TECHNISCHE UNIVERSITÄT MÜNCHEN

Lehrstuhl für Ernährung und Immunologie

Role of the intestinal microbiota in metabolic and inflammatory phenotypes in a human microbiota-associated mouse model for metabolic disorders and diet-induced obesity

Valentina Luise Ruth Schüppel

Vollständiger Abdruck der von der Fakultät TUM School of Life Sciences der Technischen Universität München zur Erlangung des akademischen Grades eines

Doktors der Naturwissenschaften (Dr. rer. nat.)

genehmigten Dissertation.

<u>Vorsitzender:</u>		Prof. Dr. Michael Schemann
<u>Prüfer der Dissertation:</u>	**1.**	Prof. Dr. Dirk Haller
	2.	Prof. Dr. Martin Klingenspor

Die Dissertation wurde am <u>02.03.2020</u> bei der Technischen Universität München eingereicht und durch die Fakultät TUM School of Life Sciences am <u>23.09.2020</u> angenommen.

Abstract

Changes in gut microbiota composition and function are linked to a great variety of disorders, including obesity and diabetes. Colonization of germfree (GF) mice with obese human microbiota provided essential insights into functional aspects of host-microbiome interactions in the context of obesity, but results are still inconsistent.

This thesis focused on the role of human gut bacteria in metabolism, gut barrier function and inflammation in gnotobiotic mice. The aim was to establish a humanized mouse model for obesity and metabolic dysfunction, based on transfer of patient-derived fecal microbiota, pre and post fecal transplantation into GF male wildtype C57BL/6N mice on control diet (CD). Obese and insulin resistant patients showing improved insulin sensitivity and reduced circular inflammation after treatment served as donors for pre and post transplantation fecal samples. As an additional control, a group of mice was associated with microbiota from a lean patient. To further elucidate mechanisms of microbe-host-diet interactions, feeding experiments of the specifically colonized mice with a diet rich in saturated fat were performed. For this, mice were fed a palm-oil based high-fat diet (HFD) for four weeks in order to provoke diet-induced obesity (DIO).

The transfer of human microbiota from obese and insulin resistant patients did not induce the respective metabolic donor phenotype in gnotobiotic mice. Recipient mice showed no change in metabolic readouts compared to animals colonized with lean microbiota. Normal body development, fat pad weight and fasting blood glucose levels were observed, independent of the human donor and pre/post treatment sample, when mice were fed CD. However, HFD feeding in colonized mice provoked obesity, insulin resistance, inflammation independent liver steatosis and low-grade adipose tissue inflammation combined with adipocyte hypertrophy regardless of the human donor and sample type. HFD feeding did not result in gut barrier impairment and intestinal inflammation.

Focusing on microbiota profiles, we observed shifts between the original patient-derived samples and the microbiota after transplantation to GF mice. These shifts were evident by a loss in number of bacterial species and changes in dominant community structure. Microbiota profiles of the colonized mice were stable over time and independent of the colonization duration.

In summary, we demonstrate that obesity and insulin resistance cannot be initialized in C57BL/6N mice by transferring patient-derived fecal microbiota. DIO, impairment of glucose tolerance and liver steatosis were independent of patient donor microbiota. In addition, transfer of human microbiota into mice resulted in a substantial change of bacterial community structure and richness, as well as diversity, suggesting that putative human obesogenic taxa remain within the group of non-transferrable bacteria.

Zusammenfassung

Veränderungen in der Zusammensetzung und Funktion der Darmmikrobiota werden mit einer Vielzahl von Erkrankungen wie Fettleibigkeit und Diabetes in Verbindung gebracht. Im Zusammenhang mit Fettleibigkeit konnten Kolonisierungen von keimfreien Mäusen mit Mikrobiota von adipösen Menschen bereits wesentliche Erkenntnisse über funktionelle Aspekte der Wirt-Mikrobiom-Interaktionen geben. Allerdings sind die bisherigen Ergebnisse widersprüchlich.

Die vorliegende Arbeit konzentrierte sich daher auf die Rolle von humaner Darmmikrobiota im Metabolismus, Darmbarrierefunktion und bei Entzündungen in gnotobiotischen Mäusen. Ziel war es, ein humanisiertes Mausmodell für Fettleibigkeit und Stoffwechselstörungen zu etablieren. Dieses basierte auf der Übertragung von fäkaler humaner Mikrobiota, generiert aus Proben einer prä- und postfäkalen humanen Transplantationsstudie, in keimfreie männliche C57BL/6N Wildtyp-Mäuse auf Kontrolldiät. Adipöse und insulinresistente Patienten, die nach der Behandlung verbesserte Insulin- und Entzündungswerte zeigten, dienten als Spender-Mikrobiota vor und nach der fäkalen Transplantation. Als zusätzliche Kontrolle wurde eine Gruppe von Mäusen mit Mikrobiota eines schlanken Patienten assoziiert. Um die Mechanismen der Wirts-Mikrobiom-Interaktionen im Kontext Ernährung weiter aufzuklären, wurden Fütterungsexperimente an den spezifisch kolonisierten Mäusen mit einer Diät, reich an gesättigten Fettsäuren, durchgeführt. Um eine ernährungsbedingte Fettleibigkeit zu provozieren, wurden die Mäuse vier Wochen lang mit Hochfettfutter, welches als Fettquelle überwiegend Palmöl enthielt, gefüttert.

Die Übertragung von Mikrobiota fettleibiger und insulinresistenter Patienten zeigte keinen entsprechenden humanen Stoffwechselphänotyp im kolonisierten Mausmodell. Darüber hinaus wurden keine Unterschiede in den Stoffwechselwerten zwischen diesen Mäusen und Tieren, die mit schlanker Mikrobiota besiedelt wurden, beobachtet. Die Mäuse zeigten außerdem, unabhängig von der humanen Spender-Mikrobiota und der Probe vor und nach der Behandlung, eine normale Körpergewichtsentwicklung sowie unbeeinflusste Fettmassen und Glukosewerte. Jedoch löste die Fütterung von Hochfettfutter bei kolonisierten Mäusen Fettleibigkeit, Insulinresistenz, eine entzündungsunabhängige Lebersteatose sowie eine niedriggradige Entzündung und Hypertrophie im Fettgewebe aus. Allerdings konnte keine Beeinträchtigung der Darmbarriere oder Entzündung im Darm bei Palmöl gefütterten Mäusen festgestellt werden. Diese Effekte waren ebenfalls unabhängig von der humanen Spender-Mikrobiota und dem Probentyp.

Es konnten Verschiebungen in der Zusammensetzung der Mikrobiota vom jeweiligen humanen Spender nach Transplantation in die keimfreien Mäuse gezeigt werden. Diese gingen mit einem Verlust bakterieller Spezies und Veränderungen der mikrobiellen Gemeinschaft einher. Des Weiteren waren die Mäuse über die gesamte Kolonisierungszeit stabil kolonisiert.

Zusammenfassend zeigt die vorliegende Arbeit, dass sowohl humane Fettleibigkeit als auch Insulinresistenz durch fäkale Mikrobiota-Transplantation nicht auf das hier eingesetzte Mausmodell übertragen werden konnte. Fettfutter-induzierte Unterschiede wie Fettleibigkeit und einhergehende Glukoseintoleranz sowie Lebersteatose manifestierten sich unabhängig vom jeweiligen humanen Spender der Mikrobiota. Darüber hinaus führte der Transfer von humaner Mikrobiota in das Mausmodell zu erheblichen Veränderungen in der bakteriellen Zusammensetzung und Vielfalt. Eine Erklärung könnte sein, dass bakterielle Spezies, die potentiell zu Fettleibigkeit beitragen, nicht den Darm der Maus besiedeln konnten.

Table of content

1   Introduction

1.1   Gut bacterial ecosystem

The gut microbiome is defined as the entity of all microorganisms (microbiota) and their collective genomes (metagenome) including bacteria, archaea, viruses, fungi and protozoa in the gastrointestinal tract. The intestinal microbiota itself is dominated by anaerobic bacteria [1], which appear in total numbers of more than 30 trillion in an average human individual [2]. Within the 12 phyla identified in gut microbiomes of human species, the most abundant phyla by far are Firmicutes and Bacteroidetes followed by Proteobacteria, Actinobacteria, Verrucomicrobia, Fusobacteria and Cyanobacteria [3, 4].

The gut microbiota is a dynamic ecosystem with large variations between each individual. Additionally, lifestyle, diet, hygiene, use of antibiotics and other drugs as well as genetics can tremendously influence the diversity, composition and metabolic function of the individual microbiome thus inducing individual differences from human to human [5-16]. Therefore, it seems difficult to define a healthy microbiota to serve as a reference control for the investigation of diseases [3]. Nevertheless, it is possible to define a so-called 'core microbiome', which comprises 90 % of bacterial species analyzed in metagenomic samples. Furthermore, most people share a core set of microbially encoded genes and thus metabolic core functions provided by the microbiome. This indicates that the core microbiome should be defined on a functional, not a taxonomical level [1, 17, 18]. In 2011, a study revealed the presence of three enterotypes defined by three robust bacterial clusters found in 261 humans independent of nation, age, gender or body mass. Each individual could be assigned to one specific enterotype, which was identified by variations in the level of one of three genera: *Bacteroides* (enterotype 1), *Prevotella* (enterotype 2) and *Ruminococcus* (enterotype 3) [19]. However, only two enterotypes, predominantly consisting of *Bacteroides* and *Prevotella*, were confirmed in follow-up studies, the third enterotype remained ambiguous [20, 21]. Recently, the human gut microbiome could be successfully partitioned into different community types. These were predictive of each other and associated with background independently of considerable intra- and interpersonal variations [22].

The gut microbiome exhibits many crucial functions as it plays an important role in the digestion of complex molecules, the production of hormones, essential amino acids as well as vitamins. In addition, the microbiota is required for development and homeostasis of the immune system, protection against invasion of opportunistic pathogens, differentiation of the host's intestinal epithelium and maintenance of tissue homeostasis [23-27]. Gut microorganisms can also affect drug metabolism, as they are able to detoxify xenobiotic compounds and influence the enterohepatic cycle of bile acids via deconjugation and dihydroxylation [28-30]. Commensal bacteria maintain gut barrier integrity by preventing colonization of pathogenic microorganisms. The innate immune system is specialized on

the recognition of microbiota-associated molecular patterns in order to defend the host against pathogenic bacteria. These pattern recognition receptors such as toll-like receptors (TLRs; e. g. TLR-2, TLR-4) expressed by intestinal epithelial and innate immune cells are sensing microbes and are activating the immune cascade [31-33]. Additionally, commensal bacteria could decrease intestinal permeability in susceptible hosts by inducing gut barrier proteins [34].

Furthermore, microbes ferment polysaccharides and proteins, produce vitamins and metabolize bile acids [30, 35]. Short-chain fatty acids (SCFAs) are bacterial fermentation end products of non-digestible dietary fibers, mainly composed of acetate, propionate and butyrate. These products function as energy source for the host, but also impact intestinal barrier function and immune responses [24, 36, 37]. Additionally, butyrate is discussed to serve as beneficial metabolite in the prevention and therapy of obesity, as it improved insulin sensitivity in obese patients [38, 39]. On the other hand, it is discussed that obese patients showed increased SCFA levels compared to lean participants [40].

But changes in the microbial composition, which is associated with specific deviations from the 'normal' gut microbiome (so called 'dysbiosis') and a functional loss of the immunological barrier in the gut, lead to the development of several diseases such as inflammatory bowel disease [41], type 1 diabetes [42] and atherosclerosis [43].

1.2   Human and mouse gut bacterial ecosystem in metabolic disorders

Diet is considered as one of the main drivers shaping the gut microbiota over life time. It has been shown that a change in diet is accompanied by rapid changes in the gut microbiota composition as well as gene expression. However, is not yet clarified if such alterations contribute to the development of metabolic disorders [8].

There has been increasing interest in the role of the microbiota in modulating metabolic disorders. Besides digestion and immunity [24, 25], the gut microbiota might also be involved in host metabolism and the development of metabolic disease, including obesity, type 2 diabetes (T2D) and non-alcoholic fatty liver disease (NAFLD) [18, 44-51] (Figure 1).
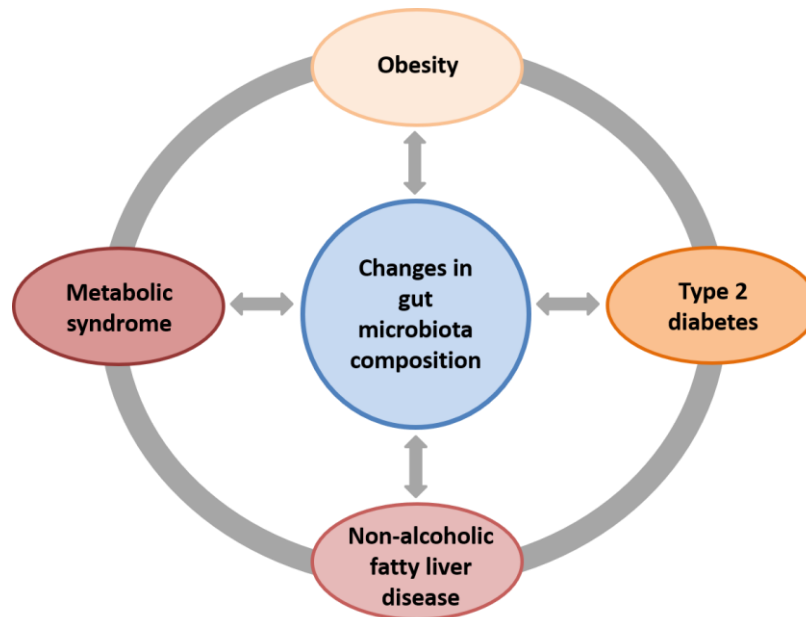
Figure 1: Changes in the gut microbial composition are associated with several metabolic diseases like obesity, type 2 diabetes, non-alcoholic fatty liver disease and metabolic syndrome.

The first study linking changes in the gut microbiota composition and function to obesity observed an increase in Firmicutes to Bacteroidetes ratio in genetically obese mice compared to lean animals [48]. Another study confirmed the differences in microbial clusters between lean and obese mice and suggested increased capacity for energy harvest from diet [36]. Further, mouse studies confirmed that obesity is associated with changes in gut microbiome associated with a reduced gut bacterial diversity [52, 53]. Fleissner and co-workers noticed a lower proportion of Bacteroidetes in favor of Firmicutes in obese mice compared to lean littermates [54].

In addition to mouse studies, the same researchers, observing differences in clusters in lean and obese mice [36], detected a decrease in the relative proportion of Bacteroidetes in obese humans compared to lean participants, which increased with weight loss. They further suggested that modulation of the gut microbial ecology might be dynamically correlated with metabolic phenotype of the host [45]. Confirmatively, compositional alterations in the gut microbiota of lean compared to T2D patients were observed [55]. In contrast, in a larger human cohort study, the comparison of microbial profiles of lean and obese twins did not reveal changes in Firmicutes abundance, but reduced levels of Bacteroidetes and a lower alpha diversity in obese individuals [18]. Additionally, in another human study no differences in the proportion of Firmicutes and Bacteroidetes in obese and weight loss patients compared to lean participants were observed [40]. In further human studies, the researchers could not find any associations between obesity and the ratio of Firmicutes to Bacteroidetes [3, 19, 56].

In conclusion, robust differences were observed between lean and obese mice with respect to gut bacterial composition on phylum level, but could not be confirmed in several human studies. Taken together, this could suggest that Bacteroidetes and Firmicutes ratios are irrelevant in human obesity, but might be relevant in murine obesity.

In a publication of Schwiertz and co-workers, who did not observe decreased Bacteroides abundance in obese and overweight subjects, SCFAs were suggested to play an important role in obesity. The total amount of fecal SCFAs was significantly higher in obese compared to lean subjects [40]. However, results are conflicting as a later publication from Ridaura *et al.* observed contradictory results in SCFA levels in mouse experiments. Lower butyrate and propionate levels in cecal contents correlated with higher fat mass in mice [57]. Noteworthy, fecal versus cecal SCFA measurements used in the studies might have an effect on the results and could explain the different outcome. The importance of SCFAs in the context of obesity is controversially discussed, as SCFAs are observed to be increased in obese patients, but also have a protective effect against diet-induced obesity (DIO) [40, 58, 59].

Despite the limited evidence for changes on phylum level in human obesity, butyrate-producing Firmicutes, namely *Roseburia* and *Eubacterium rectale*, were significantly reduced in obese patients on different weight loss diets [47]. Patients, who lost more than 4 kg body weight on a low-calorie diet, showed significantly increased abundances of *Lactobacillus* sp. and *Bacteroides fragilis* and lower levels of *Clostridium coccoides* and *Bifidobacterium longum* than before dietary intervention. The authors concluded a direct impact of weight loss on the gut microbiota composition. Nevertheless, detailed information on phylum distributions was lacking [60]. A study examining the microbiota of patients with surgery-induced weight loss observed a positive correlation between *Bacteroides*/*Prevotella* group and *Escherichia coli* abundances and the amount of lost weight. On the other hand, the abundances of lactic acid bacteria and the *Bifidobacterium* genus were negatively correlated with weight loss. The authors postulated a rapid adaptation of specific dominant bacteria to a starvation-like situation caused by bypass surgery [61].

Metagenomic analysis revealed that low bacterial richness, *i.e.* low gene counts, was associated with adiposity and insulin resistance in human individuals when comparing to participants with high bacterial richness. The authors highlighted the anti-inflammatory species *Faecalibacterium prausnitzii* which was more prevalent in high gene counts individuals. In the low richness group, the bacterial species *Bacteroides* sp. and *Ruminococcus gnavus*, which are associated with inflammatory bowel diseases, were found more frequently [44]. Although changes in specific bacterial communities are not consistent between different studies, it is widely accepted that obesity is associated with changes in fecal microbiota profiles, including altered microbial composition and reduced bacterial diversity [18, 44, 55, 62-69].

To identify indicator taxa and a general taxonomic signature of the gut microbiota in obesity, Walters *et al.* [70] and Finucane *et al.* [71] reanalyzed previously published data. Both studies concluded, based on meta-analysis of large cohorts including lean and obese subjects, that there is no association between obesity and specific taxonomic structures like differences in microbial diversity [70, 71].

In 2016, Sze and Schloss [72] went one step further and reanalyzed 10 studies, based on 16S rRNA sequencing data in combination with body mass index (BMI) values, in a meta-analysis approach. In two out of 10 studies, bacterial diversity in obese patients was significantly reduced compared to lean subjects, with the remaining studies showing a trend towards reduced diversity. When pooling all studies, significant associations between microbial richness, evenness, diversity and the status of obesity were observed. Nevertheless, the effect size of all tested parameters was quite small. Furthermore, the ratio of Bacteroidetes to Firmicutes or their individual relative abundance was not significantly associated with obesity in any of the explored studies. Taken together, these studies suggest lower diversity in obese patients compared to lean subjects, but large interpersonal variation and insufficient samples sizes are major confounders for a final conclusion.

In summary, obesity is associated with changes in microbial profiles, but a taxonomic signature of the human gut microbiota in the context of obesity is still not defined. General statements like an increased Firmicutes to Bacteroides ratio in obese compared to lean subjects are presumably superficial and incorrect, which is underlined by several studies reporting conflicting results. This still raises the question of which bacterial groups are relevant in the etiology of obesity.

Alterations of the microbial ecosystem can be either consequence of an obese physiology, which influences the intestinal environment, but also cause or amplifier of the pathology. Antibiotic treatment of obese humans with vancomycin resulted in alterations of the microbial community, but did not influence the host phenotype including insulin sensitivity, gut permeability and systemic inflammation. Additionally, there were no associations between specific characteristics of gut profiles upon antibiotics treatment and host metabolism [73]. This suggests a consequential relationship between the obese environment and microbial community alterations.

But there are also indications that bacteria can modulate host physiology in obesity. *Akkermansia muciniphila* improved host metabolism by decreasing body and fat mass weight as well as fat morphology in diabetic mice [74]. *Vice versa*, *Clostridium (C.) ramosum* DSM1402 and *Enterobacter (E.) cloacae* B29 are assumed as obesity-associated bacteria promoting obesity in HFD-fed gnotobiotic mice [75, 76].
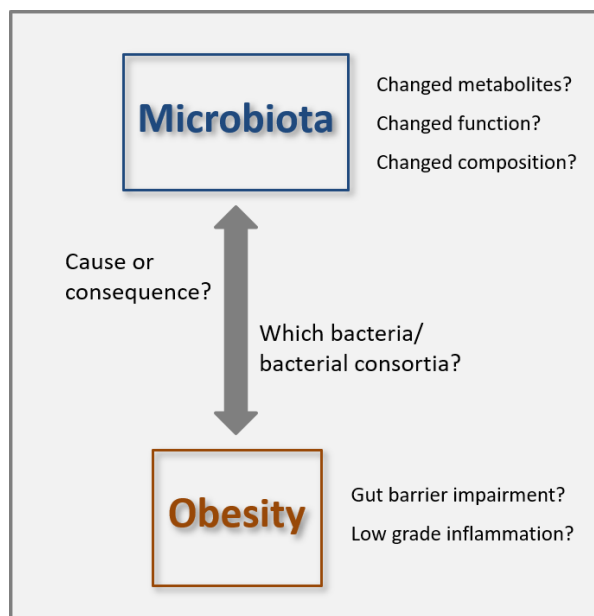
Figure 2: Interaction between the microbiome and obesity.
Cause, consequence and degree of changed microbial composition and function are still not known in the context of obesity and its possible co-morbidities.

At this stage, we are far from fully understanding which bacteria or bacterial consortia are involved in the pathogenesis of obesity. Since several lines of evidence indicate a role of the intestinal microbiota in obesity and other metabolic diseases, the identification of specific bacterial taxa and their interactions with the host is necessary to decipher disease etiology (Figure 2).

1.3 Obesity, type 2 diabetes and its pathophysiologies

Obesity is defined as abnormal or excessive fat accumulation, that may impair health and is, per definition, attributed to humans with a BMI equal or greater than 30 kg/m^2 [77]. In general, obesity is the result of an imbalanced energy intake and expenditure leading to constant energy excess. A plethora of publications confirmed that the development of obesity is triggered by the interplay of environmental, behavioral and genetic factors [78-80].

Obesity is, amongst other metabolic diseases, associated with increased blood glucose levels, insulin resistance, altered adipokine secretion, ectopic fat storage, local inflammation, mitochondrial dysfunction, dyslipidemia, hypertension, impaired gut barrier function and microbial profile changes, which are discussed to increase the risk for metabolic diseases like T2D (see section 1.2) [57, 81-87]. T2D is characterized by long-term high blood glucose levels and subsequent development of insulin resistance, defined as the inability of cells to respond to insulin properly. Beta cells within the pancreas try to compensate for the insensitivity of the body cells for insulin by releasing more and more insulin. As the disease progresses, the pancreas's insulin production decreases, due to exhaustion of the beta

cells and the consequential insufficient production of insulin. T2D is mostly provoked by an unhealthy lifestyle such as high-calorie diet and physical inactivity [88-90].

Still, the effects of obesity on intestinal barrier integrity, inflammatory processes and accompanied endotoxemia are controversially discussed in literature (Figure 2). Lipopolysaccharides (LPS), which are components of the outer cell wall of gram negative bacteria, that can induce the secretion of inflammatory cytokines [91], are believed to be relevant in the context of inflammatory processes in the gut. The release of LPS by the disaggregation of bacteria can lead to a mild increase in plasma LPS concentrations, a process known as metabolic endotoxemia. It is believed that metabolic endotoxemia is triggered by high-fat diet-induced obesity via increased gut permeability and eventually leads to low-grade inflammation in fatty tissue. Endotoxemia could further be responsible for the development of metabolic disorders including insulin resistance and hyperglycemia [82, 92-94].

In previous studies with lean and DIO mice, the authors observed a two- to three-fold increase in LPS levels, partially elevated expressions of inflammatory markers in liver, fat and muscles, higher intestinal permeability and decreased mRNA levels of junctional proteins in obese animals [82, 92, 95-98]. Also, in studies using rat models, lower levels of gut barrier proteins were found in obese animals [99, 100], but it is still elusive if these changes contribute to an altered gut barrier function and to an inflammatory status.

In contrast, a number of studies have failed to confirm impaired gut barrier function and low-grade inflammation associated with obesity and DIO in mice and humans [62, 75, 101, 102]. Kless *et al.* [101] could neither observe increased LPS levels, nor higher gut permeability and inflammation in different murine models of DIO. These data suggest that DIO-induced metabolic impairments were independent of alterations in gut barrier function. Also, housing conditions might be responsible for impaired gut barrier integrity and inflammation, as conventionally raised mice showed DIO driven pathology, but specific pathogen free (SPF)-housed mice did not [102]. Based on the inconclusive data on the presence of gut barrier problems and inflammation in the context of obesity, further studies are required to elaborate the different study outcomes.

Yet, considering the substantial amount of studies indicating impaired gut barrier function and low-grade inflammation in the context of obesity, the link between gut barrier impairment, endotoxemia and non-alcoholic fatty liver disease (NAFLD) needs to be examined in obesity [103]. NAFLD is a common DIO driven pathophysiology and characterized by excessive lipid accumulation in the liver which can progress to non-alcoholic steatohepatitis (NASH), an inflammatory response to this hepatic fat aggregation [104]. NAFLD originates from the combination of host and environmental factors, as

well as dysbiotic gut microbiota, shown by several human and animal studies with compositional shifts in the gut microbiota in subjects suffering from NALFD compared to healthy controls [50, 51, 105-107].

The primary bile acids cholic acid and chenodeoxycholic acid were produced by the liver from cholesterol and were then metabolized to secondary bile acids in the intestine from the gut microbiota [108]. Alterations in bile acid composition and an increase of total bile acid concentrations were observed in obesity and T2D [109-112]. In NAFLD patients dysbiosis of the gut microbiota is associated with changed bile acids composition and concentrations [113].

Taken together, data on gut barrier function and inflammation in the context of obesity are still inconsistent. While some studies support the existence of gut barrier impairment and associated inflammatory conditions, these observations were not confirmed by others. Inconsistencies could be due to the use of different experimental diets with regard to total energy content, the amount and composition of macronutrients, diverse housing conditions and inconsistency with respect to mouse strains. Further studies are required to increase our understanding of the link between obesity, gut function and NAFLD.

1.4 Human fecal microbiota transplantation

The human gut microbiota is considered to have enormous potential for therapeutic strategies. Fecal microbiota transplantation (FMT) is one promising option to treat a growing range of pathologies. FMT describes the transfer of fecal material from a healthy donor to a patient to increase intestinal microbial diversity and re-establish a 'normal' microbiome. The first human FMT in modern medical literature was reported as early as 1958, when four cases of enterocolitis were successfully treated with fecal enemas [114]. Over time, FMTs have also been used effectively to treat various diseases such as *Clostridium (C.) difficile* infections (CDI) and Ulcerative colitis (UC). Patients suffering from *C. difficile*-induced diarrhea showed a cure rate of 81 % after the first FMT treatment and 92 % after the second treatment, compared with a success rate of 31 % when treated with antibiotics [115]. The enormous success rate of FMT treatment in CDI could be explained by an increase in intestinal bacterial diversity in patients following the introduction of a healthy donor microbiota [115]. Hypothetically, the increase in bacterial diversity could positively impact secondary bile acid conversion and inhibit the production of bacterial toxins [116]. A meta-analysis of eleven studies, dealing with treatment of CDI patients via FMT application, confirmed the treatment success rate of over 90% and observed higher microbial diversity in cured patients [117].

There are also several controlled randomized studies on FMT that focus on the treatment of inflammatory bowel diseases (IBD). FMT treatment with a healthy donor microbiota induced remission status significantly more often in patients suffering from UC than placebo control treatment [118].

However, another study did not observe statistical differences in the response rate of UC patients treated with allogenic or autologous FMT. Nevertheless, participants achieving clinical remission after FMT treatment showed distinct differences in microbial features compared to patients not responding to FMT application [119]. Three additional studies with IBD patients revealed positive clinical responses to FMT treatment, independently if patients suffered from UC or Crohn's disease [120-122]. Overall, FMT patients showed a higher microbial diversity than before treatment. In addition, the microbial diversity of FMT-responders, that entered remission after treatment, was higher than that of non-responders [120].

1.5   Human fecal microbiota transplantation in obesity

In addition to CDI and IBD, FMT applications were extended to extra-gastrointestinal, but microbiota-associated diseases like multiple sclerosis, Parkinson and also to Kwashiorkor, a disease caused by extreme protein malnutrition and manifested by peripheral edema and muscle atrophy. A study with children discordant for malnourishment showed that mice colonized with microbiota from Kwashiorkor participants displayed significant weight loss and perturbations in amino acid, carbohydrate, and intermediary metabolism compared to mice associated with microbiota from well-nourished children [123]. These data indicate that FMT could be an appropriate approach in influencing metabolic diseases.

Recent data from microbiota transplantation studies in patients and animals suffering from obesity and co-morbidities suggest that FMT is a legitimate therapeutic intervention for the treatment of metabolic syndrome [36, 38, 57, 124, 125]. Surprisingly, there are only two published human studies from the same working group showing the efficacy of FMT in obese patients [38, 124]. Obese patients treated with fecal microbiota of a lean human donor showed increased insulin sensitivity and elevated abundance of butyrate-producing gut bacteria. Remarkably, there was no reported difference in BMI after transplantation. Although the exact mechanisms are not known, it is proposed that the application of external microbiota replaces the original bacteria with a more diverse and resilient microbiota [38].

A closer look into the microbial environment revealed a large and permanent coexistence of donor and recipient strains, still persisting three months after treatment [126]. The same working group confirmed this observation five years later. Obese patients, which got lean donor microbiota, showed improved insulin sensitivity associated with changes in plasma metabolites. Microbial profiles were also significantly changed after transfer. It is noteworthy that improvements in insulin levels were observed only up to six weeks after FMT, but FMT induced no long-term effects on body weight, insulin sensitivity and metabolites [124]. Recently, de Groot *et al.* treated humans with metabolic syndrome with fecal microbiota from either post-Roux-en-Y gastric bypass (RYGB) or metabolic syndrome (MS)

donors via FMT. The authors observed significantly decreased insulin sensitivity in MS-treated humans two weeks after FMT compared to RYGB-recipients, suggesting that donor characteristics can influence metabolic effect of FMT in human recipients [127]. But still, the effect and benefit of FMT with metabolic syndrome in humans has hardly been investigated so far.

1.6 The use of gnotobiotic mouse models and mouse fecal microbiota transplantation for the study of obesity

Mechanistic insight into the role of FMT treatment in obesity has been obtained from animal studies. Hereby, gnotobiotic experiments pose an important way to analyze the impact of the gut microbiota. Gnotobiotic mice are defined as germfree (GF) mice which are colonized with a defined intestinal ecosystem – composed of certain complex, minimal consortia or a single strain. Studies with gnotobiotic animals are a promising approach to analyze the effect of FMT on various additional diseases and to test the influence of the microbial composition on the host.

In the field of obesity and weight loss, Liou and colleagues colonized GF mice with cecal gut microbiota of gastric-bypass treated DIO mice and observed weight loss and decreased fat mass compared to placebo-surgery treated animals. These findings directly link changes in the gut microbiota with host weight, as well as adiposity due to altered production of SCFAs [128]. Confirmatively, GF mice colonized with fecal microbiota from patients after surgically-induced weight loss showed reduced fat deposition compared to animals associated with microbiota from obese humans. It is noteworthy that the results of fat gain were widely scattered: partially mice colonized with obese microbiota showed equivalent fat gain as recipients from bariatric-surgery microbiota [129].

The importance of a 'healthy' microbiota was demonstrated in a study analyzing fecal transplantation experiments in mice. Compared to mice colonized with microbiota from a healthy donor, recipients of a microbiota from undernourished children displayed growth impairments that could be improved by the introduction of two specific bacteria, namely *Ruminococcus gnavus* and *Clostridium symbiosum* [130].

Transmissibility of obesity in mice was first described by colonization of GF recipients with genetically-induced obese ob/ob-mouse microbiota, resulting in increased body fat accumulation. The authors proposed the gut microbiota as contributing factor to the pathophysiology of obesity [36]. Introduction of microbiota from conventionally raised donors into GF recipients resulted in higher weight gain compared to GF littermates when fed a Western diet [131]. In addition, a causal role of the intestinal microbiota composition for the development of obesity was supported by three independent studies transplanting fecal microbiota of obese humans into GF mice [10, 57, 132]. Goodrich *et al.* [10] colonized one set of GF mice with microbiota from an obese patient, whereas the other group received

an additional inoculation of *Christensenella minuta,* a bacterium associated with low BMI [10, 133-135]. *Christensenella minuta* treated mice showed reduced adiposity associated with changes in the microbiome composition, which gives a clear indication towards an influence of the gut microbiome on host metabolism [10]. Recently, GF mice were colonized with microbiota derived from dizygotic twins discordant for obesity. Recipient mice of obese microbiota developed increased fat mass gain, accompanied by decreased SCFAs in the intestinal content. Hence, the authors concluded that an obese phenotype is transmissible from human to mice with all its comorbidities [57].

A further study attempted to elucidate the link between the intestinal microbiota and development of diet-induced metabolic syndrome. Therefore, the authors raised rats on a standard or high-fructose diet. In addition, DIO rats were either challenged with antibiotics or fecal microbiota from control diet-fed animals. The high-fructose diet-fed mice developed DIO with typical co-morbidities including metabolic syndrome, inflammation and oxidative stress. Interestingly, the phenotype could be reversed by the treatment of DIO mice with either fecal samples of control mice or antibiotics. The authors suggested that the development of metabolic syndrome is directly correlated to specific changes in the intestinal bacterial composition. The abundance of two bacterial genera, *Coprococcus* sp. and *Ruminococcus* sp, was increased in DIO mice, but decreased after antibiotic treatment or transplantation of lean microbiota. Noteworthy, glucose levels and epididymal fat contents were not changed in mice by FMT treatment [136].

It is remarkable that even the transfer of a single bacterium seems to influence host metabolism [75, 76]. Monoassociation of GF mice with *E. cloacae* induced DIO and insulin resistance on high-fat diet, whereas GF control mice or animals colonized with Bifidobacterium did not develop the same disease phenotype upon high-fat diet feeding [76]. In line with this, gnotobiotic mice associated with a simplified human microbiota consortium containing *C. ramosum* were more susceptible to DIO than counterparts colonized with a simplified human microbiota consortium only. *C. ramosum* colonized mice showed also higher body fat as well as an increase in fat and glucose transporters. However, inflammatory status, gut barrier integrity and food intake were not different between these two association groups [75].

To further study the role of gut microbes in the etiology of metabolic syndrome, human fecal microbiota of 16 lean and 16 obese patients were transferred into GF mice by Zhang *et al.* [132]. Mice were caged in pairs for each human donor and split into two gnotobiotic isolators for each metabolic condition (in total four isolators), to prevent carry-over effects. Already one week after FMT, a significantly higher total body weight gain was observed in obese microbiota recipients compared to mice colonized with lean microbiota. Even after seven weeks of colonization body weights of obese-associated mice remained significantly increased. However, separating data according to each

individual isolator revealed a discrepancy in mice associated with lean microbiota. In one isolator, lean microbiota recipients showed comparable body weight gain as mice housed in both isolators for obese-microbiota recipients. Surprisingly, increased fat mass weights, as observed in human donors, were not transferable into mice. Additionally, different insulin levels in mice could not reflect the original human phenotypes. Although the microbial profiles of lean and obese human donors did not differ, the microbial profiles of recipient mice clustered into distinguishable groups. These data suggest that the microbiota may indeed affect metabolic phenotypes in mice, but the metabolic results of microbiota transplantation could not be predicted and were dependent on individual donor selection [132].

Transmissibility of obesity-associated comorbidities was also tested in a study on the colonization of mice with stool samples from two-week-old infants born of either normal-weight or obese women. Mice associated with the microbiota of 'obesity-born' infants showed higher gut permeability and SCFA levels, as well as increased fat tissue and liver inflammation accompanied by impaired macrophage function. Interestingly, fat mass weight was increased in 'obesity born' recipients, but total body weight did not differ between treatment groups. When mice were further challenged with HFD, weight gain and NAFLD were more pronounced in mice colonized with 'obesity-born microbiota' than in the control group [137].

In contrast to the aforementioned literature, a recently published study, investigating mouse to mouse microbiota transplantation, could not confirm transferability of obesity. Neither the microbiota from mouse stool of pre-obese – meaning microbiota from a lean mouse which development diet-induced obesity – nor from obese mice were able to induce obese phenotypes in gnotobiotic mice [138]. **These data already highlight the complexity of this topic and raises the question of the right choice of donor microbiota, mouse strain, colonization time and period.**

The gut microbiota is also discussed as a key modulator of insulin resistance, since TLR2-deficient mice were protected from diet-induced insulin resistance [139] and TLR2-deficient animals housed under conventionalized – meaning non-GF – conditions developed metabolic syndrome [140]. Conversely, treatment with antibiotics or keeping mice in a bacteria-depleted environment, rescued mice from these symptoms. Again, transplanting cecal bacterial suspension of TLR2-deficient mice into bacteria depleted wildtype mice reversed the phenotype, as TLR2-deficient recipients developed increased body and fat mass as well as higher glucose levels [140].

All these data indicate that the gut microbiota plays a major role in modulating host metabolism, as the metabolic phenotype is transmissible via FMT (Figure 3). **Therefore, all these studies indicate that allogenic fecal microbiota treatments have the potential to directly affect the host metabolism, but to what extent is not yet fully understood.**
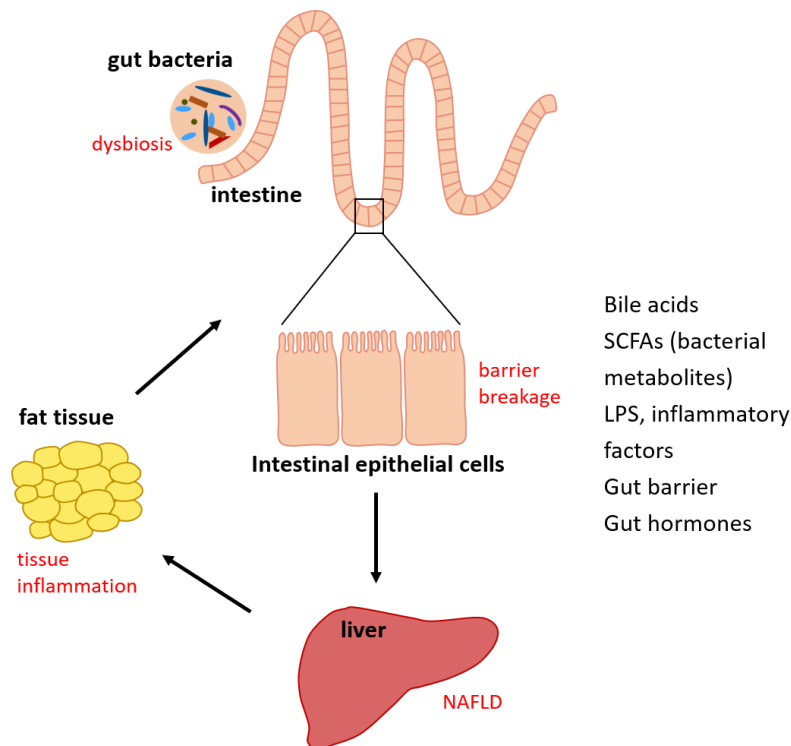
Figure 3: Potential influence of obesity and changes in gut bacteria on gut, liver and fat tissue structure and function.

Changes in gut bacterial communities (dysbiosis) caused by obesity effects the diversity of bile acids, SFCA composition, gut hormones, induces tissue inflammation as well as NAFLD and increases LPS levels and gut permeability. LPS – lipopolysaccharide, SCFAs – short chain fatty acids, NALFD – non-alcoholic fatty liver disease.

2 Aim

The gut microbiota plays an essential role in chronic diseases like obesity. Still, the microbe-host interaction in the context of obesity is not fully elucidated yet.

The primary aim of this study was to investigate the role of different human obese microbiota ecosystems in metabolism, liver, fat and gut function in a gnotobiotic mouse model for obesity and insulin resistance. Therefore, the goal was to establish a humanized mouse model for obesity and insulin resistance by transferring fecal microbiota of obese patients with different levels of adiposity, insulin resistance and circular inflammation before and after FMT therapy into GF mice. Using this experimental setup, the effects and mechanisms of microbiota interaction with the host were investigated. For that purpose, microbial compositions of patients and mice were determined to assess the success of human microbiota engraftment in recipient mice. Then, body weight development, insulin and glucose levels, inflammatory status as well as gut barrier, liver and adipose tissue structure and function of the humanized mice were analyzed.

Further, we used the humanized mouse model to challenge the animals with an additional dietary treatment in order to elucidate the effect of secondary triggers on the host´s metabolism and phenotype. Therefore, we treated the mice with high-fat diet to explore the potential aggravating effect of diet on the host focusing on metabolism, fat, gut, and liver function as well as gut microbiome.

3 Material & Methods

3.1 Ethical statement

All animal procedures were approved by the Committee on Animal Health and core of the local government (Regierung von Oberbayern, reference number ROB-55.2Vet-2532.Vet_02-14-27. The animals were housed in mouse facilities at the Technische Universität München, ZIEL - Institute for Food & Health.

3.2 Housing conditions

Sterility of germfree (GF) mice at the beginning of each experiment was confirmed by the cultivation of fecal samples on blood agar, lysogeny broth agar and Wilkins-Chalgren-Agar (WCA, Sigma Aldrich) as well as gram staining. Additionally, fecal pellets of GF mice were tested via DNA-extraction (gDNA-clean-up kit, Macherey-Nagel) followed by PCR amplification using universal 16S rRNA primers. As controls, sterile water samples and fecal pellets of conventionally housed mice were tested. A mold-trap was used to indicate the presence of mold. Only male C57BL/6N mice were used for experimental procedures and housed with constant 12 h light/dark cycles at 24 –26 °C with access to food and water *ad libitum*. Body weight development and food intake were monitored weekly. Of note, for logistical reasons, body weight developments in the isolators were assessed on different balances than end point body weights right before killing the animals. At the end of the experiment all mice were anesthetized and killed by CO_2.

3.3 Colonization of germfree mice

The colonization procedure of GF mice was adapted according to a previously described protocol [138]. Frozen human fecal material was transferred to an autoclaved mortar surrounded by liquid nitrogen to obtain a frozen and anaerobic environment and then pulverized with a sterile pestle. Aliquots of about 400 mg fecal powder were kept at -80 °C until further preparation.

On colonization day, human fecal aliquots were dissolved in 2 ml sterile filtered reduced PBS (PBS supplemented with 0.05 % L-cysteine-HCl) in an anaerobic chamber (Whitley Hypoxystation H85, Meintrup DWS Laborgeräte GmbH) containing a H_2/ N_2 gas mixture (10:90) at a constant temperature of 37 °C. The suspension was homogenized by vortexing for 5 min and incubated for 5 min at RT to allow the debris to settle. The supernatant was transferred into nitrogen-gassed autoclaved Hungate tubes and immediately taken to the animal facility for colonization. Mice were colonized via single gavage (150–200 µl) of human fecal bacterial suspension. A separate isolator was used for each human donor transplant.

After transfer of the human microbiota, colonization efficiency was tested by plating dilution series of feces one week after association and then at least every two weeks and by 16S rRNA sequencing at the end of the experiment.

3.4 Human donor selection

Human stool samples were obtained from a study on fecal microbiota transplantation (FMT) in insulin-resistant patients with metabolic syndrome at Amsterdam Medical Center (Department of Vascular Medicine; University of Amsterdam; Prof. Nieuwdorp; Figure 4). 24 Caucasian male or postmenopausal female subjects (aged 50-70 years) with metabolic syndrome were included fulfilling at least 3 out of 5 metabolic syndrome criteria of the National Cholesterol Education Program: **1)** fasting plasma glucose ≥ 5.6 mmol/l and/or homeostatic model assessment of insulin resistance (HOMA-IR) ≥ 2.5; **2)** triglycerides ≥ 1.7 mmol/l; **3)** waist-circumference > 102 cm for males and > 88 cm for females; **4)** HDL-cholesterol ≤ 1.04 mmol/l for males and ≤ 1.30 mmol/l for females; **5)** blood pressure ≥ 130/85 mmHg. For selection of FMT donors six otherwise healthy Caucasian males and postmenopausal females that lost >30% of their weight one year after bariatric surgery via RYGB (post bariatric) were used. The human study was conducted as a double blinded randomized controlled intervention trial. Half of the subjects were randomized to receive a single autologous fecal transplantation followed by 4 grams of oral sodium butyrate tablets once daily for 4 weeks. The second part of the patients (n=12) underwent a single allogenic post RYBG donor fecal transplantation followed by placebo tablets for 4 weeks (Figure 4). Butyrate derived from microbial metabolism of lean patients was observed to improve insulin sensitivity in obese patient which underwent FMT with lean microbiota [38].
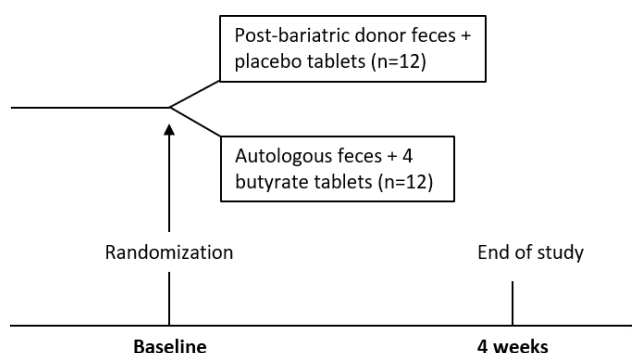
Figure 4: Human study design.

After both treatments, daily oral ingestion of sodium butyrate and a single FMT, there were no significant changes in body weight, fasting glucose levels and blood pressure in participants. However, a significant decrease in the laboratory parameters HOMA-IR and HbA1c after treatment of the allogenic FMT group was observed. Patients, who underwent sodium butyrate treatment, showed significantly altered HbA1c, total cholesterol and triglyceride levels. Inflammatory markers like CRP levels in blood were unchanged after FMT treatment in both groups.

For the present study, we selected a patient out of the human FMT trial with a moderately obese and insulin-resistant phenotype (preFMT[but]) and a participant who was classified as severely obese and insulin resistant (preFMT[lean]) before FMT treatment. Patient, designated as postFMT[but], was treated with autologous stool plus sodium butyrate tablets ([but]), while patient, termed postFMT[lean], obtained an allogenic stool transplant from a lean patient ([lean]), followed by placebo tablet treatment for 4 weeks. After treatment, both patients showed unchanged obesity categorizations, but CRP values and fasting insulin levels were improved. A post-RYGB donor, which was also used as donor for allogenic FMT treatment and which showed normal body weight and basic parameter, was selected as an additional control (lean) (Table 1).

Table 1: Human microbiota donor characteristics.

Human donor (HMb)	Weight [kg]	BMI [kg/m^2]	HbA1c [mmol/l]	Fasting glucose [mmol/l]	Fasting insulin [pmol/l]	HDL [mmol/l]	Trigly-cerides [mmol/l]	CRP [mg/l]	HOMA-IR
lean	66.6	24.5	-	5.2	24	2.60	0.63	-	0.80
preFMT[lean]	120.4	41.7	39	5.2	159	1.55	1.71	4.2	5.29
postFMT[lean]	118.6	41.0	37	5.0	105	1.54	1.34	3.5	3.36
preFMT[but]	119.0	32.6	40	6.7	108	0.97	1.07	9.8	4.60
postFMT[but]	116.4	31.9	39	6.4	74	1.00	0.99	5.1	3.03

BMI – body mass index. CRP – C-reactive protein. HbA1c – hemoglobin A1c. HDL – high-density lipoprotein. HMb – Human microbiota. HOMA-IR – insulin resistance index.

3.5   Animal experiments

Experiment 1 (establishment and high-fat diet challenge of a gnotobiotic mouse model for metabolic disorders): At the age of 4 weeks male GF C57BL/6N mice were colonized with lean-, preFMT[lean]-, postFMT[lean]-, preFMT[but]- or postFMT[but]-fecal microbiota (Table 1) and fed a control diet for 8 weeks (CD: 13 kJ% fat based on soy oil, S5745-E902, Ssniff, Soest, Germany; Table 2) *ad libitum*. Mice either remained on CD for another 4 weeks (n = 10–13 for each colonization group) or were switched to a high-fat diet (HFD: 48 kJ% fat based on a soy and palm oil mixture, S5745-E912, Ssniff, Soest, Germany; Table 2; n = 10–13 for each colonization group) to provoke diet-induced obesity (Figure 5). Both diet groups were divided in two parts, which either received an oral glucose tolerance test or were subjected to an intestinal permeability measurement.

Experiment 2 (kinetic evaluation of a gnotobiotic mouse model for metabolic disorders): At the age of 4 weeks, male GF C57BL/6N mice were colonized with preFMT[but]- or postFMT[but]-fecal microbiota for 4 (T1), 8 (T2) or 12 (T3) weeks and fed *ad libitum* with CD throughout the experiment (n= 10–13 for each time point and colonization group (Figure 5). All kinetic groups were divided into two groups, which either received an oral glucose tolerance test or were subjected to an intestinal permeability measurement.

Experiment 3 (HFD pre-challenge in short-term colonized mice): At the age of 3.5 weeks, male GF C57BL/6N mice were fed *ad libitum* with either CD (n = 7) or HFD (n = 5) throughout the experiment. After 3 days on the specific diet, mice were associated with preFMT^{lean}-fecal microbiota for 4 weeks and then sacrificed (Figure 5).
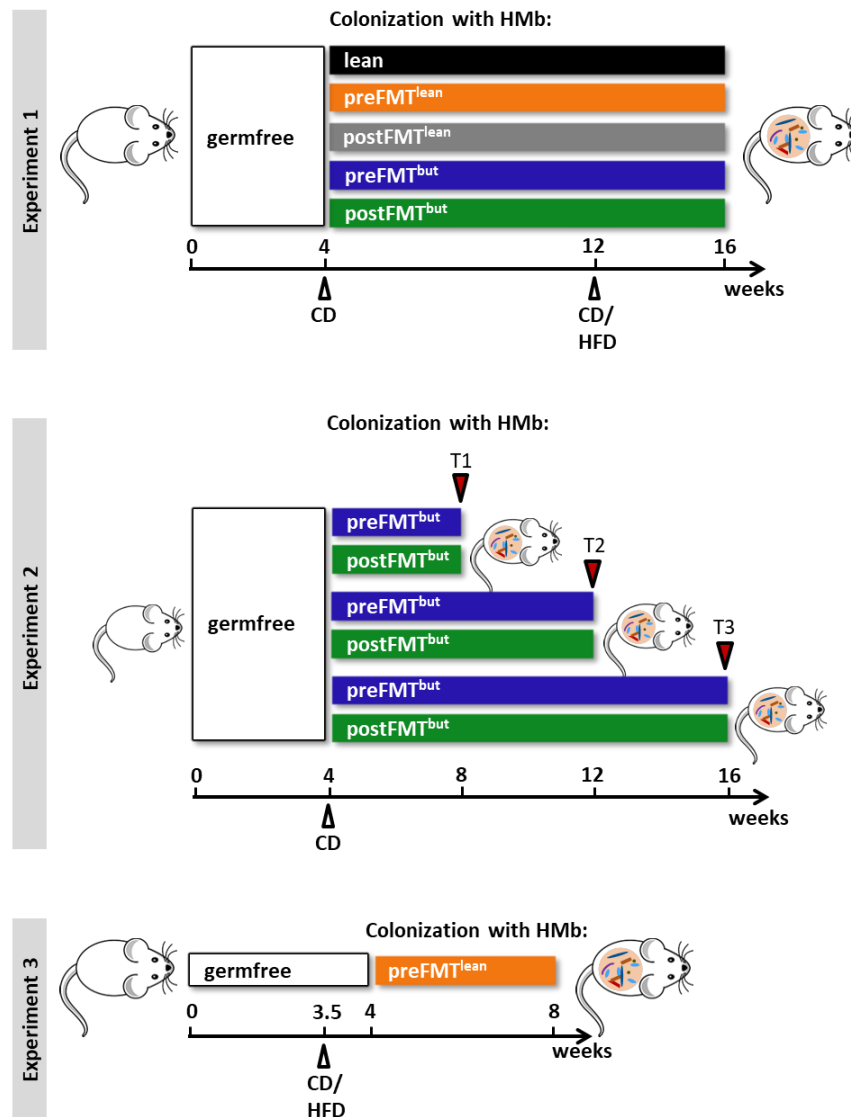
Figure 5: Design of animal experiments.
Germfree male C57BL6/N mice were colonized at the age of 4 weeks by single gavage of a complex human microbiota (HMb). In **experiment 1,** mice were associated with lean-, preFMT^{lean}-, postFMT^{lean}-, preFMT^{but}- or postFMT^{but}-fecal microbiota and received an experimental CD for 12 weeks. 4 weeks prior to sampling, mice either remained on CD or switched to HFD. In **experiment 2,** mice were colonized with preFMT^{but}- or postFMT^{but}-fecal microbiota for 4 (T1), 8 (T2) or 12 (T3) weeks and received CD throughout the experiment. In **experiment 3,** mice were fed CD or HFD three days prior to association with preFMT^{lean}-fecal microbiota. Mice were then colonized for 4 weeks while remaining on the respective diet. CD – control diet. HFD – high-fat diet. HMb – Human microbiota.

Table 2: Composition of the diets.

	Control diet (S5745-E902)	High-fat diet (S5745-E912)
Metabolizable energy [MJ/kg]	**15.3**	**19.7**
Protein [kJ%]	**23**	**18**
Fat [kJ%]	**13**	**48**
Carbohydrates [kJ%]	**64**	**34**
Casein [weight %]	24	24
Corn starch [weight %]	47.8	27.8
Maltodextrin [weight %]	5.6	5.6
Sucrose [weight %]	5	5
Cellulose [weight %]	5	5
L-Cysteine [weight %]	0.2	0.2
Vitamins [weight %]	1.2	1.2
Mineral & Trace elements [weight %]	6	6
Choline chloride [weight %]	0.2	0.2
Soy oil [weight %]	5	5
Palm oil [weight %]	**-**	**20**
Crude protein [weight %]	21	21
Crude fat [weight %]	5.1	25.1
Crude fiber [weight %]	5	5
Crude ash [weight %]	5.4	5.4
Starch [weight %]	45.9	26.7
Sugar [weight %]	6.1	6.1
NfE [weight %]	56.8	37.7
Lysine [weight %]	1.76	1.76
Methionine	0.77	0.77
Methionine + Cysteine [weight %]	1.06	1.06
Threonine [weight %]	0.93	0.93
Tryptophan [weight %]	0.28	0.28
Calcium [weight %]	0.92	0.92
Phosphate [weight %]	0.65	0.65
Sodium [weight %]	0.19	0.19
Magnesium [weight %]	0.21	0.21
C12:0 [weight %]	0.01	0.01
C14:0 [weight %]	0.02	0.21
C16:0 [weight %]	0.58	9.18
C18:0 [weight %]	0.18	1.11
C20:0 [weight %]	0.02	0.1
C16:1 [weight %]	0.01	0.05
C18:1 [weight %]	1.29	9.19
C18:2 [weight %]	2.65	4.67
C18:3 [weight %]	0.29	0.35
Vitamin A [IU/kg]	18000	18000
Vitamin D_3 [IU/kg]	1800	1800
Vitamin E [mg/kg]	180	180
Vitamin K_3 [mg/kg]	24	24
Vitamin C [mg/kg]	36	36
Copper [mg/kg]	14	14

3.6   Food intake measurement

Food intake was measured by weighing food pellets each week and dividing the weight by the number of mice in the cage. Energy uptake was then calculated using the energy content of the diets as specified by the manufacturer (Table 2).

3.7 Fecal energy content

Fecal pellets were removed from all embedding and food residues and dried for at least 48 h at 60 °C. Until further analysis, feces were stored air-tight at room temperature. Fecal pellets were then grinded in 35 ml devices (1/3 feces, 1/3 metal balls, 1/3 air) using a refiner (Tissue Lyser II, Retsch, Haan, Germany) at 30 Hz for approx. 3 min until a homogenous powder was obtained. 1 to 1.3 g of fecal powder was pressed and pelleted (Typ C21, Janke & Kunkel, Staufen, Germany). The exact weight of the pellet was noted by using an accuracy balance. Utilizing a 6300 bomb calorimetry (Parr Instrument Company, Moline, IL, USA), fecal pellets were completely burned under high pressure (30 bar) of oxygen and gross energy contents were measured:

$$caloric\ value\ \left[\frac{J}{g}\right] = \frac{EE * \Delta T}{m}$$

EE = energy equivalent value of the calorimeter [J/°C]
ΔT = increase in temperature by combustion [°C]
m = sample weight [g]

3.8 Glucose tolerance test

Oral glucose tolerance test (oGTT) was performed in order to test the response to an orally administered glucose dosage. Briefly, mice were fasted for 6 hours (6 am to 12 am) prior to oral administration of 2 mg glucose per g body mass (G-40 % glucose concentrate, B. Braun, Melsungen, Germany). Blood glucose was measured from the tail tip immediately pre- (time 0) and at 15, 30, 60 and 120 min post-gavage using a glucose meter (Abbott, Chicago, IL, USA). The total area under curve (AUC) of blood glucose levels was calculated for each animal.

3.9 Plasma measurements

3.9.1 Insulin concentration

During conduction of the oGTT, approximately 40 µl blood from *Vena facialis* was taken 30 min before and 15 min after the glucose administration and plasma was separated and frozen at -80 °C to determine insulin sensitivity. HOMA-IR was calculated as fasting glucose (mmol/l) × insulin (µU/ml)/22.5. Plasma insulin levels from *Vena facialis* were determined with an ELISA kit (Mercodia, Uppsala, Sweden) according to the manufacturer's instructions.

Briefly, 10 µl of calibrators, control and plasma samples were pipetted into pre-coated wells. 100 µl of enzyme conjugate was added to each well and plate was homogenized by shaking (700-900 rpm) for 2 h at RT. After six rinsing steps with wash buffer, 200 µl of substrate solution was added to each well and incubated for 15 min. Reaction was blocked by applying 50 µl of stop solution in every well. The

plate was then agitated for 5 sec to ensure mixing of all reagents and optical density was measured at 450 nm wavelength. Quantification was performed using the linear equation of the calibrator values.

3.9.2 Endotoxin concentration in portal vein plasma

Endotoxin levels in hepatic portal vein plasma of mice were quantified using a limulus amoebocyte lysate chromogenic endpoint assay for a concentration range of 0.015–1.2 EU/ml (Charles River, Ecully, France) as described previously [103]. Plasma samples were diluted 1:30 in endotoxin-free water, heated to 70 °C for 20 min and measured according to manufacturer's instructions. Measurements were conducted by Anika Nier from University of Vienna, Department of Nutritional Sciences, Molecular nutritional sciences, Prof. Bergheim.

3.9.3 Measurement of acute phase protein SAA

Serum amyloid A (SAA) levels in abdominal aorta plasma were quantified by ELISA (Immunology Consultant Laboratories, Portland, OR) according to manufacturer's instructions. Shortly, samples were diluted 1:1000 with dilution buffer and 100 µl of each sample and standard dilutions were added to designated wells. The plate was covered and incubated for 1 h at RT. After aspiration of supernatants, the plate was washed four times prior to adding 100 µl of enzyme antibody conjugate to each well. After an incubation period of 30 min in the dark, the plate was rinsed again four times with washing buffer. 100 µl of substrate solution was added to each well and the plate was incubated for 10 min. To interrupt the enzymatic reaction, 100 µl stop solution was added to each well. The absorbance was measured at 405 nm wavelength. Quantification of SAA quantification was performed using the linear equation of the standard dilutions.

3.9.4 Lipopolysaccharide binding protein (LBP) measurements

Lipopolysaccharide binding protein (LBP) concentrations in systemic plasma were measured using a LBP ELISA assay (Biometec, Greifswald, Germany). The samples were diluted 1:800 in dilution buffer and 100 µl of each sample and standard were applied to pre-coated plates according to the manufacturer's protocol. After 1 h incubation at RT under agitation (300 rpm), the plate was washed three times and 100 µl detection antibody was added to each well. The plate was then incubated for 1 h followed by three washing steps. 100 µl substrate solution was pipetted into each well followed by an incubation time of 12 min without shaking. After adding 100 µl stop solution, the plate was gently mixed and the absorbance at 450 nm with reference wavelength of 620 nm was measured. LBP concentrations were quantified by plotting optical densities of standard dilutions.

3.10 Gut permeability analysis

3.10.1 Transepithelial resistance and intestinal permeability

Immediately after dissection, segments of jejunum, distal ileum, proximal and distal colon were placed in ice-cold Krebs buffer (113.6 mM NaCl, 21 mM NaHCO$_3$, 5.4 mM KCl, 2.4 mM Na$_2$HPO$_4$, 1.2 mM CaCl$_2$, 1.2 mM MgCl$_2$, 0.6 mM NH$_2$PO$_4$, 10 mM glucose, pH 7.4) and then fixed on Sylgard® plates to open them longitudinally along the mesenteric border. Spread-out tissues were fixed with pins to transfer each intestinal segment into individual Ussing chambers (Warner Instruments, Hamden, CT, USA). Luminal and serosal surfaces of intestinal pieces were constantly exposed to carbogen-gassed Krebs buffer at 37 °C. Tissues were equilibrated for 45 min in the presence of 125 µM fluorescein (Sigma Aldrich, St. Louis, USA) on the luminal side. Transepithelial resistance (TER) was calculated from the tissue responses in the current clamp configuration after the equilibration period. At the end of the experiment, 100 µl of 1 M EGTA was applied in each Ussing chamber on both the luminal and serosal side to induce gut barrier breakage and to determine residual background TER, which was subtracted from 45 min TER values. Using the software 'Acquire and Analyze' (Physiological Instruments, San Diego, USA), TER values were recorded, analyzed and expressed as $\Omega * cm^2$ tissue.

For permeability measurements, fluorescence intensity of the serosal buffer was determined after 45 and 60 min of equilibration and then used to calculate paracellular permeability in cm per second. Fluorescence intensity was measured at wavelength 485/520 nm in a microplate reader, concentration of the paracellular marker was computed and flux (J) as well as permeability (P) were determined according to the following equations:

$$J \left[\frac{\mu M}{h * cm^2} \right] = \frac{(c_2 - c_1) * V}{(t_2 - t_1) * A}$$

c_1, c_2 = concentration on the serosal side at time point 1 respectively 2 [µM]
V = volume of the chamber [ml]
t_1, t_2 = time point 1 respectively 2 [h]
A = tissue area exposed to fluorescence marker [cm^2]

$$P \left[\frac{cm}{s} \right] = \frac{J}{c}$$

J = flux
c = difference of permeability marker concentration between luminal and serosal sides at time point 0 min [µM]

3.10.2 FITC Dextran permeability assay

One group of mice (see section 3.5) was removed from food and water for 6 h and then gavaged with 0.6 mg FITC dextran (4000 Da, Sigma) per g body weight dissolved in 1x PBS. Blood samples were collected 2 h post inoculation and centrifuged immediately at 2000 g for 10 min at 4 °C. Plasma

samples were then diluted 1:4 and the absorbance was measured with a fluorometer at 538 nm wavelength. A standard curve with serial dilutions of FITC dextran in PBS was used to determine plasma concentrations of FITC dextran.

3.11 Metagenomic DNA isolation from fecal and cecal contents

Frozen human fecal and murine cecal contents were thawed on ice, transferred to 2 ml screw cap tubes containing 500 mg zirconia/silica beads (0.1 mm; Carl Roth, Karlsruhe, Germany) and mixed with 600 µl stool DNA stabilizer (Stratec Biomedical, Birkenfeld, Germany). After addition of 250 µl 4 M Guanidinethiocyanat (Sigma Aldrich, St. Louis, USA) and 500 µl 5 % N-laurolylsarcosine (Sigma Aldrich), samples were homogenized for 60 min at 70 °C with constant shaking (700 rpm). Mechanical lysis of the samples was executed by using a bead-beater (3 times, 40 sec, 6.5 m/ sec) (FastPrep®-24, MP Biomedicals, Santa Ana, USA). 15 mg Poly(vinylpolypyrrolidone) (PVPP, Sigma Aldrich) was applied to each sample, followed by vortexing and centrifugation for 3 min at 15.000 x g and 4 °C.

The supernatant was transferred into a new 2 ml tube and again centrifuged for 3 min at 15.000 x g and 4 °C. 500 µl of the clear supernatant was applied to a new 2 ml tube, mixed with 5 µl RNase (stock concentration 10 mg/ ml; VWR International, Radnor, USA) and incubated for 20 min at 37 °C with constant shaking (700 rpm). Afterwards, DNA was extracted and purified using NucleoSpin® gDNA clean-up kit (Machery&Nagel, Düren, Germany). Briefly, 500 µl of each sample was mixed with 1500 µl of binding buffer, transferred to the provided clean-up columns and centrifuged at 10.000 x g for 30 sec. After three washing steps with 600 µl wash buffer, including 2 sec vortex and centrifugation for 30 sec at 11.000 x g, columns, were again centrifuged at 11.000 x g for 2 min. DNA was eluted with a total of 100 µl corresponding elution buffer with two 1 min centrifugation steps at 11.000 x g and DNA quantity and quality were measured by using NanoDrop® (Thermo Fisher Scientific, Waltham, USA).

3.12 High throughput 16S rRNA gene amplicon sequencing

For analysis of gut microbiota profiles, next generation sequencing (NGS) of 16S rRNA genes was conducted at the core facility microbiome unit NGS (TUM, Prof. Neuhaus) [141]. After DNA isolation (see section 3.11), the V3/V4 region of 16S rRNA genes was amplified (25 cycles) from 12 ng of metagenomic DNA by using primer 341F and 785R [142], followed by a 2-step procedure to limit amplification bias [143]. Libraries were double-barcoded (8-nt index sequence on each forward and reverse primer). Amplicons were purified using the AMPure XP system (Beckmann Coulter, Brea, USA), pooled in an equimolar amount, and sequenced in paired-end modus (PE275) using a MiSeq sequencer (Illumina, San Diego, USA) following the manufacturer's instructions.

Raw sequence reads were then processed using IMNGS approach [144], an in-house program based on UPARSE [145]. In brief, sequences were demultiplexed (allowing a maximum of 2 errors in

barcodes), trimmed to the first base with a quality score <3, and then paired. Sequences with <300 and >600 nucleotides and paired reads with an expected error >3 were excluded from the analysis. Remaining reads were trimmed by 5 nucleotides on each end. Operational taxonomic units (OTUs) were picked at a threshold of 97 % similarity. Only those OTUs with a relative abundance above 0.5 % total reads in at least one sample were kept. The RDP classifier [146] was used to assign taxonomy. Further analysis was performed in the R programming environment using in-house developed pipeline Rhea [147]. All details of the analysis and the scripts are available online (https://lagkouvardos.github.io/Rhea/). For estimation of diversity within samples (alpha-diversity), species richness and Shannon-effective counts were calculated as described by Jost *et al.* [148]. Diversity between species (beta-diversity) was determined based on generalized UniFrac distances [149]. EzTaxon classification [150] was used to identify specific OTUs with differential abundances between groups.

3.13 RNA isolation

3.13.1 Liver

450 µl RA1 buffer (Macherey-Nagel) supplemented with 10 mM DTT (Sigma Aldrich) was added to 30 mg of frozen liver tissue, which was homogenized with a plastic pastille. The samples were loaded onto QIAshredder columns (QIAGEN) and centrifuged for 2 min at maximum speed. The flow-through was used for RNA isolation according to the manufacturer's instructions (NucleoSpin® RNAII kit; Macherey-Nagel). RNA was eluted in 60 µL RNase-free water and RNA concentration and quality were measured using NanoDrop® (Thermo Fisher Scientific).

3.13.2 Jejunum

400 µl RA1 buffer (Macherey-Nagel), supplemented with 10 mM DTT (Sigma Aldrich), was added to 50 mg frozen jejunal tissue. The tissue was smashed with a plastic pastille and then stored at -80°C for at least 24 h. The samples were further homogenized using a 0.9 mm syringe needle and loaded onto QIAshredder columns (QIAGEN). The flow-through was used for RNA isolation according to the manufacturer's instructions (NucleoSpin® RNAII kit; Macherey-Nagel). RNA was eluted in 40 µL RNase-free water and RNA concentration and quality were measured using NanoDrop® (Thermo Fisher Scientific).

3.13.3 White adipose tissue (WAT)

100 mg of epididymal (e) WAT was diluted in 1 ml of Isol-RNA lysis reagent (5 Prime/VWR), homogenized using Ultra-Turrax (Art-Miccra D-1, ART modern Labortechnik) for 20 sec and incubated 5 min at RT. After centrifugation at 2500 g for 5 min, the homogenates were taken off through the fat phase. 200 µl ice cold chloroform (Carl Roth) was added, the samples were mixed thoroughly for 15 sec

and incubated for 2 min at RT. The samples were then centrifuged for 15 min at 12.000 x g and 4 °C to obtain the aqueous RNA-containing phase. The aqueous phase was then transferred to a new eppendorf tube and the RNA was isolated according to the manufacturer's instructions (Direct-zol RNA MiniPrep, Zymo Research). Concentration and quality of the RNA were measured using NanoDrop® (Thermo Fisher Scientific).

3.13.4 Reverse transcription (RT) PCR and quantitative real-time PCR (qPCR)

Complementary DNA (cDNA) was synthesized from 500 ng (eWAT) or 1000 ng (jejunum, liver) RNA template in 13 µl PCR-grade H_2O using random hexamers and M-MLV RT Point Mutant Synthesis System (Promega, Madison, USA) (Table 3).

Table 3: Reagents and protocol for RT-PCR.

Components	Volume per sample
mRNA (500 or 1000 ng)	x µl
Random-Hexamer [200ng/µl]	1 µl
PCR grade H_2O	up to 14 µl
5 min 70°C	
Cool down to 4°C for 5 min.	
5x 1. Strang Puffer (Promega)	5µl
PCR grade H_2O	3,1 µl
rRNasin® (Promega)	0,65 µl
dNTP Mix 10mM	1,25µl
M-MLV (200U/µl) (Promega)	1µl
10 min 25°C	
50 min 48°C	
15 min 70°C	
Store at 10°C	

Table 4: Primer sequences used for qPCR.

Gene name	Forward primer	Reverse primer
IL-6	tgatggatgctaccaaactgg	ttcatgtactccaggtagctatgg
IFNγ	cctttggaccctctgacttg	agcgttcattgtctcagagcta
IL-1ß	tgtaatgaaagacggcacacc	tcttctttgggtattgcttgg
SAA	atgctcgggggaactatgat	acagcctctctggcatcg
TNF	tgcctatgtctcagcctcttc	gaggccatttgggaacttct
MCP-1	catccacgtgttggctca	gatcatcttgctggtgaatgagt
LBP	ccctgaccccagagtcct	aggatgggacggagtcaag
F4/80	cctggacgaatcctgtgaag	ggtgggaccacagagagttg
Leptin	caggatcaatgactttcacaca	gctggtgaggacctgttgat
Occludin	cacgacaggtggggagtc	ttgatctgaagtgataggtggatatt
ZO-1	aggcagctcacgtaggtctc	ggttttgtctcatcatttcttcag
Housekeeper		
Rpl13a	atccctccaccctatgacaa	gccccaggtaagcaaactt
GAPDH	gggttcctataaatacggactgc	ccattttgtctacgggacga
HPRT	tcctcctcagaccgctttt	cctggttcatcatcgctaatc

To examine gene expression levels, quantitative real-time PCR was performed using the LightCycler® 480 system (Roche Diagnostics, Mannheim, Germany) with 200 nM Probe, 400 nM forward and reverse primer, 2x Probe Master Mix (Agilent Technologies, Santa Clara, USA) and 1 µl cDNA. Primers and probes were designed using the universal probe library (Roche) (Table 4).The relative induction of mRNA expression was calculated using the equation $2^{-\Delta\Delta Cp}$ [151] and normalized to the expression of the geometric mean of *gapdh*, *rpl13a* and *hprt.* Data were expressed as fold-changes against mice associated with lean microbiota fed with CD.

3.14 Western Blot analysis

20 mg of jejunal tissue was lysed in 200 µl lysis buffer, homogenized using ultrasound (0.5 Hz, 40 µm amplitude) and protein concentration was determined with Pierce 660 nm Protein Assay (Thermofisher Scientific, Waltham, MA) following the instructions of "Microplate Procedure" (working range 50–2000 µg/mL) of the producer's protocol. Afterwards, protein lysates were heated in Laemmli buffer at 70 °C for 10 min, separated by size in SDS-polyacrylamide gel and transferred by electroblotting to a polyvinylidene difluoride membrane. Anti-occludin (1:2000; Sigma-Aldrich, St. Louis, USA) and anti-β-Actin (1:5000; Cell signaling, Cambridge, UK) antibodies diluted in 0.2 % ECL Prime Blocking Reagent (GE Healthcare, Buckinghamshire, UK) were used to bind immunoreactive proteins of interest. For detection, the appropriate HRP-coupled secondary antibody (goat anti-rabbit IgG, Dianova, Hamburg, Germany) was diluted 1:10000 using an enhanced chemiluminescence light detecting system with ECL Prime Western Blotting Detection Reagent (GE Healthcare, Buckinghamshire, UK). Quantification of protein expression was conducted with the 'Quantity One 1D Analysis Software' (BioRad, Munich, Germany).

3.15 Fat histology and adipocyte size measurements

Formalin-fixed epididymal adipose tissue samples were embedded in paraffin and cut in sections of 5 µm using a rotary microtome (Leica R2252, Leica Microsystems, Wetzlar, Germany). Then, slices were transferred to SuperFrost® microscope slides and dried overnight. On the next day, sections were incubated at 60 °C for 15 min and stained with hematoxylin and eosin (H&E) using a multistainer station (LeicaST5020, Leica Microsystems) and covered with embedding medium (Carl Roth). Stained sections were scanned using Digital microscope M8 (PreciPoint GmbH, Freising, Germany). The mean relative proportion and mean surface area of the adipocytes were estimated by Digital microscope M8 combined with a program, which measured the size of the adipocytes called AdipocyteAnalyser (img.ai UG (haftungsbeschränkt), Munich, Germany).

3.16 Histology and immunohistochemistry of liver

Liver histology of 2 µm H&E stained sections (see section 3.15) was assessed by scoring photomicrographs at University of Vienna, Department of Nutritional Sciences (Prof. Bergheim) as previously described [152]. Briefly, liver sections were judged using the semi quantitative 'Nonalcoholic Steatohepatitis Clinical Research Network System for Scoring Activity and Fibrosis in Nonalcoholic Fatty Liver Disease' (modified from [153]). According to this system, scores were as follows: steatosis grade, 0: <5 %, 1: 5–33 %, 2: 34–66 %, 3: >66 %; lobular inflammation, 0: none, 1: <2, 2: 2–4, 3: 4; hepatocellular ballooning, 0: none, 1: few ballooned cells, 2: many ballooned cells. To determine means, the counts from 8 fields of each tissue section were used. 4 µm sections of TissueTek (FisherScientific, Schwerte, Germany) embedded liver slices were used to stain with SudanRed at the German Cancer Research Center, Division of Chronic Inflammation and Cancer, Heidelberg, Germany (Prof. Heikenwälder). Afterwards, SudanRed positive area was calculated using SudanRedAnalyzer (img.ai UG). Images were generated using Digital microscope M8 (PreciPoint GmbH).

3.17 Short chain fatty acids

Colon contents were weighed and then prepared and analyzed at the chair of food chemistry and molecular sensory science (Technical University of Munich, Freising, Germany) as described previously [154].

3.18 Statistics

All statistical tests were performed with GraphPad Prism (GraphPad Software version 7.0, San Diego, USA).

Experiment 1: To compare dietary effects, we used unpaired, parametric t-test. Differences between feeding groups were considered significant if p-values were $< 0.05(*)$, $< 0.01(**)$ or $< 0.001(***)$. One-way ANOVA followed by Tukey's multiple comparison test was applied to compare donor effects within the same feeding group. Therefore, squares referred to p-values $< 0.05(\blacksquare)$, $< 0.01(\blacksquare\blacksquare)$ or $< 0.001(\blacksquare\blacksquare)$. Data are shown as means ± standard deviation (SD).

Experiment 2: We used unpaired, parametric t-test to compare donor effects and one-way ANOVA followed by Tukey's multiple comparison test to compare differences between colonization periods within the same human donor. Differences between human donors were considered significant if p-values were $< 0.05(*)$, $< 0.01(**)$ or $< 0.001(***)$, when not elsewhere indicated. Squares represented colonization effects and referred to p-values $< 0.05(\blacksquare)$, $< 0.01(\blacksquare\blacksquare)$ or $< 0.001(\blacksquare\blacksquare\blacksquare)$. Data are depicted as means ± SD.

Experiment 3: Unpaired, parametric t-test was utilized to compare dietary group effects. Differences between diets were considered significant if p-values were < 0.05(*), < 0.01(**) or < 0.001(***), when not elsewhere indicated. Data are shown as means ± SD.

4 Results

4.1 Human donor characteristics

To establish a humanized mouse model of obesity, we selected human donors from a controlled FMT-study based on their metabolic parameters. The 'lean' human donor, which underwent RYGB surgery, showed overall normal metabolic parameters without pathological findings (Table 1). Compared to the selected obese donors termed preFMT^{lean}, postFMT^{lean}, preFMT^{but} and postFMT^{but}, the lean donor displayed distinctly lower body weight, BMI, fasting insulin, triglycerides and HOMA-index, while no differences were detected in glycated hemoglobin HbA1c. Glucose levels of the lean donor were indistinguishable to preFMT^{lean} and postFMT^{lean}, but lower compared to preFMT^{but} and postFMT^{but} donors. Additionally, the level of high-density lipoprotein (HDL) was higher in the lean donor compared to obese counterparts.

We selected two obese patients that underwent either allogenic or autologous FMT and showed both an improvement of metabolic parameters after treatment. The participant named as preFMT^{lean} (120.4 kg; BMI 41.7 kg/m^2), who received allogenic FMT from the lean patient described above, showed a body weight loss of approximately 1.5 % (postFMT^{lean}; 118.6 kg), but was still classified as 'very severely obese' in terms of BMI (41 kg/m^2) after FMT. While HbA1c and fasting glucose levels did not change, triglyceride levels improved from 'borderline high risk' for cardiovascular disease (CVD) before transplantation to 'normal range' after treatment. Patient preFMT^{lean} showed pathologically elevated levels of C-reactive protein (CRP), insulin and HOMA-IR as well as low HDL values and was still defined as insulin resistant after transplantation (postFMT^{lean}). However, inflammatory marker (CRP) and HOMA-IR values including fasting insulin improved remarkably after FMT therapy (Table 1).

The second selected patient termed preFMT^{but} (119.0 kg; BMI 32.6 kg/m^2), who got an oral bolus of sodium butyrate tablets once daily followed by an autologous fecal transplantation, recorded a body weight loss of 2.2 % (postFMT^{but}; 116.4 kg), but was still classified as 'moderately obese' according to the BMI (31.9 kg/m^2). The participant showed normal HbA1c and triglyceride levels both before and after FMT, while HDL and glucose values displayed a risk for CVD and fasting glucose levels were impaired. CRP values improved from a near 'acute risk' before FMT therapy to a 'great risk' for CVD after FMT therapy. The HOMA-IR including fasting insulin level also decreased after FMT intervention. However, the patient was still classified as insulin resistant (Table 1).

4.2 Fecal microbiota transfer from lean and obese patients to mice and HFD challenge

To verify the hypothesis that the human phenotype is transmissible to mice by FMT, male GF wildtype mice were colonized with fecal samples from obese and insulin resistant patients, referred to as preFMT^{lean}, postFMT^{lean}, preFMT^{but} and postFMT^{but}, to establish a humanized mouse model for metabolic disorders. Mice associated with microbiota of a lean human donor served as control (lean).

To investigate the metabolic effect of colonization with obese human microbiota, one group of mice from each colonization group was perpetually fed with CD and sacrificed 12 weeks after fecal transplantation. The second group of mice was switched to HFD 4 weeks prior to sampling to elucidate the metabolic effect of a dietary challenge in different microbial environments (Figure 5; **Experiment 1**).

4.2.1 Stable colonization of GF mice with complex human microbiota

Mice were colonized with a single gavage of human fecal supernatant at the age of 4 weeks. One week after colonization, all mice showed a comparable colonization density of 8 x 10^{10} to 5 x 10^{11} colony forming units (CFU) per gram feces, which remained stable within the next weeks (Figure 6A). CFUs in ileal, cecal, colonic contents as well as feces were determined at sampling day and revealed colonization densities from 10^8 CFU/g in ileum to 10^{11} CFU/g in cecum, colon and feces. In the ileum, all association groups showed similar colonization densities. In cecum and colon, lean-mice fed CD showed significantly lower colonization density than the two corresponding preFMT-mouse groups. Colonization densities in feces did not fully reflect the results obtained for colonic content. Lower colonization densities in lean-associated CD-fed-mice were not observed. Furthermore, postFMT^{lean}-mice on both diets showed significantly lower CFU numbers than preFMT^{but}- and postFMT^{but}-association groups (Figure 6B–E). **Taken together, all mice were stably colonized along the entire gastrointestinal tract throughout the experiment.**
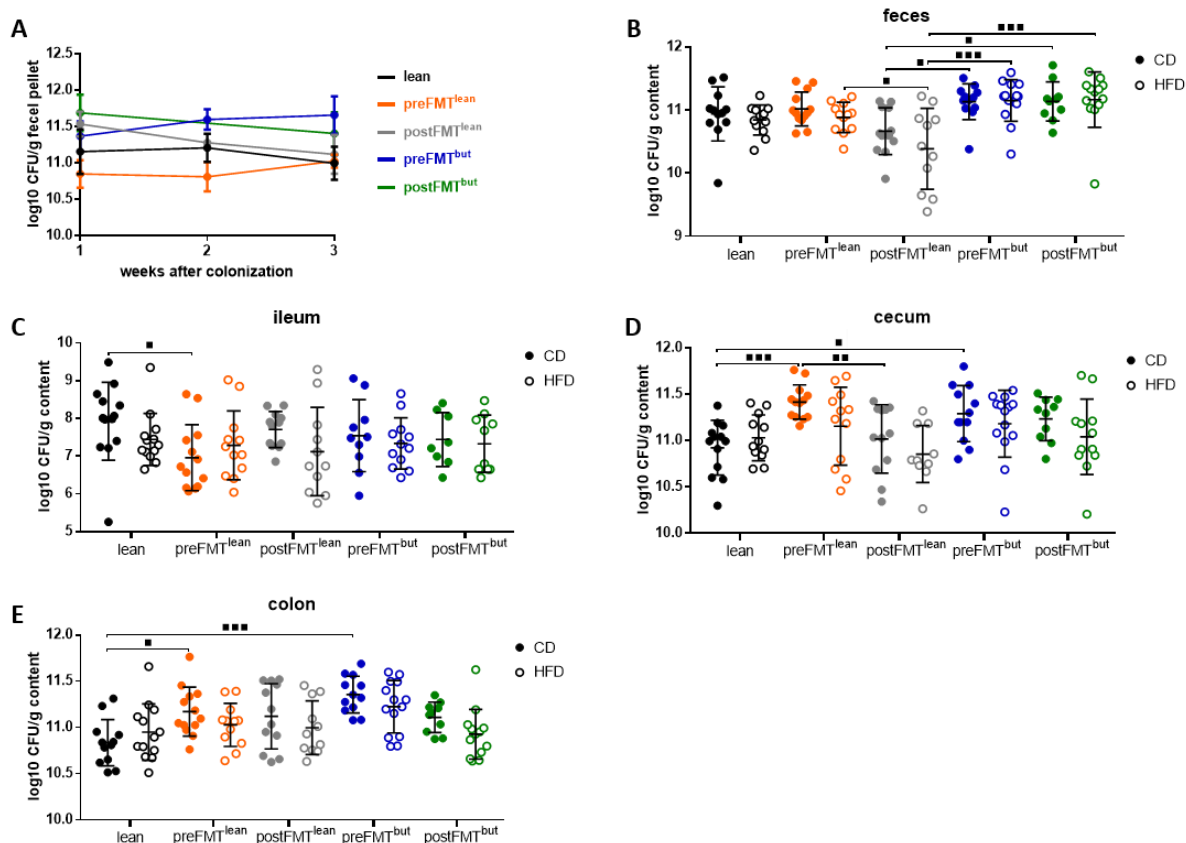
Figure 6: Mice were sufficiently and stably colonized with complex human microbiota.
(A) Colonization density in mouse feces shown as log10 CFU/g. Analyzed samples were taken at week one, two and three of association. CFU/g at week 12 of colonization in **(B)** fecal, **(C)** ileal, **(D)** cecal and **(E)** colonic content. Statistics: ▪p< 0.05; ▪▪p< 0.01; ▪▪▪p< 0.001; One-way ANOVA followed by Tukey's to compare donor effects within the same feeding group (3.18). Data are shown as means ± SD. N = 10-14 per group. CD – control diet. HFD – high-fat diet. CFU – colony forming units. SD – standard deviation. N – number of mice measured.

4.2.2 Obesity and insulin resistance are not transferable from human to mice

Looking at mice, that were exclusively fed CD and colonized with lean-microbiota, showed the same weight development as animals treated with obese microbiota (Figure 7A). Body weight curve of preFMT^{but}-mice was lower compared to the other colonization groups, but this could be explained by lower cumulative food intake (Figure 7D). Also, in contrast to human donors, final body mass of mice at sampling date was not distinguishable between colonization groups. This applied to both the CD and HFD feeding mouse groups (Figure 7B). When comparing feeding groups, mice fed HFD gained significantly more body weight accompanied by a higher energy intake than CD-fed animals (Figure 7B, D). To determine the direct effect of HFD on body weight, the gain in body mass was calculated. However, no donor-specific differences were observed between colonization groups on the same diet (Figure 7C).
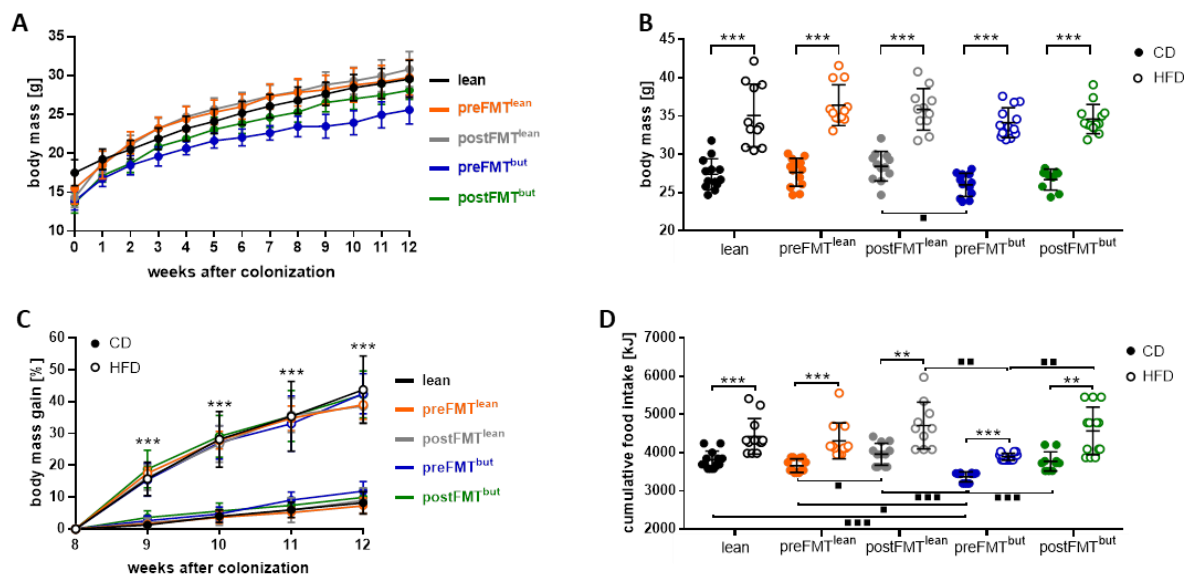
Figure 7: Obese phenotypes from patients were not transferable into mice, but HFD induced obesity regardless of human donor.
(A) Body mass development from 0 to 12 weeks after colonization. **(B)** Body mass measurements after 12 weeks of association. **(C)** Body weight gain (%) after switch to CD or HFD from week 8 to 12 after colonization. **(D)** Cumulative food intake (kJ) after 12 weeks of feeding. Statistics: *p< 0.05; **p< 0.01; ***p< 0.001; unpaired, parametric t-test to compare dietary effects within the same colonization group; ■p< 0.05; ■■p< 0.01; ■■■p< 0.001; One-way ANOVA followed by Tukey's to compare donor effects within the same feeding group (3.18). Data are shown as means ± SD. N = 10-14 per group. CD – control diet. HFD – high-fat diet. SD – standard deviation. N – number of mice measured.

We further analyzed whether the phenotype of insulin resistance from human donors were transferable to gnotobiotic mice. Oral glucose tolerance was reduced in HFD-fed mice compared to mice receiving CD, as indicated by significantly increased AUC in lean-, preFMT[lean]- and postFMT[but]-colonization groups and mildly increased AUC in postFMT[lean]- and preFMT[but]-groups (Figure 8A–F). In a second group of mice (FITC-dextran mouse group, see section 3.10.2) fasting glucose levels increased in preFMT[lean]-, postFMT[lean]- and preFMT[but]-groups. However, lean- and postFMT[but]-mice showed no differences in glucose parameters (Figure 8G).

Regarding fecal association groups, preFMT[lean]-recipients fed HFD displayed the highest response to a glucose bolus compared to mice colonized with butyrate-treated microbiota. In addition, preFMT[lean]-animals also showed increased glucose levels compared to lean- and postFMT[but]-groups (Figure 8F, G). HFD feeding resulted in higher insulin concentrations before and after glucose treatment in all association groups. Insulin resistance indices (HOMA-IR), which are based on fasting glucose and insulin levels, were significantly increased in postFMT[lean]-, postFMT[but]- and postFMT[but]-recipients and elevated in animals colonized with lean- and preFMT[lean]-microbiota. Insulin secretion was also slightly affected by diet, as HFD-fed mice showed higher levels of Δinsulin, but alterations were only significant for postFMT[lean]-mice. Differences between association groups were only seen between CD-fed lean-

and preFMT[lean]-recipients by a slight increase in HOMA-indices and insulin secretion in animals colonized with obese microbiota. No differences in insulin levels were observed between mice colonized with pre- and postFMT[but]-microbiota (Figure 8H-J).
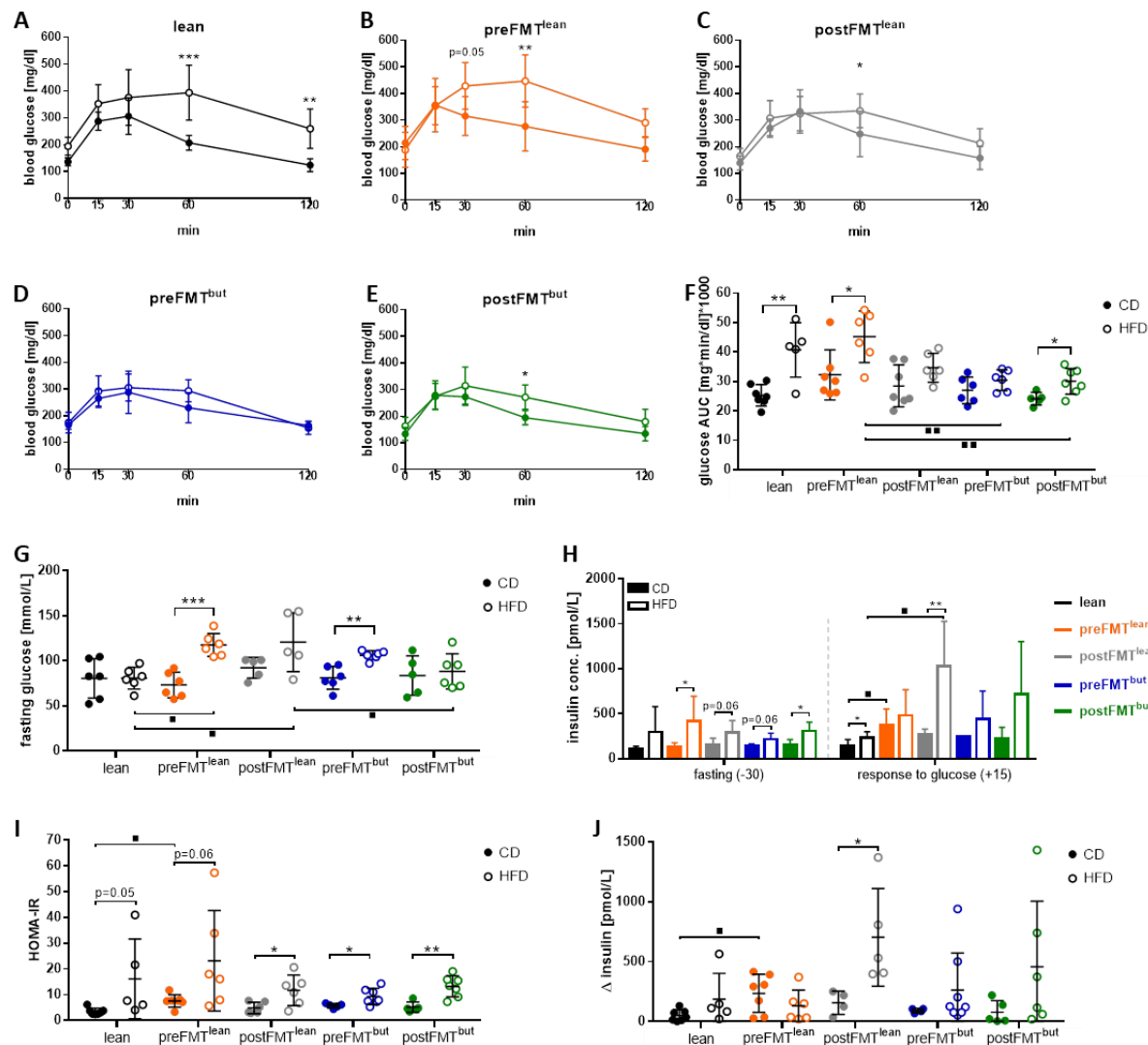

Figure 8: Phenotypes of insulin resistance are not transferable from human to mouse by microbiota transfer, but HFD interfered with mouse metabolism.
All measurements were performed 12 weeks after colonization. oGTTs (2 mg glucose per kg body mass) of **(A)** lean-, **(B)** preFMT[lean]-, **(C)** postFMT[lean]-, **(D)** preFMT[but]-, **(E)** postFMT[but]-associated mice after a 6-hour fasting period and **(F)** calculated AUC. **(G)** Fasting blood glucose levels measured after a 6-hour fasting period in FITC-dextran mouse groups (see section 3.10.2). **(H)** Fasting plasma insulin levels (-30) and values 15 minutes after oral glucose administration (+15) in oGTT-mouse groups. **(I)** HOMA-IR included fasting glucose and insulin values. **(J)** Glucose-induced insulin secretion after glucose administration. Statistics: $*p < 0.05$; $**p < 0.01$; $***p < 0.001$; unpaired, parametric t-test to compare dietary effects within the same colonization group; ▪$p < 0.05$; ▪▪$p < 0.01$; ▪▪▪$p < 0.001$; One-way ANOVA followed by Tukey's to compare donor effects within the same feeding group (3.18). Data are shown as means ± SD. N = 4-7 per group. CD – control diet. HFD – high-fat diet. oGTT – oral glucose tolerance test. AUC – area under the curve. Conc. – concentration. HOMA-IR – homeostatic model assessment of insulin resistance. SD – standard deviation. N – number of mice measured.

Overall, the phenotypic differences in body weight as well as glucose and insulin levels of human donors could not be transferred to colonized mice (Figure 7; Figure 8; Table 1). Phenotypic differences in weight, glucose tolerance and insulin resistance were only triggered by high-fat feeding, but not by different microbial environments.
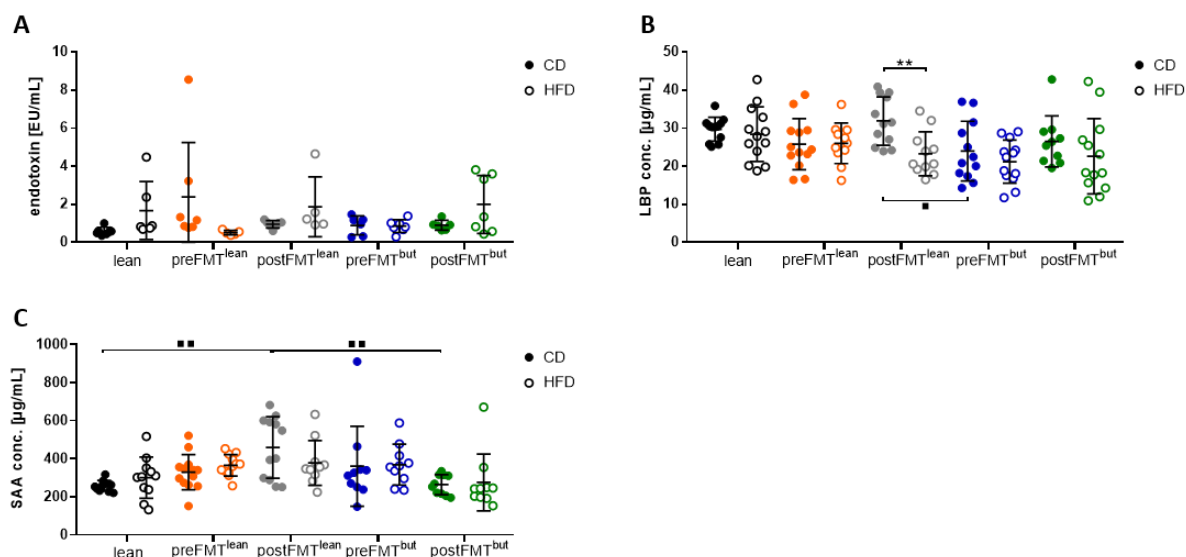

Figure 9: Colonization with obese human microbiota did not induce endotoxemia and systemic inflammation in mice.
All measurements were performed 12 weeks after colonization. **(A)** Endotoxin levels in portal vein plasma. N = 4-7 per group. **(B)** LBP protein and **(C)** SAA levels in systemic plasma. N = 10-13 per group. Statistics: *p< 0.05; **p< 0.01; ***p< 0.001; unpaired, parametric t-test to compare dietary effects within the same colonization group; ▪p< 0.05; ▪▪p< 0.01; ▪▪▪p< 0.001; One-way ANOVA followed by Tukey's to compare donor effects within the same feeding group (3.18). Data are shown as means ± SD. CD – control diet. HFD – high-fat diet. Conc. – concentration. LBP – lipopolysaccharide binding protein. SAA – serum amyloid A. SD – standard deviation. N – number of mice measured.

As metabolic endotoxemia - defined as moderate increase in plasma LPS levels - is linked to metabolic disease [82], we determined LPS concentration in portal vein plasma. Endotoxin levels as marker for development of metabolic syndrome were not influenced by diet or human microbiota composition (Figure 9A). Accordingly, LPS binding protein (LBP) levels in systemic plasma as well as the levels of acute phase protein serum amyloid A (SAA) were similar for all dietary and colonization groups. Only postFMT[lean]-recipients showed mildly increased LBP levels compared to preFMT[but]-mice and elevated SAA values compared to lean-, preFMT[but]- and postFMT[but]-groups (Figure 9B, C). **Taken together, the differences in inflammatory status in human donors were not transferable to mice by microbiota transplantation.**

4.2.3 Microbiota composition changes after the transfer from human to mice

In order to evaluate the success of the transfer of complex human microbiota to GF mice, we analyzed the engraftment efficiency. 16S rRNA gene amplicon analysis was performed to assess the alpha-diversity and microbial composition of human fecal donor microbiota and recipient mouse microbiota. We observed a loss of bacterial species richness and Shannon effective counts in all association groups when transferring human stool to mice (Figure 10A, B). The greatest drop in richness after microbiota transfer was observed for the lean-mouse group with a loss of 42 % of bacterial species, followed by preFMT^{lean}- and postFMT^{lean}-mice with 39 % and 36 % species loss, respectively. The transfer of preFMT^{but}- and postFMT^{but}-microbiota resulted in a loss of 26 % and 30 % species, respectively.

Looking at bacterial richness in colonized mice, CD-fed preFMT^{but}-animals showed significantly more bacterial species than all other colonization groups. An effect of HFD feeding was observed only for preFMT^{but}- and postFMT^{but}-groups with a decrease of 5 % of bacterial species under HFD (Figure 10A).

Shannon effective counts, which additionally take into account the evenness of bacterial species, also dropped remarkably (with a loss of about 44 % of bacteria) in all obese microbiota mouse groups compared to the respective human donors. Recipients of lean-microbiota had only half the number of species detected in the human donor. Lean- and preFMT^{lean}-mice showed higher Shannon counts than all other groups. The only effect of HFD feeding on Shannon effective counts was a higher number of bacterial species in the postFMT^{lean} HFD-group compared to CD-fed mice (Figure 10B).

Beta-diversity indicates the similarity of different microbial profiles. UniFrac distances, which additionally take into account the abundances of bacterial species, showed a transfer efficiency of about 50 to 60 % for all association groups, which indicates an incomplete engraftment of fecal human microbiota to mice. The lowest similarity between mouse microbiota and the respective human donor microbiota was detected for lean- and preFMT^{lean}-groups, while pre- and postFMT^{but}-groups showed highest similarity. HFD negatively influenced the similarity of microbial profiles in lean- and pre-/postFMT^{but}-groups, which was not the case for pre-/postFMT^{lean}-colonization groups (Figure 10C).

Furthermore, beta-diversity analysis showed that the relative abundances of bacterial phyla in recipients differed from those of the respective human donors. Independent of the association groups, FMT resulted in a loss of Actinobacteria and Firmicutes in favor of Verrucomicrobia, Bacteriodetes and Proteobacteria.

Compared to the human donor, mice showed about 1.5-fold higher levels of Bacteroidetes and Proteobacteria, as well as two-fold higher abundances of Verrucomicrobia. On the other hand, Firmicutes and Actinobacteria were two-fold and more than three-fold decreased, respectively,

compared to human feces. Only postFMT[but]-mice showed similar numbers of Actinobacteria as the respective human donor (Figure 10D).
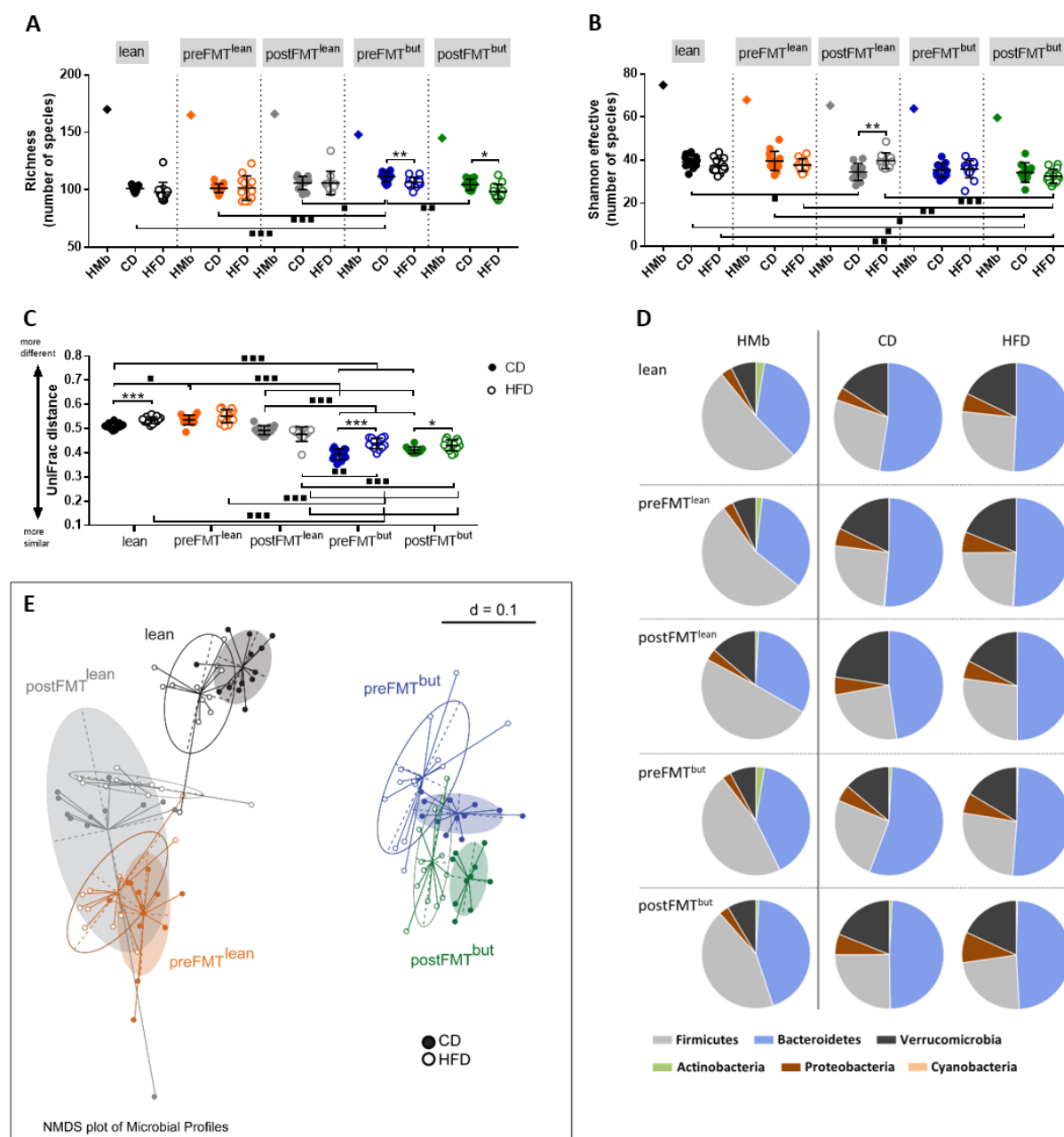

Figure 10: Transplantation of human microbiota into germfree mice resulted in incomplete transfer of donor microbiota.

All measurements were performed 12 weeks after colonization. Number of bacterial species depicted as **(A)** richness and **(B)** Shannon effective in HMb and corresponding mice. **(C)** Transfer efficiency from human to mice displayed by UniFrac distances. **(D)** Relative abundances of bacterial phyla in HMb and corresponding mice. **(E)** NMDS plot of microbial profiles showing distances in colonized mice. Statistics: *p< 0.05; **p< 0.01; ***p< 0.001; unpaired, parametric t-test to compare dietary effects within the same colonization group; ▪p< 0.05; ▪▪p< 0.01; ▪▪▪p< 0.001; One-way ANOVA followed by Tukey's to compare donor effects within the same feeding group (3.18). Data are shown as means ± SD. N = 10-14. CD – control diet. HFD – high-fat diet. HMb – human microbiota. NMDS – non-metric multidimensional scaling. SD – standard deviation. N – number of mice measured.

In humans, the treatment with autologous or allogenic stool resulted in a >2.5-fold decrease in Actinobacteria levels. In line with this, we observed a lower number of Actinobacteria in postFMT[but]-compared to preFMT[but]-mice. However, a similar effect could not be detected in mice colonized with FMT[lean]-microbiota, which can be explained by the low abundance of Actinobacteria in the mice (approximately below 0.1%). It is noteworthy that HFD feeding did not influence microbial composition on phylum level and bacterial diversity as well as Firmicutes to Bacteroidetes ratio in mice (Figure 10D).

The analysis of phylogenetic distances, as shown by a NMDS plot, revealed only significant differences between CD and HFD for preFMT[lean]- and postFMT[but]-groups, all other colonization groups were not affected by diet. The focus on bacterial composition in relation to association groups showed differences between pre and post autologous FMT (pre-/postFMT[but]) treatment, but surprisingly not between allogenic FMT groups (pre-/postFMT[lean]). The NMDS plot also revealed that each individual human donor shaped its own significant microbiome in recipients, independently of the treatment status (Figure 10E).

The recipients developed a stable microbiota after FMT. Yet, composition analyses revealed alterations between fecal mouse and human donor samples with respect to relative abundances. A look at lower taxonomic levels showed that OTUs, which were highly present in humans, were mostly not detectable in mice and *vice versa* (Figure 11A-E). Regardless of human donor-groups, mice lost most of the OTUs belonging to *Ruminococcaceae* and *Lachnospiraceae* families. Among *Ruminococcaceae*, *Faecalibacterium prausnitzii*, one of the most abundant commensal and anti-inflammatory bacteria in healthy humans were detected in patients, but not in mice [155, 156]. In contrast, two other OTUs of the *Lachnospiraceae* and *Bacteroidaceae* family, were below detection level in humans of 0.5% relative abundance, but were present in mice, independent of the donor. Interestingly, OTUs occurring in both - human and mouse groups - mainly belonged to *Bacteroidaceae, Porphyromonadaceae and Rikenellaceae* families with similar relative abundances. *Akkermansia muciniphila*, known as commensal strain inversely correlated with inflammation (IBD) and obesity [157-160], was detected in high relative abundances (Figure 11F).

A

lean

B

preFMT^lean

C

postFMT^lean

D

preFMT^but

E
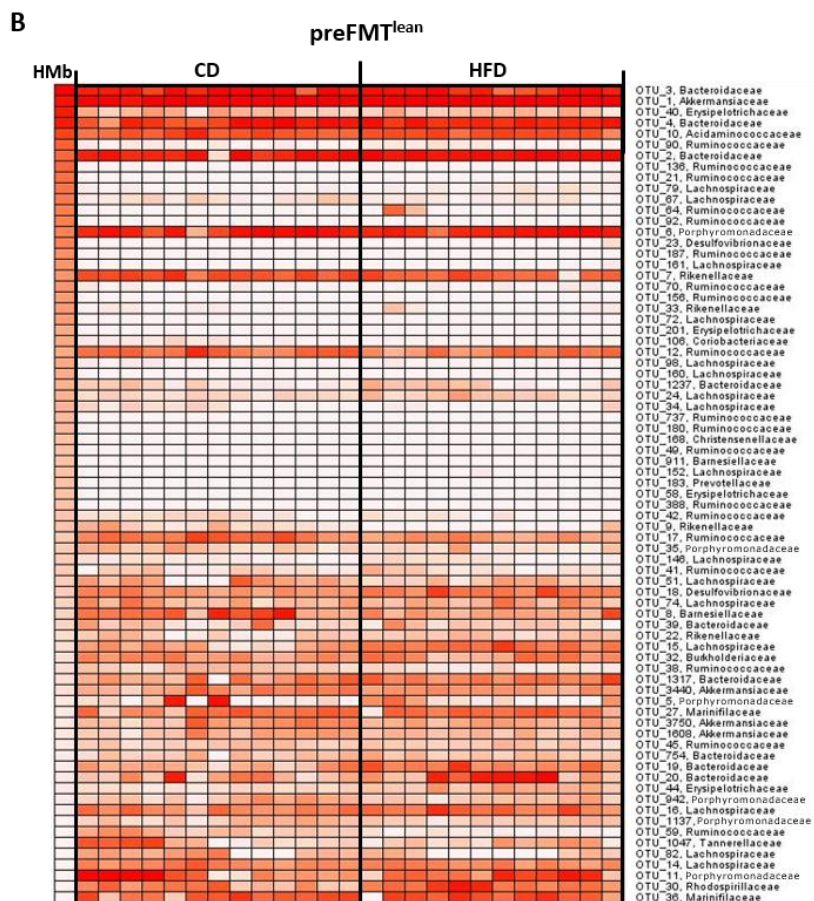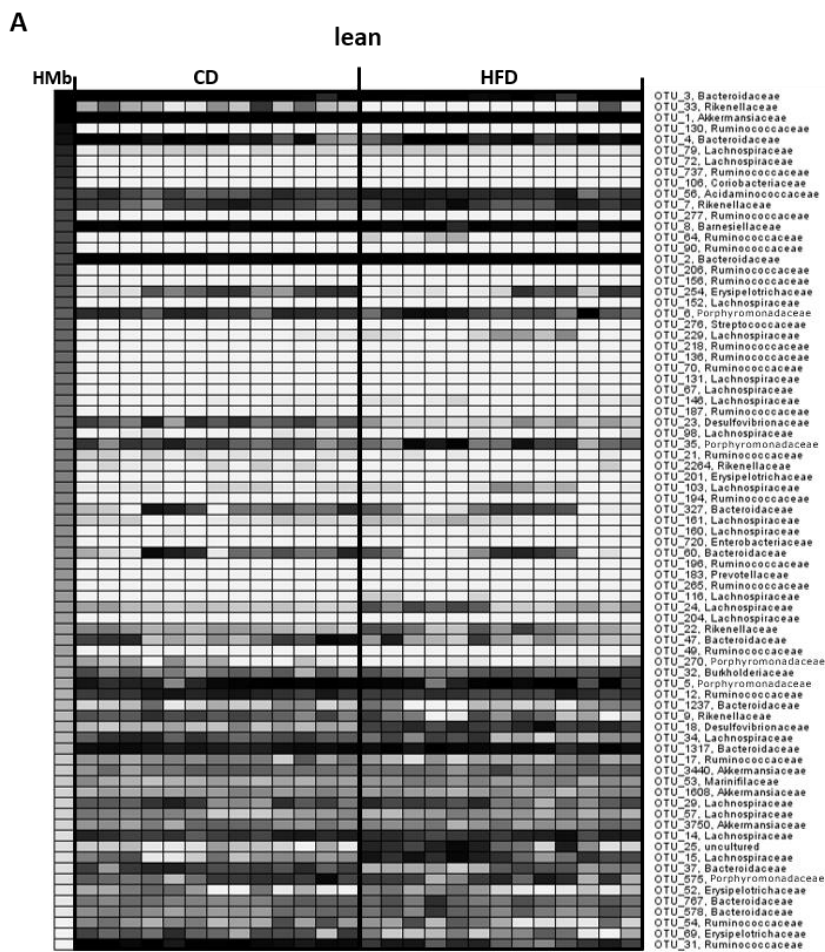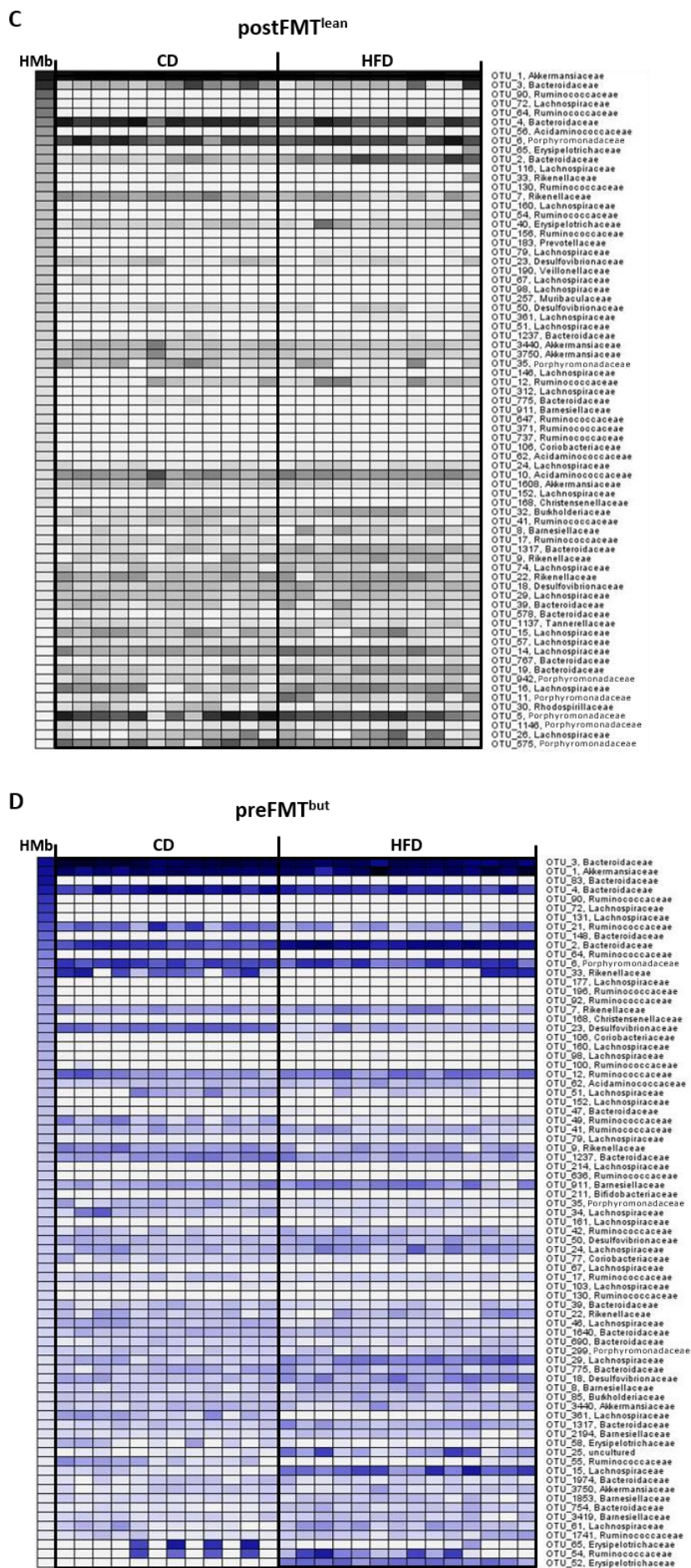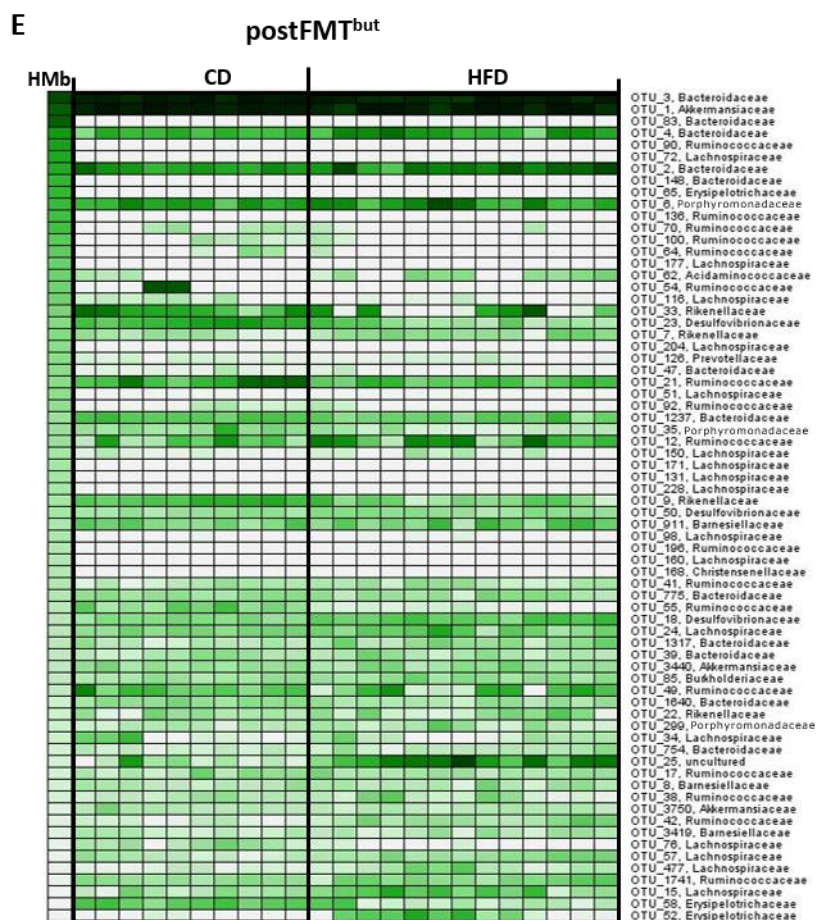
F

OTUs	Family level	Sequence similarity [%]	Closest match
TOP OTUs human only			
OTU_64	*Ruminococcaceae*	99.1	*Gemmiger formicilis*
OTU_72	*Lachnospiraceae*	99.3	*Agathobacter rectalis*
OTU_90	*Ruminococcaceae*	98.8	*Faecalibacterium prausnitzii*
OTU_98	*Lachnospiraceae*	99.1	*Fusicatenibacter saccharivorans*
OTU_160	*Lachnospiraceae*	99.5	*Blautia wexlerae*
TOP OTUs mice only			
OTU_15	*Lachnospiraceae*	99.1	*Hungatella hathewayi*
OTU_1317	*Bacteroidaceae*	97.1	*Bacteroides massiliensis*
TOP OTUs shared			
OTU_1	*Akkermansiaceae*	99.5	*Akkermansia muciniphila*
OTU_2	*Bacteroidaceae*	98.9	*Bacteroides massiliensis*
OTU_3	*Bacteroidaceae*	98.7	*Bacteroides vulgatus*
OTU_4	*Bacteroidaceae*	99.1	*Bacteroides thetaiotaomicron*
OTU_6	*Porphyromonadaceae*	98.9	*Parabacteroides distasonis*
OTU_7	*Rikenellaceae*	99.1	*Alistipes putredinis*
OTU_9	*Rikenellaceae*	99.1	*Alistipes inops*
OTU_35	*Porphyromonadaceae*	99.1	*Parabacteroides johnsonii*

Figure 11: The fecal microbiota composition of lean, preFMT[lean], postFMT[lean], preFMT[but] and postFMT[but] human patients differed from that of respective colonized mice.

Heat map of OTUs on family level of **(A)** lean, **(B)** preFMT[lean], **(C)** postFMT[lean], **(D)** preFMT[but] and **(E)** postFMT[but] groups with ≥0.5 % relative abundance in human and ≥0.5 % relative abundance in ≥50 % of the mice. **(F)** TOP OTUs present in humans only, mice only or in both species. Classification was done with EZBioCloud. N = 10-14 per group CD – control diet. HFD – high-fat diet. HMb – human microbiota. OTU – operating taxonomic unit. N – number of mice measured.

To get a deeper insight into microbial activities, cecum to body weight ratios as a marker of colonization efficacy were determined, as cecum weights in GF animals are significantly increased compared to colonized animals. PreFMT[lean]- and postFMT[lean]-mice showed a lower ratio of cecum to body weight compared to the other association groups. HFD feeding led to a further reduction in the ratio of cecum to body weight in all groups (Figure 12A). Since reduced cecum weights suggest higher feed efficiency through energy harvest [36], we determined residual energies in mouse feces. Upon HFD feeding, fecal energy was reduced in mice colonized with lean-, preFMT[but]- and postFMT[but]-microbiota, compared to CD-fed animals. In preFMT[lean]- and postFMT[lean]-recipients, however, we did not observe this massive reduction in fecal energy in HFD-fed mice. PreFMT[lean]- and postFMT[lean]-mice fed with CD were almost as efficient in energy harvesting as the remaining mouse groups upon HFD (Figure 12B).
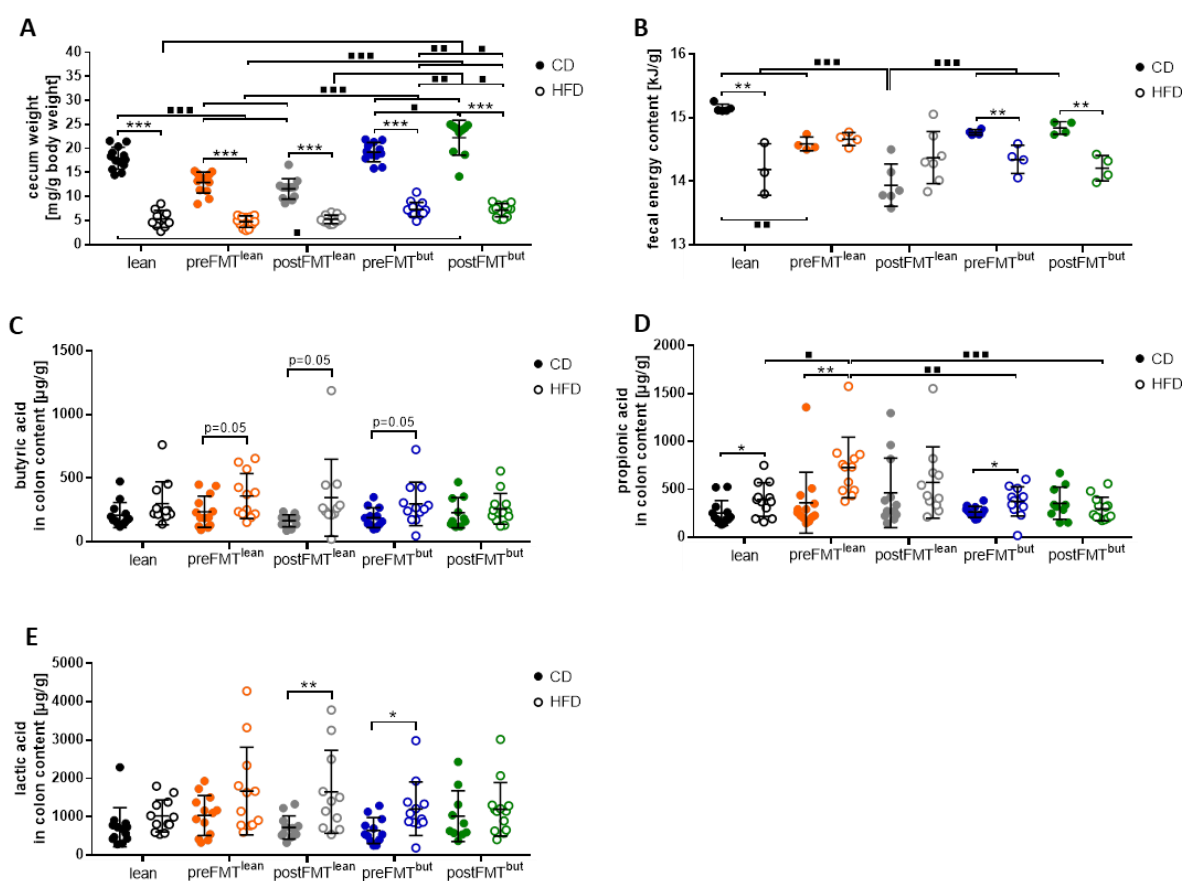

Figure 12: HFD feeding, but not human microbiota composition influenced mouse metabolism and microbial activities.
All measurements were performed 12 weeks after colonization of the mice. **(A)** Cecum to body weight ratio. N = 10-14 per group. **(B)** Fecal energy. N = 3-7 per group. Concentrations of SCFAs **(C)** butyrate, **(D)** propionate and **(E)** lactate in colonic contents. N = 10-13 per group. Statistics: *p< 0.05; **p< 0.01; ***p< 0.001; unpaired, parametric t-test to compare dietary effects within the same colonization group; ▪p< 0.05; ▪▪p< 0.01; ▪▪▪p< 0.001; One-way ANOVA followed by Tukey's to compare donor effects within the same feeding group (3.18). Data are shown as means ± SD. CD – control diet. HFD – high-fat diet. SCFA – short chain fatty acid. SD – standard deviation. N – number of mice measured.

SCFAs were often shown as markers for efficient energy harvest and were mostly elevated upon high-fat feeding or obesity [36, 40]. Confirmatory, in our study butyrate, propionate and lactate levels in colonic contents were significantly increased in most DIO mice (Figure 12C-E). It is remarkable that postFMT-mouse groups did not show elevated butyric acid levels, although human donors were treated with either butyrate tablets (postFMT[but]) or feces from a patient high in butyrate producing bacteria (Figure 12C). Other SCFAs like Isobutyrate, Methylbutyrate and Isovalerate were not significantly altered, neither by diet nor by donor groups (data not shown).

In summary, many bacterial species were lost when human microbiota was transferred into mice. Similarity analysis revealed that only half of the human bacteria were detected in the corresponding recipients. Furthermore, DIO was not necessarily a trigger for changes in microbial profiles.

4.2.4   Obese human microbiota does not influence gut barrier function

As obesity is associated with inflammation [92, 99], gut histology of colonized mice was evaluated. However, neither different microbial environments nor higher fat contents in food influenced jejunum and colon histology or induced gut inflammation (Figure 13A, C–F). Furthermore, villus heights were reduced in HFD-fed mice, but were not distinguishable between human donors, except for postFMT[but]-mice, which showed no villus length reduction upon HFD (Figure 13B).

To further validate gut barrier integrity, we analyzed transepithelial resistance (TER) and translocation of fluorescein in different intestinal segments *ex vivo*. Jejunal TER was significantly reduced in all mouse groups fed with HFD compared to CD mice. In line with this, jejunal permeability increased, but only reached significance in preFMT[but]-mice. However, the other intestinal compartments were not affected in TER or permeability by diet or by colonization with human donor microbiota (Figure 14B, C). Furthermore, *in vivo* translocation of the bigger sized fluorescein FITC-Dextran (4kDa), measured by fluorescence recovery in the upper gastrointestinal tract, was found at same levels in plasma (Figure 14A). Since TER was reduced in jejunum, we further determined gene expression levels for barrier markers. However, no differences in occludin and ZO-1 regulation could be observed (Figure 14D, E). In line with this, occludin protein levels did not differ between diet groups with the exception of lean colonized mice showing slightly decreased occludin concentrations triggered by HFD (Figure 14F, G).

In summary, obese human microbiota did not induce gut barrier dysfunction or changes in gut histology. Also, HFD did not induce intestinal inflammation or total gut impermeability despite decreased jejunal transepithelial resistance.
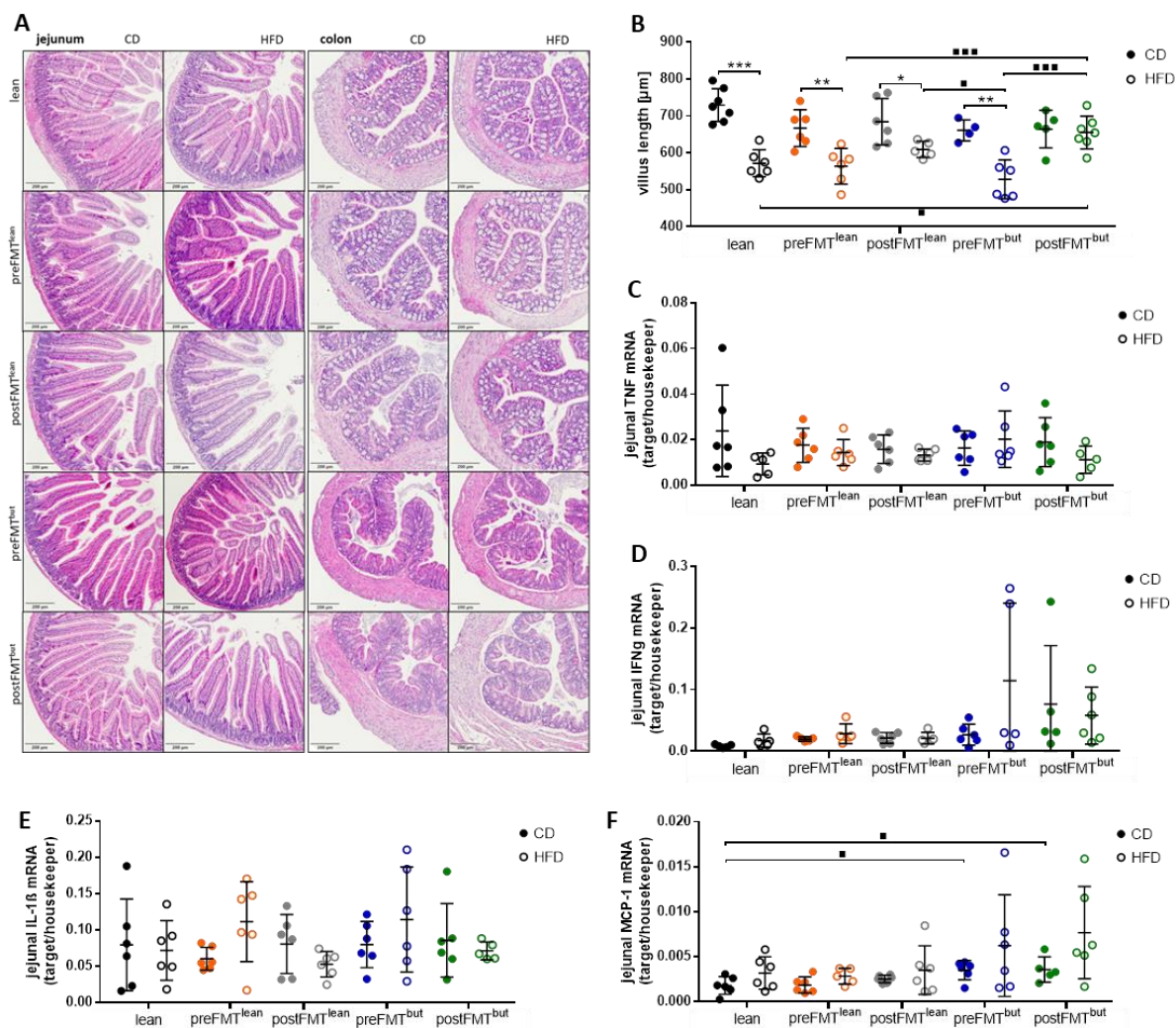
Figure 13: Neither obese human microbiota nor HFD feeding induced gut pathology or inflammation.
All measurements were performed 12 weeks after colonization. **(A)** Representative H&E staining of jejunal and colonic tissue sections. **(B)** Villus lengths measured in jejunum. Gene expression levels of **(C)** TNF, **(D)** IFNγ, **(E)** IL-1ß and **(F)** MCP-1 shown as fold-change normalized to the housekeeping genes GAPDH, RPL13A and HPRT. Statistics: *p< 0.05; **p< 0.01; ***p< 0.001; unpaired, parametric t-test to compare dietary effects within the same colonization group; ▪p< 0.05; ▪▪p< 0.01; ▪▪▪p< 0.001; One-way ANOVA followed by Tukey's to compare donor effects within the same feeding group (3.18). Data are shown as means ± SD. N = 5-6 per group. CD – control diet. HFD – high-fat diet. TNF – tumor necrosis factor. IFN – interferon. IL – interleukin. MCP – monocyte chemoattractant protein. SD – standard deviation. N – number of mice measured.
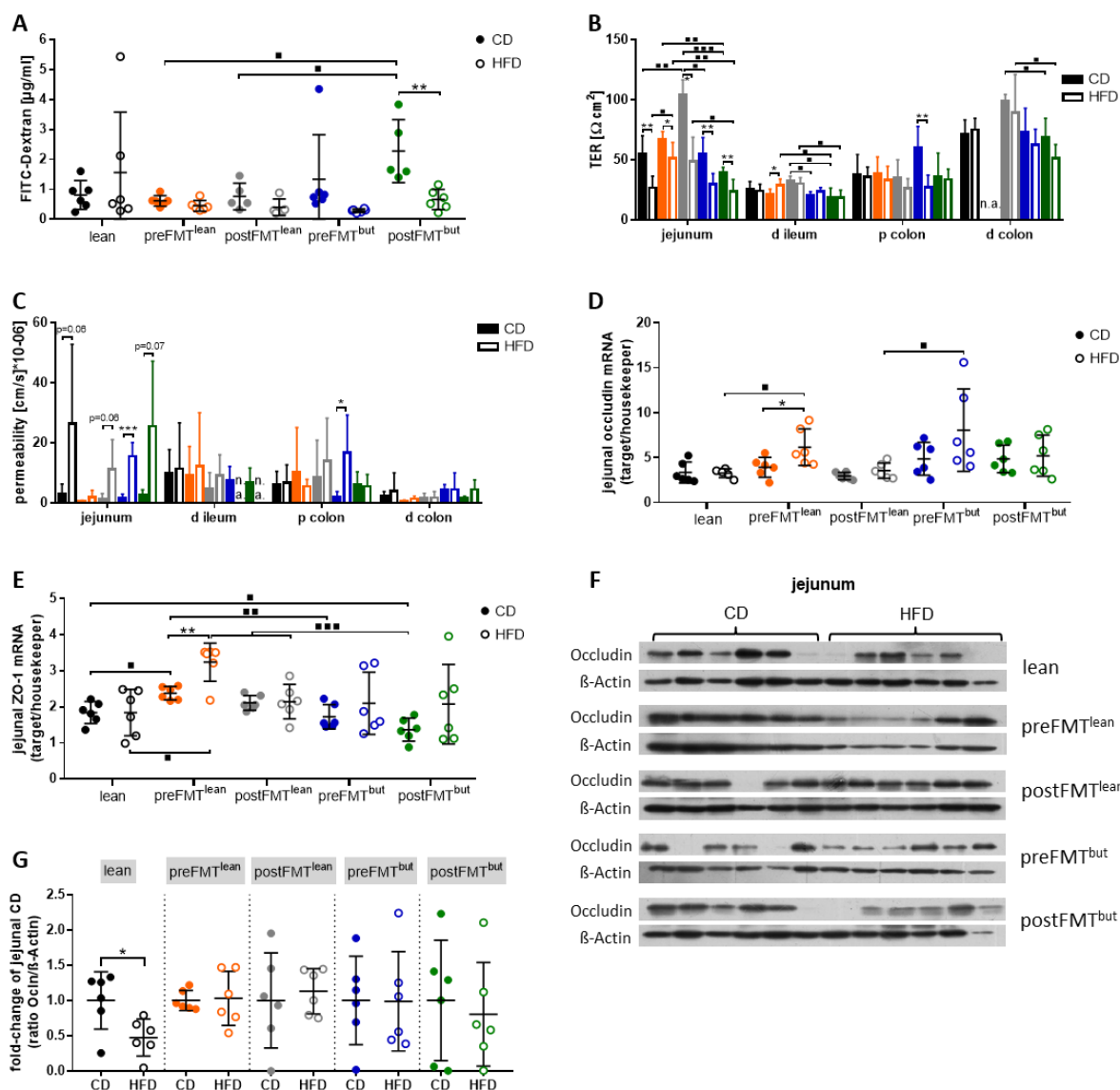
Figure 14: Obese human microbiota had no effect on gut barrier function, but HFD slightly reduced the resistance in the jejunal epithelium in the absence of inflammation.

All measurements were performed 12 weeks after colonization. **(A)** FITC-Dextran recovery in plasma analyzed *in vivo* two hours post gavage. **(B)** Transepithelial resistance (TER) and **(C)** translocation of fluorescein (permeability) of jejunum, distal ileum, proximal and distal colon analyzed using Ussing chambers. Gene expression levels of **(D)** occludin and **(E)** ZO-1 shown as fold-change normalized to the housekeeping genes GAPDH, RPL13A and HPRT. **(F)** Protein levels of occludin in total jejunal tissue were assessed by Western blotting using ß-Actin as loading control. **(G)** Protein expression was then quantified and displayed as fold-change of CD in relation to housekeeping gene ß-Actin. Statistics: *$p < 0.05$; **$p < 0.01$; ***$p < 0.001$; unpaired, parametric t-test to compare dietary effects within the same colonization group; ▪$p < 0.05$; ▪▪$p < 0.01$; ▪▪▪$p < 0.001$; One-way ANOVA followed by Tukey's to compare donor effects within the same feeding group (3.18). Data are shown as means ± SD. N = 4-6 per group. CD – control diet. HFD – high-fat diet. FITC – fluorescein isothiocyanate. TER – transepithelial resistance. d –distal. p – proximal. ZO – zona occludens. SD – standard deviation. N – number of mice measured.

4.2.5   HFD feeding, but not obese human microbiota induces hepatic steatosis

Hepatic inflammation and steatosis are often associated with HFD feeding or DIO [161, 162]. However, the analysis of inflammatory markers in total liver tissue revealed no induction of TNF, IL-1ß and IL-6 mRNA levels upon HFD feeding (Figure 15E–G).
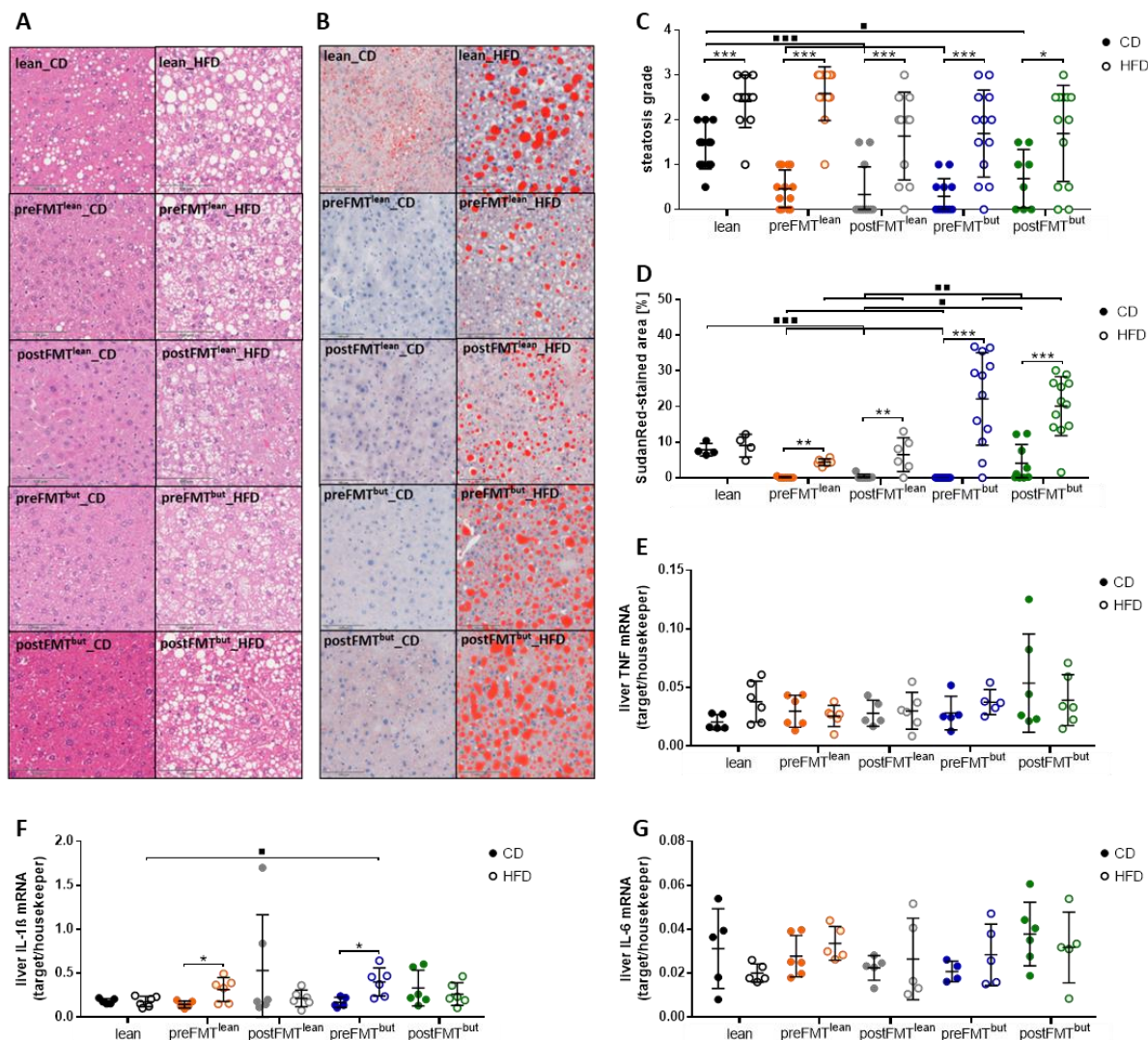

Figure 15: Liver histology was not influenced by colonization with obese human microbiota, but HFD feeding induced liver steatosis without the occurrence of inflammation.
All measurements were performed 12 weeks after colonization. **(A)** H&E staining of liver tissue sections **(C)** used for the assessment of liver steatosis scores. **(B)** SudanRed staining of liver tissue sections **(D)** used for the quantification of lipids in the liver tissue. Gene expression levels of **(E)** TNF, **(F)** IL-1ß and **(G)** IL-6 in liver tissue shown as fold-change normalized to the housekeeping genes GAPDH, RPL13A and HPRT. Statistics: *p< 0.05; **p< 0.01; ***p< 0.001; unpaired, parametric t-test to compare dietary effects within the same colonization group; ∎p< 0.05; ∎∎p< 0.01; ∎∎∎p< 0.001; One-way ANOVA followed by Tukey's to compare donor effects within the same feeding group (3.18). Data are shown as means ± SD. N = 4-13 per group. CD – control diet. HFD – high-fat diet. TNF – tumor necrosis factor. IL – interleukin. SD – standard deviation. N – number of mice measured.

Additionally, fat accumulation in the liver was measured by determining lipid droplets and calculating the degree of steatosis based on the number and size of lipid droplets. A 4 weeks HFD feeding period was already sufficient to induce steatosis in mice. Colonizing mice for 12 weeks with obese human microbiota and feeding them with CD induced no or only mild signs of steatosis. Surprisingly, tissue histology revealed that lean-microbiota recipients fed with CD developed steatosis (Figure 15A, C). Steatosis in lean-CD mice was also confirmed by SudanRed staining of hepatic lipid droplets (Figure 15B, D). **In summary, it can be concluded that not human microbiota, but HFD feeding caused liver steatosis without development of liver inflammation.**

4.2.6 HFD feeding, but not colonization with obese human microbiota triggers low-grade fat inflammation and changes in adipocyte morphology

In our study, HFD feeding induced obesity accompanied by a significant increase of the sum of epididymal, mesenteric and subcutaneous white adipose tissue weights (WAT) and epididymal WAT mass to body weight ratios (Figure 16A, B). It is noteworthy that mice fed with CD and colonized with preFMT^{lean}- and postFMT^{lean}-microbiota showed significantly increased fat pad mass compared to residual association groups without showing differences in body weights (Figure 7B; Figure 16A, B). Regardless of the human donor, HFD feeding led to increased fat cells and to higher abundances of larger adipocytes compared to CD-fed mice. Corresponding to increased epididymal fat mass, mean adipocyte size was significantly higher in the preFMT^{lean}-group than in pre- and postFMT^{but}-groups (Figure 16C–E).

Further characterization of fat metabolism revealed, as expected, high levels of leptin in the adipose tissue. Leptin levels in preFMT^{lean}-associated mice were significantly higher than in the preFMT^{but}-group, which was already reflected in increased fat mass (Figure 16B; Figure 17A).
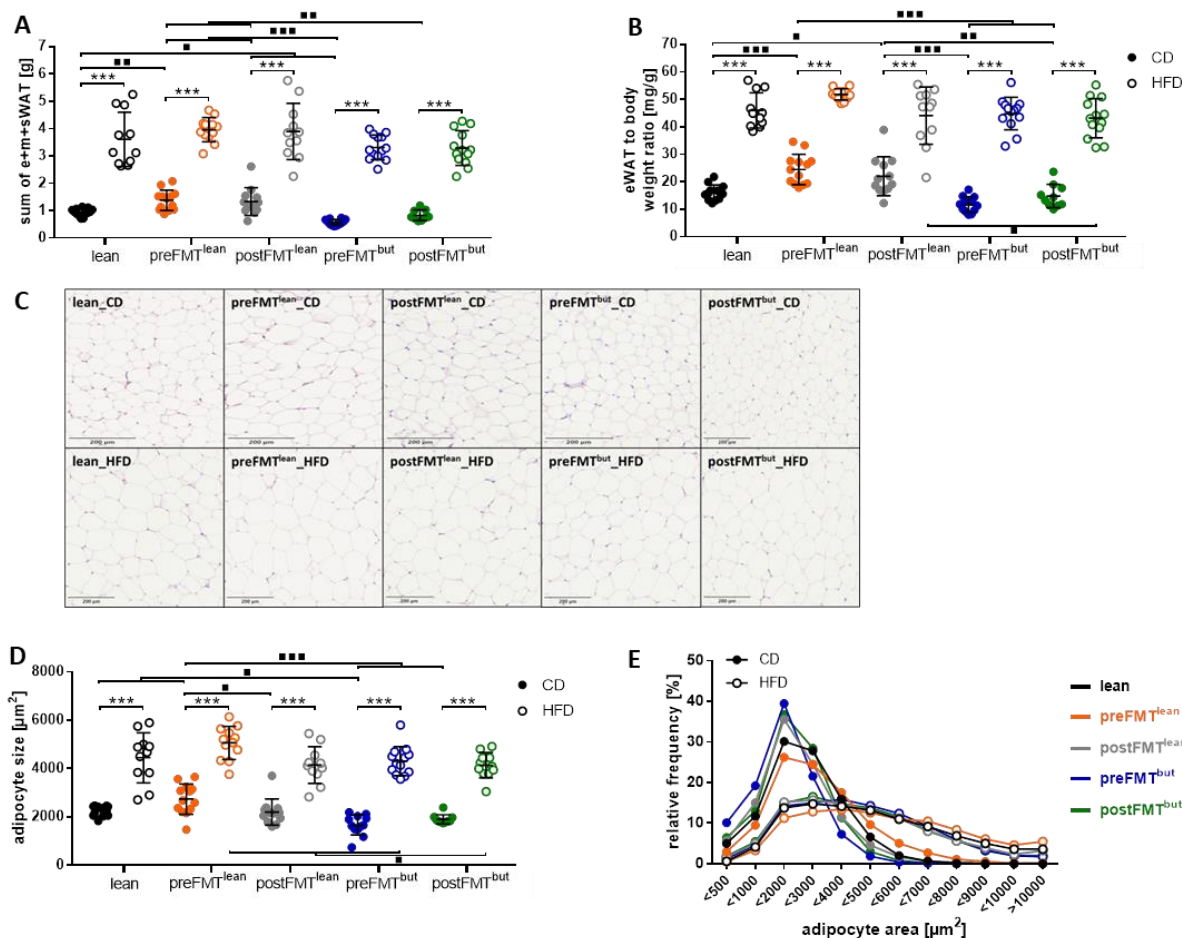
Figure 16: Obese human microbiota induced partly different fat morphologies in mice, but HFD provoked a fat mass gain and massive hypertrophy independent of the human donor.

All measurements were performed 12 weeks after colonization. **(A)** Sum of fat weights (eWAT, mWAT and sWAT). **(B)** eWAT to body weight ratios. **(C)** H&E stained eWAT adipocytes. **(D)** Size and **(E)** relative frequency of eWAT adipocytes. Statistics: $*p< 0.05$; $**p< 0.01$; $***p< 0.001$; unpaired, parametric t-test to compare dietary effects within the same colonization group; $\blacksquare p< 0.05$; $\blacksquare\blacksquare p< 0.01$; $\blacksquare\blacksquare\blacksquare p< 0.001$; One-way ANOVA followed by Tukey's to compare donor effects within the same feeding group (3.18). Data are shown as means ± SD. N = 10-14 per group. CD – control diet. HFD – high-fat diet. eWAT – epididymal white adipose tissue. mWAT – mesenteric white adipose tissue. sWAT – subcutaneous white adipose tissue. SD – standard deviation. N – number of mice measured.

Obesity, DIO and diabetes are often characterized by a low-grade inflammation in the adipose tissue, also known as chronic or metabolically triggered inflammation. Low-grade inflammation of adipose tissue is triggered by macrophage infiltration and expressed as a two- to three-fold increase of inflammatory marker [163-165]. In accordance with previous studies, the expression levels of MCP-1 and F4/80 as markers for macrophage infiltration were three-fold elevated in HFD mice compared to CD groups (Figure 17B, C). Additionally, expression levels of different inflammatory marker in epididymal tissue were tested. We were able to confirm slightly increased levels of TNF in all

colonization groups fed with HFD compared to CD-fed littermates with the exception of the lean-group. However, this can be explained by the high basal TNF expression values of CD-fed mice (Figure 17D).
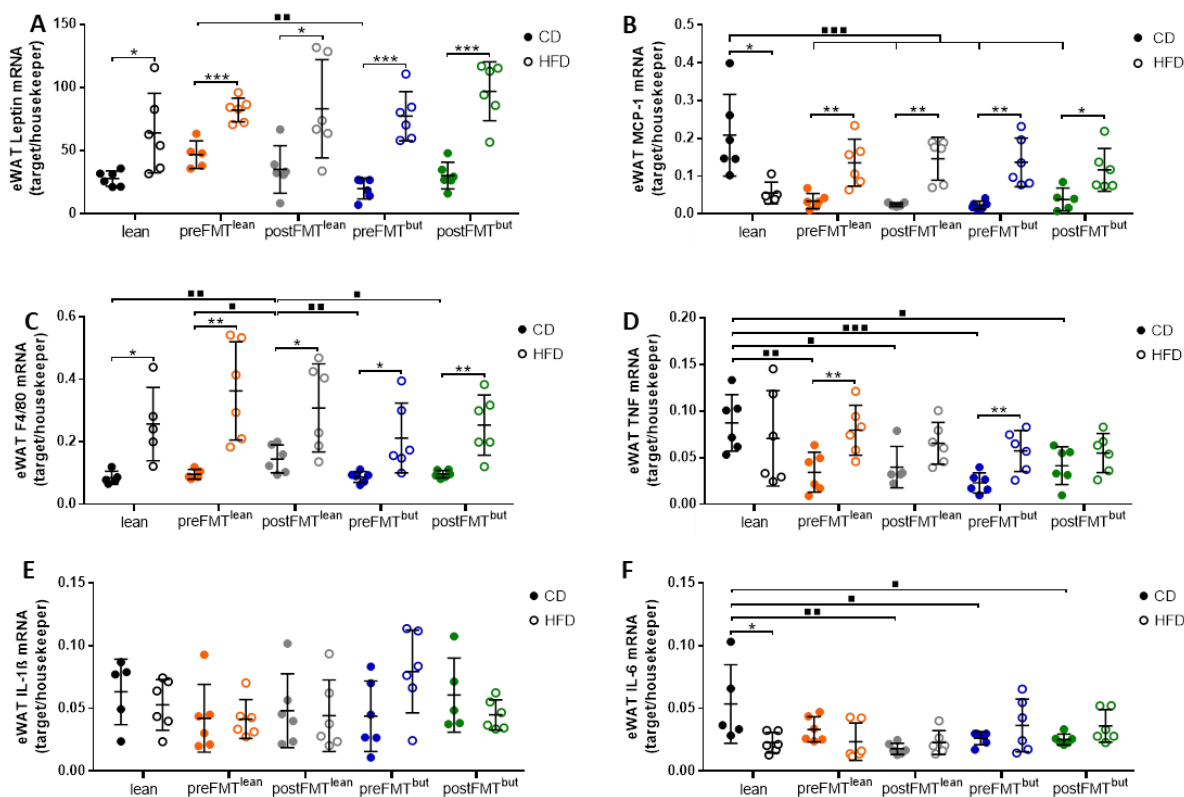

Figure 17: HFD feeding, but not colonization with obese human microbiota induced adipose tissue inflammation.
All measurements were performed 12 weeks after colonization. Gene expression levels of **(A)** leptin, **(B)** MCP-1, **(C)** F4/80, **(D)** TNF, **(E)** IL-1ß and **(F)** IL-6 in adipose tissue shown as fold-change normalized to the housekeeping genes GAPDH, RPL13A and HPRT. Statistics: *p< 0.05; **p< 0.01; ***p< 0.001; unpaired, parametric t-test to compare dietary effects within the same colonization group; ■p< 0.05; ■■p< 0.01; ■■■p< 0.001; One-way ANOVA followed by Tukey's to compare donor effects within the same feeding group (3.18). Data are shown as means ± SD. N = 5-6 per group. CD – control diet. HFD – high-fat diet. eWAT – epididymal white adipose tissue. MCP – monocyte chemoattractant protein. TNF – tumor necrosis factor. IL – interleukin. SD – standard deviation. N – number of mice measured.

IL-1ß and IL-6 expression levels were not distinguishable in all mouse groups (Figure 17E, F). With respect to human microbiota donors, we could not detect any differences in the inflammatory status and macrophage infiltration pattern, except for high baseline levels of TNF, MCP-1 and IL-6 in the lean-mouse group fed with CD. Furthermore, the postFMT^lean-group fed CD showed significantly higher expression levels in MCP-1 than residual mouse sets (Figure 17B–F).

Overall, human obese microbiota did not trigger changes in fat morphology or inflammation, but HFD feeding induced low-grade inflammation accompanied by adipocyte hypertrophy in all mouse groups.

4.3 Transfer of fecal microbiota from obese patients to mice with different colonization periods

To test whether different colonization durations can induce the human obese and insulin resistant phenotype in mice, 4 weeks old male GF mice were associated with fecal microbiota of a moderate obese patient ('preFMT^but') for 4 (T1), 8 (T2) and 12 (T3) weeks. The human donor showed decreased insulin levels and HOMA-IR after autologous FMT in combination with butyrate tablet treatment ('postFMT^but') (Table 1; Figure 5, **Experiment 2**).

4.3.1 Different colonization periods do not provoke human obese phenotype in mice

Intestinal segments were adequate and equally colonized regardless of association, mouse groups and duration of colonization (Figure 18A, B). The transfer of microbiota from human to mice resulted in a significant drop of bacterial species as it was already shown in the long-term experiment (Figure 18C, D; Figure 10A, B). It is noteworthy, that there was no loss of bacterial species regarding colonization over time and numbers of bacterial species independently of association group. Shannon effective results showed rather an increase of bacterial counts over time in pre- and postFMT^but mouse groups (Figure 18C, D).
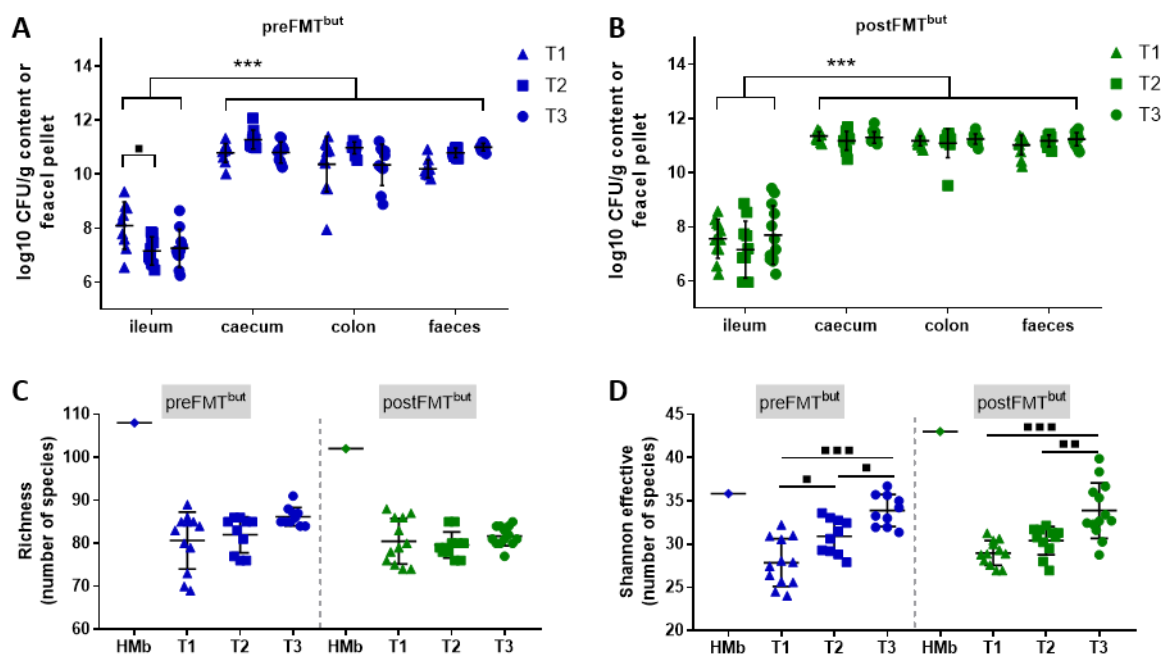

Figure 18: Different colonization periods led to stable and unchanged colonization over time.
All measurements were performed after 4 (T1), 8 (T2) and 12 (T3) weeks of colonization. **(A, B)** log10 CFU/g intestinal contents. **(C)** Richness and **(D)** Shannon effective in HMb and corresponding mice. Statistics: *p< 0.05; **p< 0.01; ***p< 0.001; Two-way ANOVA followed by Tukey's to compare intestinal compartment effects within the same colonization period group; ■p< 0.05; ■■p< 0.01; ■■■p< 0.001; One-way ANOVA followed by Tukey's to compare colonization period effects within the same donor group (3.18). Data are shown as means ± SD. N = 10-13. CFU – colony forming units. HMb – human microbiota. SD – standard deviation. N – number of mice measured.
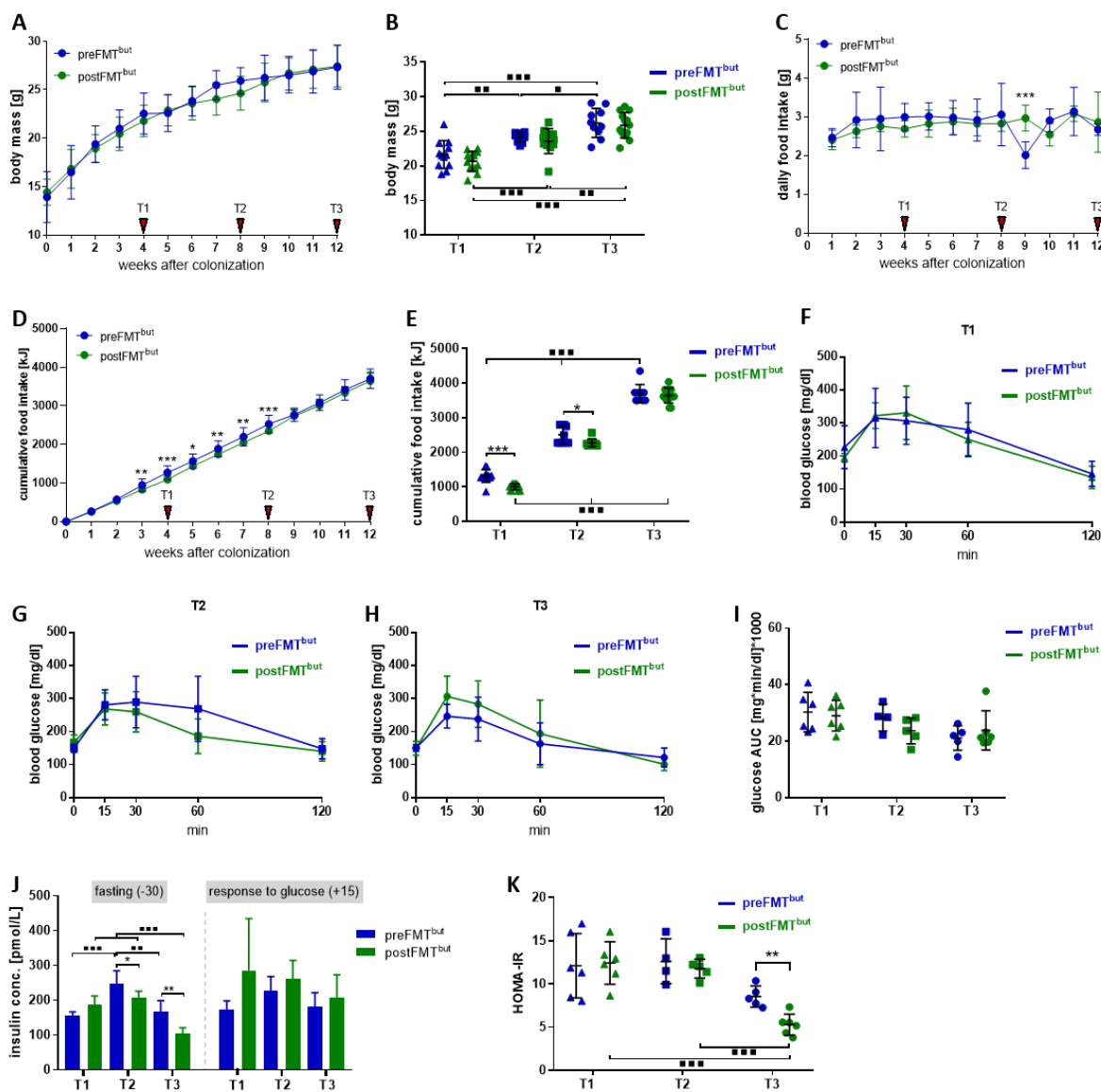
Figure 19: Human donor microbiota did not influence the obesity phenotype in colonized mice regardless of the colonization period.

Mice were sacrificed after 4 (T1), 8 (T2) and 12 (T3) weeks of colonization **(A)** Body mass development from 0 to 12 weeks after colonization. **(B)** Body mass measurement at T1, T2 and T3. **(C)** Daily food intake per mouse from week 1 to 12 after colonization. **(D)** Cumulative food intake from week 1 to 12 after colonization. **(E)** Total cumulative food intake after 12 weeks of colonization. oGTTs (2 mg/kg body mass) of **(F)** T1 **(G)** T2, **(H)** T3 mouse groups after 6 hours fasting period and **(I)** calculated AUC. **(J)** Fasting plasma insulin levels (-30) and plasma insulin levels 15 minutes after oral glucose administration (+15). **(K)** Insulin resistance index (HOMA-IR). Statistics: *p< 0.05; **p< 0.01; ***p< 0.001; unpaired, parametric t-test to compare donor effects within the same colonization period group; ▪p< 0.05; ▪▪p< 0.01; ▪▪▪p< 0.001; One-way ANOVA followed by Tukey's to compare colonization period effects within the same donor group (3.18). Data are shown as means ± SD. N = 10-13 per group for (A) - (E), N = 5-6 per group for (F) - (K). oGTT – oral glucose tolerance test. AUC – area under the curve. Conc. – concentration. SD – standard deviation. N – number of mice measured.

Since duration of colonization may be essential for the induction of an obese phenotype in mice by the transfer of human microbiota, a kinetic evaluation of mice was conducted. Phenotypic characterization revealed that mice showed normal body development throughout the colonization experiment and

that endpoint body weights were not different between the two association groups. Pre- and postFMT^but-mice showed significant increase of body mass over time (Figure 19A, B).

Daily food intake and cumulative food intake were slightly lower in the postFMT^but-group, but this was not reflected in higher body weights (Figure 19C–E). All three colonization groups did not differ in oral glucose tolerance as indicated by comparable blood glucose levels before and after glucose administration and the calculated area under the curve (Figure 19F–I). As shown in human donors, insulin levels were significantly decreased in postFMT^but-mice colonized for 8 and 12 weeks (Figure 19J). Confirmatively, insulin resistance index was decreased in 12 weeks colonized mice comparing pre- and post-treatment groups. (Figure 19K).

Colonization of mice with post-treatment compared to pre-treatment human microbiota had no influence on the inflammatory status, as shown by equal systemic SAA levels (Figure 20A). Also, LBP levels were not different between the groups (Figure 20B). Further phenotypic characterization revealed that mice showed normal epididymal fat pad weights which naturally increased with age and body weight, but were not influenced by the microbiota donor group (Figure 20F).

With regard to gut barrier function, all animals showed unchanged FITC-Dextran recovery in plasma and *ex vivo* TER as well as permeability in jejunum, ileum and colon (Figure 20C–E).

Concerning adipose tissue inflammation, we could not observe changes in expression levels of markers of inflammation and macrophage infiltration in the pre- and postFMT^but-treatment groups which was consistent with unaffected epididymal fat pad weights (Figure 20F–I).

In summary, changes in the colonization period were not sufficient to induce human obesity phenotypes in mice by microbiota transfer.
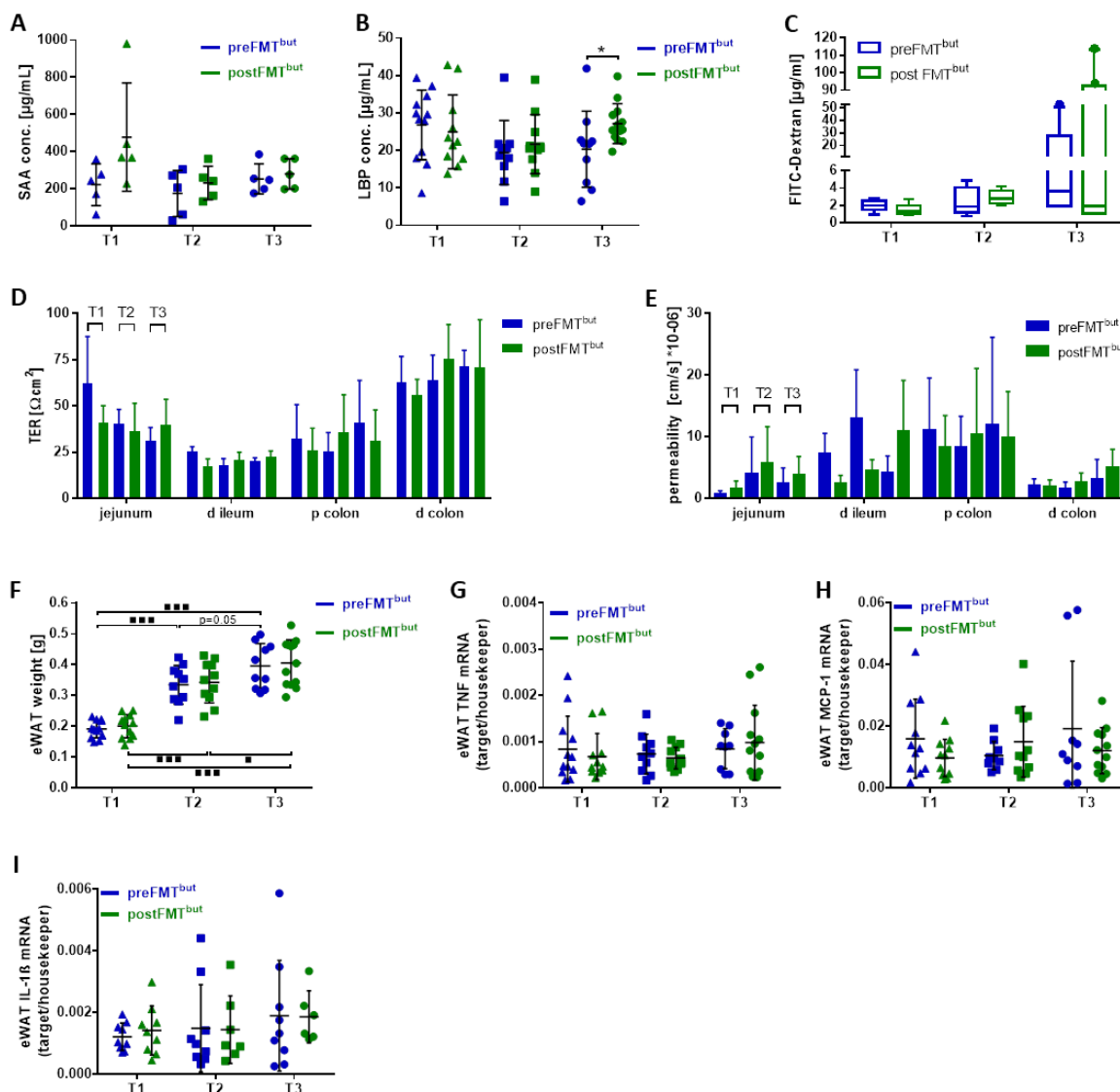
Figure 20: Colonizing mice with obese human microbiota for different periods of time did not induce systemic inflammation, adipose tissue inflammation or a loss of gut barrier integrity.

All measurements were performed after 4 (T1), 8 (T2) and 12 (T3) weeks of colonization. **(A)** SAA levels in plasma. N = 5 per group. **(B)** LBP levels in plasma. N = 10-13 per group. **(C)** FITC-Dextran recovery in plasma analyzed *in vivo* two hours post gavage. N = 5-7 per group. **(D)** Transepithelial resistance (TER) and **(E)** translocation of fluorescein (permeability) of jejunum, distal ileum, proximal and distal colon analyzed using Ussing chambers. N = 4-7 per group. **(F)** eWAT weights. N = 10-13 per group. Gene expression levels of **(G)** TNF, **(H)** MCP-1 and **(I)** IL-1ß in adipose tissue shown as fold-change normalized to the housekeeping genes GAPDH, RPL13A and HPRT. N = 6-13 per group. Statistics: *$p< 0.05$; **$p< 0.01$; ***$p< 0.001$; unpaired, parametric t-test to compare donor effects within the same colonization period group; ▪$p< 0.05$; ▪▪$p< 0.01$; ▪▪▪$p< 0.001$; One-way ANOVA followed by Tukey's to compare colonization period effects within the same donor group (3.18). Data are shown as means ± SD. SAA – serum amyloid A. LBP – lipopolysaccharide binding protein. FITC – fluorescein isothiocyanate. TER – transepithelial resistance. d –distal. p – proximal. eWAT – epididymal white adipose tissue. TNF – tumor necrosis factor. MCP – monocyte chemoattractant protein. IL – interleukin. SD – standard deviation. N – number of mice measured.

4.4 Fecal microbiota transfer of an obese patient to mice using short-term colonization and high-fat diet pre-challenge

To test whether a pre-challenge of mice with HFD and a colonization time of 4 weeks in total are capable of inducing an obese human phenotype upon colonization with human obese microbiota, mice were first challenged with CD or HFD three days prior to association with fecal microbiota originating from a severely obese patient (preFMT^lean short) (Table 1; Figure 5, **Experiment 3**).

4.4.1 No induction of insulin resistance upon HFD feeding in short-term colonized mice

Short-term colonized mice (preFMT^lean short) fed with HFD showed a significantly higher body weight from 3.5 weeks of age until the end of the experiment in week 8. Looking at body mass development curve of preFMT^lean short-mice, the human obese microbiota has not induced an equivalent phenotype in mice (Figure 21A). In the current experiment, cumulative food-energy intake was significantly increased by HFD (Figure 21B).
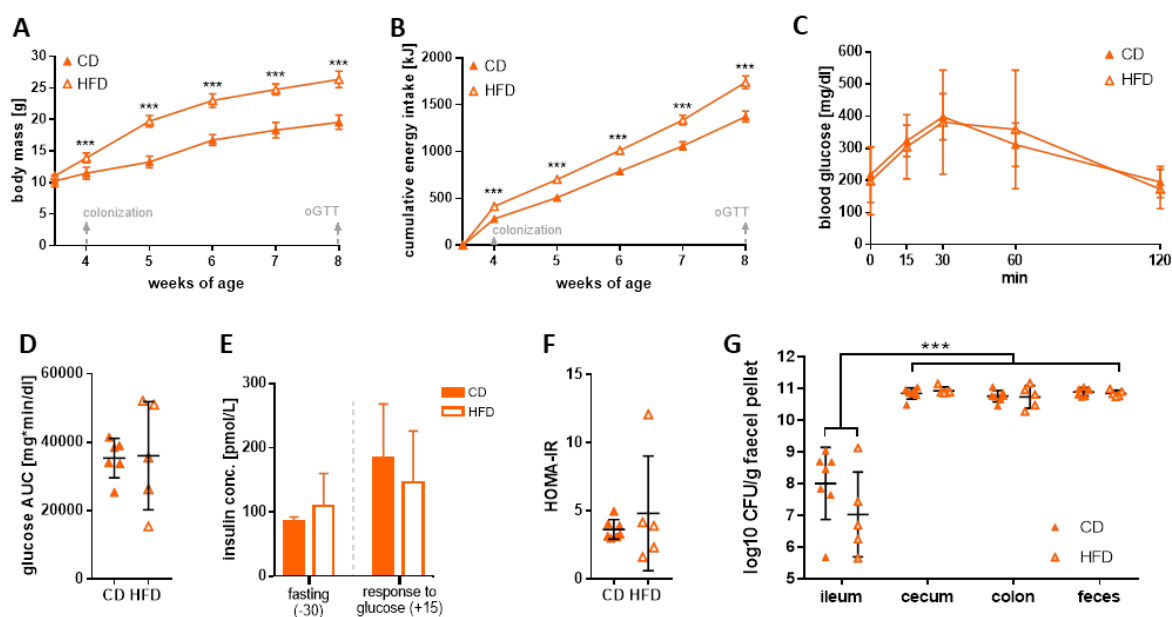

Figure 21: Simultaneous transfer of obese human microbiota und HFD challenge in mice did not induce insulin resistance, but promoted diet-induced obesity.
Mice were switched to CD or HFD at 3.5 weeks of age and were colonized 3 days later for 4 weeks. **(A)** Body weight development from 3.5 to 8 weeks of age. **(B)** Cumulative food intake from 3.5 to 8 weeks of age. **(C)** oGTT after 8 weeks of age and **(D)** calculated AUC. **(E)** Fasting plasma insulin levels (-30) and values 15 minutes after oral glucose administration (+15). **(F)** Insulin resistance index (HOMA-IR). Statistics: *p< 0.05; **p< 0.01; ***p< 0.001; unpaired, parametric t-test to compare dietary group effects (3.18). **(G)** CFU of fecal contents after 4 weeks of colonization. Statistics: ***p< 0.001; Two-way ANOVA followed by Tukey's to compare intestinal compartment effects within the same colonization group. Data are shown as means ± SD. N = 5-7 per group. CD – control diet. HFD – high-fat diet. oGTT – oral glucose tolerance test. AUC – area under the curve. Conc. – concentration. HOMA-IR – homeostatic model assessment of insulin resistance. CFU – colony forming units. SD – standard deviation. N – number of mice measured.

However, preFMT[lean]short-colonized mice did not show elevated fasting glucose and insulin levels as well as glucose intolerance induced by HFD (Figure 21C–F). Insulin resistance was again not induced in these mice comparing insulin levels, meaning that the transfer of obese human fecal microbiota did not induce equivalent phenotype in mice (Figure 21E, F). Intestinal segments were adequate and equally colonized comparing dietary groups (Figure 21G). **Taken together, HFD induced obesity without influencing glucose metabolism.**

4.4.2 No fat hypertrophy and liver steatosis upon HFD in short-term colonized mice

PreFMT[lean]short-animals revealed significantly bigger fat pads and a higher fat to body weight ratio after a 4 weeks HFD feeding period. This was accompanied by raised leptin expression levels (Figure 22A–C). However, equal sizes of adipocytes of epididymal tissues displayed no fat hypertrophy in mice fed HFD. Also, relative frequency of adipocytes showed no difference between CD- and HFD-fed mice (Figure 22D–F).
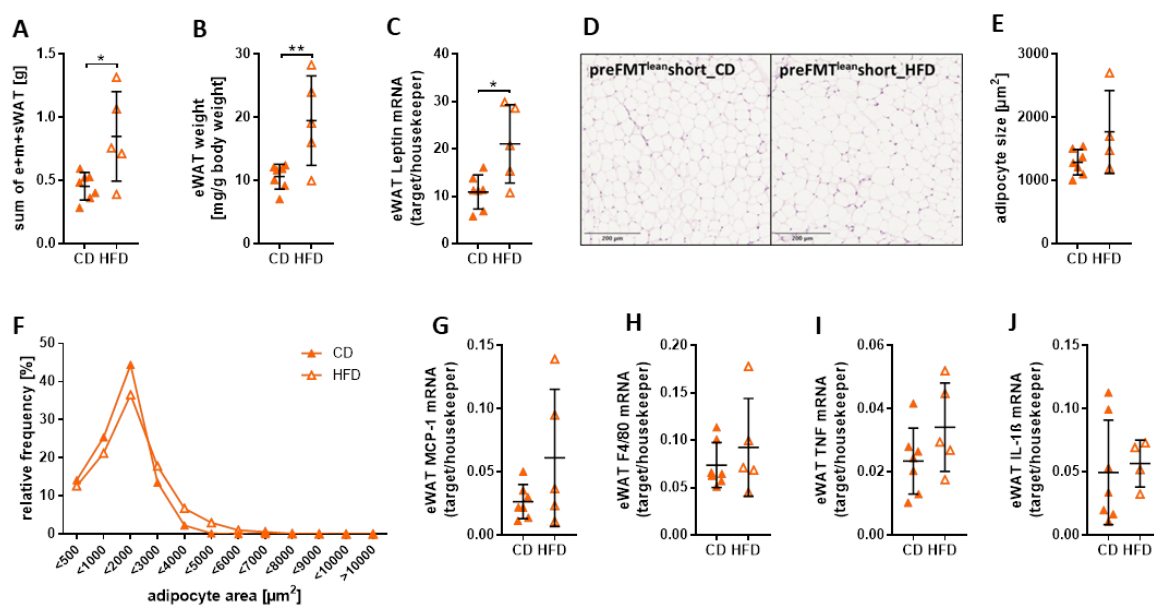

Figure 22: Simultaneous transfer of obese human microbiota und HFD challenge in mice led to fat mass gain without inducing hypertrophy, but did not promote low-grade fat inflammation.
All measurements were performed after 8 weeks of age when mice were colonized for 4 weeks. **(A)** Sum of fat weights (eWAT, mWAT and sWAT). **(B)** eWAT to body weight ratio. **(C)** Gene expression levels of leptin in adipose tissue shown as fold-change normalized to the housekeeping genes GAPDH, RPL13A and HPRT. **(D)** H&E stained eWAT adipocytes. **(E)** Size and **(F)** relative frequency of eWAT adipocytes. Gene expression levels of **(G)** MCP-1, **(H)** F4/80, **(I)** TNF and **(J)** IL-1ß in adipose tissue shown as fold-change normalized to the housekeeping genes GAPDH, RPL13A and HPRT. Statistics: *p< 0.05; **p< 0.01; ***p< 0.001; unpaired, parametric t-test to compare dietary group effects (3.18). Data are shown as means ± SD. N = 5-7 per group. CD – control diet. HFD – high-fat diet. eWAT – epididymal white adipose tissue. mWAT – mesenteric white adipose tissue. sWAT – subcutaneous white adipose tissue. MCP – monocyte chemoattractant protein. TNF – tumor necrosis factor. IL – interleukin. SD – standard deviation. N – number of mice measured.

Although adipose tissue increased significantly in weight in HFD-fed mice, there was no induction of low-grade inflammation. Equal expression levels of MCP-1, F4/80, TNF and Il-1ß were observed between CD- and HFD-fed mice (Figure 22G–J).

Systemic inflammation was detected in short-term colonized mice fed HFD, but endotoxin levels were equal, which stands in contrast to significantly raised LBP values of HFD-fed mice compared to CD-fed littermates (Figure 23A–C). Interestingly, obese microbiota in short-term colonized mice fed HFD did not induce liver steatosis as liver stainings revealed no signs of fat incorporation (Figure 23D–G). In contrast, preFMT^lean short-mice showed liver inflammation as expression levels of inflammatory markers were significantly increased by HFD (Figure 23H–J).
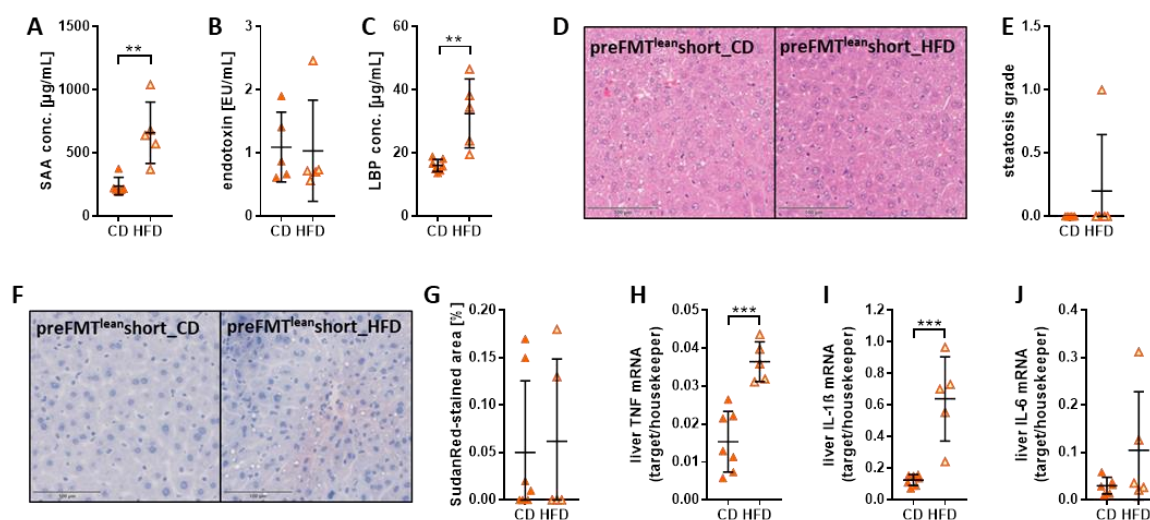

Figure 23: Simultaneous transfer of obese human microbiota und HFD challenge induced systemic and liver inflammation in the absence of liver steatosis.
All measurements were performed after 8 weeks of age when mice were colonized for 4 weeks. **(A)** SAA levels in plasma. **(B)** Endotoxin levels in portal vein plasma. **(C)** LBP levels in plasma. **(D)** H&E stainings from liver tissue **(E)** for liver steatosis scoring. **(F)** SudanRed staining **(G)** to quantify lipids in the liver tissue. Gene expression levels of **(H)** TNF, **(I)** IL-1ß and **(J)** IL-6 in liver tissue shown as fold-change normalized to the housekeeping genes GAPDH, RPL13A and HPRT. Statistics: *p< 0.05; **p< 0.01; ***p< 0.001; unpaired, parametric t-test to compare dietary group effects (3.18). Data are shown as means ± SD. N = 5-7 per group. CD – control diet. HFD – high-fat diet. SAA – serum amyloid A. LBP – lipopolysaccharide binding protein. TNF – tumor necrosis factor. IL – interleukin. SD – standard deviation. N – number of mice measured.

In summary, 8 weeks old short-term colonized mice fed HFD showed systemic and hepatic inflammation, but were protected from liver steatosis. Furthermore, HFD did not influence fat morphology and inflammation in these mice.

5 Discussion

The microbiota plays an important role in the development of several disease like obesity and diabetes. It is widely accepted that obesity is linked to changes in gut microbiota composition, but which bacteria may be involved in microbe-host interaction is not fully elucidated yet. The present work investigated the role of human gut bacteria in metabolism, gut barrier function and inflammation in gnotobiotic mice. To address microbe-host interactions in the context of obesity, the aim was to establish a humanized mouse model for obesity and metabolic dysfunction. Therefore, obese and insulin resistant patient-derived fecal microbiota pre and post transplantation of autologous feces and butyrate tablets or allogenic feces from a lean human donor were transferred into GF male wildtype mice. To further elucidate diet-microbe-host interactions, an additional HFD challenge of specifically colonized mice was conducted.

The current study shows no transfer of obesity from human to mouse via FMT

In the present study, we demonstrated that the microbiota of selected obese patients showing different levels of impaired insulin sensitivity and systemic inflammation was not able to induce an equivalent phenotype in gnotobiotic wildtype male mice. Recipients of the microbiota from obese patients showed no signs of obesity or altered weight development when compared to animals associated with lean-microbiota. Also, fat distribution, pad weight and metabolism were not different.

The human FMT study, which included the patients used for the humanized mouse model also showed unchanged body weights and inflammatory markers in patients after FMT treatment, which confirms our observed lack in phenotypic changes upon FMT in the different recipient mouse groups. Only fasting insulin levels of human subjects treated with allogenic FMT were significantly decreased after the treatment, whereas patients of the butyrate tablet group did not show changed insulin sensitivity [166].

Existing studies dealing with the effect of obese microbiota on host organism have shown controversial data. Some previous studies observed increased fat accumulation in mice treated with obese microbiota [36, 57]. However, Turnbaugh and coworkers [36] used mouse to mouse microbial transfer of obesity in C57BL/6J animals which makes comparability to our study difficult. Ridaura *et al.* [57] also used the C57BL/6J mouse model in their study, while C57BL/6N animals were used in the present study. It is known that C57BL/6J mice are more sensitive to DIO and glucose intolerance [167], which may explain different outcome.

However, in accordance with our data, Rabot *et al.* [138] did not observe mouse to mouse transferability of obesity in C57BL/6J. Additionally, Di Luccia and co-workers were also unable to influence total body weight, epididymal fat contents and glucose intolerance in high-fructose-fed rats

through FMT application of microbiota obtained from CD-fed lean animals [136]. Confirmatory, a recent study could also not observe an increase of fat mass in Swiss Webster mice humanized with lean or obese human microbiota [132]. These controversial study results underline that there is no common conclusion on this intriguing question of microbe-host-metabolism. Furthermore, the phenotype of type 1 diabetes, including beta cell loss, was not transmissible from human to mouse via FMT, suggesting difficulties in transmitting disease without the concurrent genetically or environmentally driven predisposition [168].

In the present study, the selected obese patients showed improved insulin levels, including HOMA indices and decreased CRP-values after FMT treatment compared to pre-treatment levels. These phenotypic differences could not be transferred to GF mice by colonization with the respective human microbiota. Based on our data, it could be concluded that transfer of obesity from human to mouse is not possible via FMT. However, the choice of donor microbiota may be of crucial importance in this context, which will be discussed in detail in the following chapter.

Furthermore, also the choice of animal model could play a central role in the transmission of an obese phenotype from donor to recipient. The anatomical dissimilarities - and resulting differences in the intestinal ecosystem - between human and murine models are frequently discussed in the scientific society.

Moreover, not only rodent models for FMT applications should be considered, but also transplantation studies with pigs which pronounced more similarity to humans regarding anatomy, physiology and metabolism of the digestive system [169]. Some studies already revealed human microbiota-associated porcine models as a suitable approach to research the development of gastrointestinal-related and metabolic diseases [170, 171], but FMT experiments of pigs in the context of obesity are still lacking.

Obesity-related FMT studies are heterogeneous

An important approach to unravel microbial signatures associated with obesity and comorbidities, is to detect confounding factors influencing study outcomes. In the present study, human phenotypes were not reproduced in mice after FMT. As already discussed, the human FMT study could also not show phenotypic changes after transfer of lean microbiota into obese patients [166]. In our experiments, potential reasons for not reproducing human disease in mice may be due to incorrect colonization periods, application time, selected animal model as well as selected human donors, or a combination of these factors.

The aim of FMT is to regain host health by increasing microbial diversity and function. Several routes and techniques have been used to transplant fecal microbiota from one individual to another.

Applications range from self to medically-administered enemas, oral capsules or nasogastric tube to colonic or duodenal endoscopy. As a consequence, there is no standardization of the processing, pretreatment of donor samples or form of application [172, 173]. Nevertheless, recently, guidelines for FMT treatments concerning donor recruitment and selection as well feces preparation and storage were published [174, 175]. A panel of European FMT experts agreed to establish a stool bank in order to improve standardization of FMT applications and working protocols [174].

In addition, variable approaches of microbiome analysis lead to different outcomes and interpretation of gut microbial profiles [176, 177]. Different methods for the analysis of the gut microbial composition, from collection and storage of feces to DNA extraction and NGS evaluation, challenge the comparability of study results as researchers are using different techniques and platforms [172]. One recent publication claimed that the outcome of the gut microbiota analysis strongly depended on the 16S rDNA target region of the selected primers, while the route of DNA extraction had little effect on the gut microbial profile [178]. **In summary, it is difficult to compare microbiome data without standardizing the NGS platform and analysis.**

The timing and duration of colonization trials also vary depending on the FMT study [57, 179-181]. Capturing the right time frame could be crucial in humanization trials for obesity and related comorbidities. In addition, inconsistent literature on diets used in FMT studies as well as lack of descriptions of dietary content do not allow final conclusions to be drawn.

Different diets and mouse models were used in obesity driven FMT trials with GF mice [54, 57, 131, 182]. It was first claimed that GF mice are resistant to DIO [131], which was contradicted by other studies as it turned out to be a diet-dependent effect [54, 182]. The role of diet in inducing a shift in bacterial composition and function is not understood either, as different dietary compositions were used in the studies [54, 171, 183-186]. Furthermore, metformin, which is used as an antidiabetic, could also be a major confounder in studies analyzing microbial profiles in obese patients. It has been shown that metformin medication *per se* alters the composition of the gut microbiome by increasing *Escherichia* and decreasing *Intestinibacter* species abundances [69].

In mouse studies, non-standardized chow diets, often used as a reference diet for DIO, may be an important confounder. Chow diets contain equal nutritional values, but the composition of macronutrients such as fat sources, fibers and proteins is not uniformly defined [187]. It should further be noted that it is in general complex to assess study results and the degree of obesity, since often only relative fat and body weight changes and not total weight data are displayed [36, 57, 128, 132, 137]. Without showing total body mass, it cannot be conclusively clarified whether animals really

become obese, as aggravation of phenotype - *i.e.* body weight, fat gain and adiposity index – might be observed only, if FMT and HFD are combined.

Dalby *et al.* compared the effect of HFD on the microbial composition and host physiology in mice using two reference diets - chow and a refined low-fat control diet. They observed that differences between the two control diets were more pronounced than differences between low-fat control diet and HFD [188]. This suggests that interactions between diet, microbe and host in (diet-induced) obesity are far more complex than originally thought and underlines the importance of a clear and standardized study design.

The transmission of obesity from human to mouse could depend on the selection of the human donor. Since the inter-individual differences in the human microbiome are huge [3], it may be important which obese human donor is finally selected for humanization studies [132]. In order to make a final statement, it is needed to increase the final number of selected human donors. Here, we used stool samples from a controlled human study with limited numbers. The patchy outcome of studies using FMT approaches already reveals the difficulties in finding the appropriate human donor [36, 57, 131, 132, 137, 173, 189]. One approach could be to use so-called super donors, as studies have shown that certain donors implant positive effects on recipients via FMT [38, 190]. **The selection of a so-called super donor could be crucial, but there is still a lack of additional profound and confirmatory literature. To date, there is no standardization of donors selected for FMT trials.**

Finally, it is essential to include a suitable control donor as reference for comparison of results. Here, we used a lean donor which underwent RYGB treatment before and served as a donor for the human FMT trial. Therefore, using a RYGB donor might have a cofounding effect on the outcome of the present study as gastric-bypass individuals showed different microbial composition than obese or lean counterparts [56, 128]. For future experiments, one may consider to increase the number of reference donors and to include not only a lean donor obtaining RYGB surgery [128, 132, 191]. In addition, using donors with the highest bacterial richness might be most promising, as studies showed a higher richness in lean compared to obese humans [18, 44, 64].

In summary, heterogeneous findings on bacterial species involved in the etiology and development of human obesity may be based on different study designs, number of subjects, microbiota-profiling methodologies, as well as so far unknown confounding factors.

Differences in donor and recipient microbiota are a potential explanation for lack of phenotype transfer

The microbiome of humans differs from that of mice [192]. Although the two dominant phyla Firmicutes and Bacteroidetes are shared, major differences in deeper taxonomic classification are

detectable. Ley *et al.* [48] reported that 85 % of mouse bacterial genera are not present in humans. Our data showed that after FMT treatment with the human microbiota, bacterial composition in the murine organism differed greatly from the human donor. This is probably the consequence of milieu differences resulting in the selection of different dominant bacteria as reported earlier [192].

Nevertheless, several FMT studies show a transfer of the respective human phenotype into mice [10, 57, 132]. One reason for these divergent results could be the loss of bacteria that may be responsible for triggering the obese phenotype. These 'obese' bacteria could be lost either before or after colonization of recipient mice. As fecal samples are difficult to process and need to be stored under strict anaerobic conditions, some obligate anaerobe bacteria will be lost between defecation, processing and inoculation of mice [191]. This would argue for a potential loss of strict anaerobic bacteria as a consequence of the transfer procedure and could be one explanation for differences in relative abundances between human donor microbial composition and the microbial composition in recipient mice. A loss of obesity-associated bacteria due to transfer conditions could thus explain the absent metabolic phenotype in recipients.

One example of an obesity-associated bacterium is *C. ramosum* [75], which was not found to be increased in the relevant mouse groups in this study. Additionally, we observed a loss of *Ruminococcaceae* which are also connected with human obesity [193]. A potential loss of obesity-associated bacteria - independent of transfer conditions - could further be due to the adaptation of the microbial community to the new habitat of the murine gut. The environmental conditions between human and murine gut are different with respect to nutrients, anatomical structures, pH value and bile acids [192].

We have achieved transfer efficiencies of about 50 % from human to mouse, which is comparable to published data [57, 132, 194, 195]. Nevertheless, the question arises why obesity-triggering bacteria engrafted in the murine intestinal habitat in other studies, but were lost in the present study. Possible explanations could be the genetic background of recipients and the diets used. A possible solution to prevent loss of obesity-associated bacteria from a complex human microbiota during transfer could be in using a defined bacterial consortium instead of a complex ecosystem.

In this study, we colonized GF mice with four complex human microbiota ecosystems of two patients. One selected obese human donor received autologous FMT additionally to a daily dose of butyrate tablets (pre/postFMT[but]). The other obese donor got FMT from a lean participant and placebo tablets (pre/postFMT[lean]). Surprisingly, mice colonized with preFMT[lean]-microbiota showed no significant changes in bacterial community structures after the patient's treatment (postFMT[lean]-mice). However, animals transplanted with preFMT[but]-microbiota exhibited significant differences in microbial profiles

compared to postFMT[but]-colonized mice. These results could be explained by the more scattered microbial profiles in FMT[lean]-mouse groups than in FMT[but]-groups, which showed more homogenous outcomes.

The causative contribution of the gut microbiota to obesity-related pathologies is uncertain

In general, the overall interest for usage of FMT in the context of human disease is increasing, which goes along with an increase in research studies. Currently, FMT is primarily and efficiently used to treat recurrent *C. difficile* infections [115] or IBD [120]. In addition, FMT studies have also been conducted with patients suffering from obesity and associated disorders, but there is only limited literature on the subject and outcome varies with respect to insulin sensitivity after FMT treatment (Table 5) [38, 124, 125]. Studies with humanized mouse models in which GF or antibiotic treated mice have been colonized with microbiota, originating from humans with a distinct disease, are becoming more frequent, but inconsistent (Table 5) [57, 132, 179]. Humanized mouse models were introduced to enhance translation of general processes in human pathology development. Transplantation of a complex fecal gut microbiome is an approach to transfer the human phenotype and to elucidate the potential causative role of gut microbes in the context of diseases like obesity [196]. But still, there is inconsistent literature on failure and success rates of FMT studies [191, 197].

Table 5: Examples of human-to-human or human-to-mouse FMT studies in the context of obesity

Study	Human donor stool	Recipient	Experimental setup	Main findings
Vrieze *et al.* [38]	Lean adults	Metabolic syndrome adults	Transfer of lean microbiota; readouts after 6 wks of FMT	Increased insulin sensitivity after FMT; no changes in body weight, fat mass and glucose levels
Kootte *et al.* [124]	Lean adult	Metabolic syndrome adults	Transfer of lean microbiota; readouts after 6 wks and 18 wks of FMT	Increased sensitivity after 6 wks, which diminished after 18 wks; no changes in body weight and glucose levels
Smits *et al.* [125]	Lean vegan adults	Metabolic syndrome adults	Transfer of lean microbiota; readouts after 2 wks of FMT	No changes in body weight, insulin and glucose levels
Turnbaugh *et al.* [179]	Healthy adult HM lean and obese mice	GF C57BL/6J mice	Dietary intervention (LFD vs. WD) of HM mice, subsequently transfer of HM microbiota; readouts after 2 wks of FMT	Responsiveness to diet of HM mice; phenotypic transfer of adiposity from HM mice to GF mice after FMT
Ridaura *et al.* [57]	Lean and obese twins	GF C57BL/6J mice	Transfer of lean and obese microbiota; readouts after 2 wks of FMT	Phenotypic transfer of adiposity
Zhang *et al.* [132]	Lean and obese adults	GF Swiss Webster mice	Transfer of lean and obese microbiota; readouts after 52 days of FMT	Partly phenotypic transfer of obesity; no changes in fat mass; differences in insulin levels after FMT did not match with donor situation

FMT – Fecal microbiota transplantation. GF – germfree; Wks – weeks. HM – humanized. LFD – Low-fat diet. WD – Western diet (high-fat/high-sugar diet).

Scientific findings for obesity-induced pathologies are controversial

Cani *et al.* [82, 92] stated that HFD feeding is associated with increased levels of endotoxin in systemic blood serum as a consequence of changes in the gut flora. In our study, we could not confirm a connection between DIO and serum LPS levels. Additionally, DIO-induced microbial composition changes were not accompanied by changes in the ratio of Firmicutes to Bacteriodetes or a loss of bacterial richness which is contrary to literature [36, 45], but mirrors observation of others [3, 40, 56].

In the present study, HFD-triggered obesity induced distinct clusters in microbial profiles compared to CD-fed mice. However, feeding effects were only observed in postFMT[but]- and preFMT[lean]-microbiota associated mice, whereas microbial profiles of residual colonization groups were not affected by diet. It is widely accepted that HFD feeding and/or DIO is associated with changes in microbial composition [36, 45, 48, 55, 198], but it is still controversially discussed which bacterial cluster(s) or specific strains are involved [1, 8, 40, 64, 71, 199]. The differences in study outcomes could be due to chow versus HFD-diet effects. HFD-driven changes in the murine gut microbiota are regarded to be rather nutritional than obesity-induced. In addition, glucose intolerance in mice is associated with HFD, independent of changes in the gut microbiota [188].

In accordance with literature, we showed that HFD triggered an increase in glucose levels, as well as a two- to three-fold elevation in fat tissue inflammation [82, 92]. Nevertheless, intestinal inflammation and gut barrier breakage were not associated with DIO in this study. The connection between DIO, intestinal inflammation and gut barrier breakage in general is controversially discussed in literature [82, 97, 101].

The response of GF mice to HFD was shown to be dependent on the type of high-calorie diet given to the animals, with a particular importance of dietary fat source [54, 131]. Kübeck *et al.* [182] showed that a palm-oil based diet induced obesity in GF mice, whereas a lard-based diet did not. As a consequence, it is essential to look at macronutrients involved in the diet, as the main difference between the diets used in this study was the higher cholesterol content in the lard-based diet. It was then hypothesized that mice on lard-based diet were less efficient in fat absorption and revealed a higher metabolic rate.

Taken together, data on microbial composition, gut barrier function and inflammation in context of obesity are still inconsistent. Possible reasons for the inconsistent outcome of studies could be differences in the used diets in terms of total energy content as well as the amount and composition of macronutrients like fat sources, fibers and proteins.

Obesity-related microbiota does not affect the development of liver steatosis in the current study

Non-alcoholic fatty liver disease (NAFLD) is linked to obesity [200], adipose tissue inflammation [201] and gut dysfunction [49]. Gut dysfunction is defined by increased gut permeability, changes in microbial derived SCFAs and compositional shifts in the gut microbiome [49]. In this study, we were able to show that HFD induced liver steatosis regardless of the donor microbiota. Microbial composition changes have been associated with humans and mice suffering from NAFLD or non-alcoholic steatohepatitis (NASH) [50, 105, 200]. Here, steatosis was observed in CD-fed lean-mice, but not in animals colonized with any obese microbiota. Hence, different human microbial ecosystems can lead to different phenotypes in the murine liver, but no correlation between obese human microbiota and liver steatosis was observed.

Experimental setup is a crucial confounding factor for translational FMT studies

Two sets of GF mice were colonized with human obese microbiota (preFMT[lean]) in order to examine the effect of colonization period and colonization time. The first group was colonized with preFMT[lean]-microbiota for 12 weeks und was subsequently challenged with HFD for 4 weeks. The second group was simultaneously colonized with preFMT[lean]-microbiota and challenged with HFD for four weeks (preFMT[lean]short). In both experimental groups, mice fed HFD showed a significant gain in body mass compared to mice fed CD. In contrast to the preFMT[lean]-group, preFMT[lean]short-mice showed no elevated fasting glucose and insulin levels and no HFD-induced glucose intolerance. Similar to the long-term colonized mice, transfer of obese human fecal microbiota did not lead to an equivalent phenotype in mice. Although, preFMT[lean]- and preFMT[lean]short-mice showed significantly bigger fat pads and a higher fat to body weight ratio after 4 weeks of HFD feeding, a shorter colonization period rescued the recipients from fat hypertrophy in epididymal tissues, maybe due to age-dependent metabolic changes, in contrast to the 12 weeks colonization group.

Low-grade inflammation of adipose tissue, which was shown in 16 weeks old mice (preFMT[lean]-group), was diminished in short-term colonized mice. Compared to 16 weeks old mice, 8 weeks old mice (preFMT[lean]short) fed HFD were protected from liver steatosis. In contrast, preFMT[lean]short-mice showed hepatic inflammation upon HFD, which was not the case in preFMT[lean]-animals. Possibly due to the age and lower initial weight of the preFMT[lean]short-group prior to treatment, they responded differently in terms of glucose, fat and liver metabolism.

In literature, age-dependent differences in phenotype in response to treatment were confirmed, but controversially discussed to data seen in this study [202-205]. Noteworthy, there is only literature on age-dependent differences in elder mice existing, so a direct comparison of the data was not possible.

Another explanation for different outcomes of the long- and short-term experiments in response to HFD could be mucus-maturation of the gut. In GF animals, mucus formation is incomplete and only fully established in six weeks after confrontation with bacteria [206]. Mice of preFMT[lean]short-group were challenged with HFD and fecal microbiota simultaneously, meaning that the gut barrier was maybe not yet adapted to bacteria when opposed to HFD. As a consequence, fatty acids could be differently metabolized in preFMT[lean]short-mice in comparison to preFMT[lean]-animals. Furthermore, the current study revealed significant changes in microbiota composition between preFMT[lean]- and preFMT[lean]short-colonized mice (data not shown). Due to divergent gut environments, mice could respond differently to HFD with respect to host metabolism as well as gut, liver, fat structure and function.

6 Conclusion and perspective

This study showed that a human obese phenotype is not transferable to GF mice by fecal microbiota transplantation under the selected experimental conditions. Obese human microbiota per se had no influence on the recipient´s phenotype, including metabolism and inflammation. Independent of donor microbiota, colonized mice showed no sign of obesity or insulin resistance. Diet, but not human microbiota induced an increase in body weight, insulin resistance, adipose tissue inflammation and liver steatosis.

The transferability of obesity from mouse to mouse or human to mouse has been controversially discussed in literature before. The question arises as to whether FMT trials are suitable or optimal models for transferring a complex human microbiota into a GF mouse model. It is also proposed to use FMTs with conventional or antibiotic treated mice rather than gnotobiotic or sterile recipients, which better reflects the clinical situation. Also, the consideration whether other animal models – *e.g.* pigs – might be more suitable for dietary intervention studies, should be applied. Hence, the role of intestinal microbiota on metabolic and inflammatory phenotypes is still not fully clarified. Further research on an increased number of human donors, different onsets and duration of colonization and an optimized colonization process will be needed to clarify the hypothesis that obesity is transferable into mice via FMT.

For future experiments it would be also a promising approach to start with mouse to mouse microbiota transfer, as the transfer efficiency of microbes was higher than in human to mouse transplantations [57, 195]. Additionally, FMT in rats would be another attempt as transfer rates were higher than in mice [194]. As a next step transferring of consortia with defined bacterial organisms based on human strains could be a fruitful approach for the future.

FMTs in humans are often used in clinical studies to treat diseases like CDI, IBD and recently obesity with different outcomes. Still, the question if the microbiota is causative or associative factor in pathology development has to be resolved. Confirmatively, FMTs using in mouse models show both, fail and success regarding the transferability of disease.

List of Figures

List of Tables

Abbreviations

AUC	Area under the curves
BMI	Body mass index
bp	Base pairs
C.	*Clostridium*
CD	Control diet
cDNA	Complementary DNA
cfu/g	Colony forming units per gram
CRP	C-reactive protein
CVD	Cardiovascular disease
DIO	Diet-induced obesity
DNA	Deoxyribonucleic acid
DSM	Deutsche Sammlung von Mikroorganismen
DTT	Dithiothreitol
E.	*Enterobacter*
EDTA	Ethylenediaminetetraacetate
EGTA	Ethyleneglycol-bis-tetraacetate
eWAT	Epididymal white adipose tissue
F4/80	Macrophage marker
FITC	Fluorescein isothiocyanate
GAPDH	Glyceraldehyde 3-phosphate dehydrogenase
GF	Germfree
H	Hour
Hba1c	Hemoglybin A1c
HDL	High-density lipoprotein
HFD	High-fat diet
HOMA-IR	homeostatic model assessment of insulin resistance
HPRT	Hypoxanthine-guanine phosphoribosyltransferase
IL	Interleukin
INF	Interferon
IR	Insulin resistance
LPB	Lipopolysaccharide binding protein
LPS	Lipopolysaccharide
MCP	Monocyte chemoattractant protein
min	Minutes
mRNA	Messenger RNA
mWAT	Mesenteric white adipose tissue
NaCl	Sodium chloride
NALFD	Non-alcoholic fatty liver disease
NASH	Non-alcoholic steatohepatitis
NfE	Nitrogen free extracts
OGTT	Oral glucose tolerance test
OTU	Operational Taxonomic Units
PBS	Phosphate buffered saline
PCR	Polymerase chain reaction
qPCR	Quantitative polymerase chain reaction
rRNA	Ribosomal ribonucleic acid
RT	Room temperature
RYBG	Roux-en-Y gastric bypass
SAA	Serum amyloid A
SCFA	Short-chain fatty acid
SD	Standard deviation
sWAT	Subcutaneous white adipose tissue
T2D	Type 2 diabetes
TER	Transepithelial resistance
TLR	Toll-like receptor
TNF	Tumor necrosis factor

UPL	Universal Probe Library
V3/V4	Variable regions 3 and 4
WAT	White adipose tissue
WCA	Wilkins-Chalgren-Agar
WKS	Weeks
ZO	Zona occludens

References

1. Qin, J., et al., *A human gut microbial gene catalogue established by metagenomic sequencing.* Nature, 2010. **464**(7285): p. 59-65.
2. Sender, R., S. Fuchs, and R. Milo, *Revised Estimates for the Number of Human and Bacteria Cells in the Body.* PLoS Biol, 2016. **14**(8): p. e1002533.
3. Human Microbiome Project, C., *Structure, function and diversity of the healthy human microbiome.* Nature, 2012. **486**(7402): p. 207-14.
4. Hugon, P., et al., *A comprehensive repertoire of prokaryotic species identified in human beings.* Lancet Infect Dis, 2015. **15**(10): p. 1211-1219.
5. Li, J., et al., *An integrated catalog of reference genes in the human gut microbiome.* Nat Biotechnol, 2014. **32**(8): p. 834-41.
6. Ley, R.E., D.A. Peterson, and J.I. Gordon, *Ecological and evolutionary forces shaping microbial diversity in the human intestine.* Cell, 2006. **124**(4): p. 837-48.
7. Vrieze, A., et al., *The environment within: how gut microbiota may influence metabolism and body composition.* Diabetologia, 2010. **53**(4): p. 606-13.
8. David, L.A., et al., *Diet rapidly and reproducibly alters the human gut microbiome.* Nature, 2014. **505**(7484): p. 559-63.
9. Nicholson, J.K., et al., *Host-gut microbiota metabolic interactions.* Science, 2012. **336**(6086): p. 1262-7.
10. Goodrich, J.K., et al., *Human genetics shape the gut microbiome.* Cell, 2014. **159**(4): p. 789-99.
11. Faith, J.J., et al., *The long-term stability of the human gut microbiota.* Science, 2013. **341**(6141): p. 1237439.
12. Dore, J., et al., *Hot topics in gut microbiota.* United European Gastroenterol J, 2013. **1**(5): p. 311-8.
13. Maurice, C.F., H.J. Haiser, and P.J. Turnbaugh, *Xenobiotics shape the physiology and gene expression of the active human gut microbiome.* Cell, 2013. **152**(1-2): p. 39-50.
14. Jernberg, C., et al., *Long-term ecological impacts of antibiotic administration on the human intestinal microbiota.* ISME J, 2007. **1**(1): p. 56-66.
15. Tyakht, A.V., et al., *Human gut microbiota community structures in urban and rural populations in Russia.* Nat Commun, 2013. **4**: p. 2469.
16. Sommer, F. and F. Backhed, *The gut microbiota--masters of host development and physiology.* Nat Rev Microbiol, 2013. **11**(4): p. 227-38.
17. Nielsen, H.B., et al., *Identification and assembly of genomes and genetic elements in complex metagenomic samples without using reference genomes.* Nat Biotechnol, 2014. **32**(8): p. 822-8.
18. Turnbaugh, P.J., et al., *A core gut microbiome in obese and lean twins.* Nature, 2009. **457**(7228): p. 480-4.
19. Arumugam, M., et al., *Enterotypes of the human gut microbiome.* Nature, 2011. **473**(7346): p. 174-80.
20. Wu, G.D., et al., *Linking long-term dietary patterns with gut microbial enterotypes.* Science, 2011. **334**(6052): p. 105-8.
21. Liang, C., et al., *Diversity and enterotype in gut bacterial community of adults in Taiwan.* BMC Genomics, 2017. **18**(Suppl 1): p. 932.
22. Ding, T. and P.D. Schloss, *Dynamics and associations of microbial community types across the human body.* Nature, 2014. **509**(7500): p. 357-60.
23. Smith, K., K.D. McCoy, and A.J. Macpherson, *Use of axenic animals in studying the adaptation of mammals to their commensal intestinal microbiota.* Semin Immunol, 2007. **19**(2): p. 59-69.
24. Kau, A.L., et al., *Human nutrition, the gut microbiome and the immune system.* Nature, 2011. **474**(7351): p. 327-36.
25. Round, J.L. and S.K. Mazmanian, *The gut microbiota shapes intestinal immune responses during health and disease.* Nat Rev Immunol, 2009. **9**(5): p. 313-23.

26. Hooper, L.V., D.R. Littman, and A.J. Macpherson, *Interactions between the microbiota and the immune system.* Science, 2012. **336**(6086): p. 1268-73.

27. Sorbara, M.T. and E.G. Pamer, *Interbacterial mechanisms of colonization resistance and the strategies pathogens use to overcome them.* Mucosal Immunol, 2018.

28. Jia, W., et al., *Gut microbiota: a potential new territory for drug targeting.* Nat Rev Drug Discov, 2008. **7**(2): p. 123-9.

29. Backhed, F., *Programming of host metabolism by the gut microbiota.* Ann Nutr Metab, 2011. **58 Suppl 2**: p. 44-52.

30. Fukuda, S. and H. Ohno, *Gut microbiome and metabolic diseases.* Semin Immunopathol, 2014. **36**(1): p. 103-14.

31. Goto, Y. and Ivanov, II, *Intestinal epithelial cells as mediators of the commensal-host immune crosstalk.* Immunol Cell Biol, 2013. **91**(3): p. 204-14.

32. Goto, Y., *Epithelial Cells as a Transmitter of Signals From Commensal Bacteria and Host Immune Cells.* Front Immunol, 2019. **10**: p. 2057.

33. Jimenez-Dalmaroni, M.J., M.E. Gerswhin, and I.E. Adamopoulos, *The critical role of toll-like receptors--From microbial recognition to autoimmunity: A comprehensive review.* Autoimmun Rev, 2016. **15**(1): p. 1-8.

34. Krumbeck, J.A., et al., *Probiotic Bifidobacterium strains and galactooligosaccharides improve intestinal barrier function in obese adults but show no synergism when used together as synbiotics.* Microbiome, 2018. **6**(1): p. 121.

35. Tremaroli, V. and F. Backhed, *Functional interactions between the gut microbiota and host metabolism.* Nature, 2012. **489**(7415): p. 242-9.

36. Turnbaugh, P.J., et al., *An obesity-associated gut microbiome with increased capacity for energy harvest.* Nature, 2006. **444**(7122): p. 1027-31.

37. Marchix, J., G. Goddard, and M.A. Helmrath, *Host-Gut Microbiota Crosstalk in Intestinal Adaptation.* Cell Mol Gastroenterol Hepatol, 2018. **6**(2): p. 149-162.

38. Vrieze, A., et al., *Transfer of intestinal microbiota from lean donors increases insulin sensitivity in individuals with metabolic syndrome.* Gastroenterology, 2012. **143**(4): p. 913-6 e7.

39. Canfora, E.E., et al., *Gut microbial metabolites in obesity, NAFLD and T2DM.* Nat Rev Endocrinol, 2019. **15**(5): p. 261-273.

40. Schwiertz, A., et al., *Microbiota and SCFA in lean and overweight healthy subjects.* Obesity (Silver Spring), 2010. **18**(1): p. 190-5.

41. Gevers, D., et al., *The treatment-naive microbiome in new-onset Crohn's disease.* Cell Host Microbe, 2014. **15**(3): p. 382-392.

42. Kostic, A.D., et al., *The dynamics of the human infant gut microbiome in development and in progression toward type 1 diabetes.* Cell Host Microbe, 2015. **17**(2): p. 260-73.

43. Koeth, R.A., et al., *Intestinal microbiota metabolism of L-carnitine, a nutrient in red meat, promotes atherosclerosis.* Nat Med, 2013. **19**(5): p. 576-85.

44. Le Chatelier, E., et al., *Richness of human gut microbiome correlates with metabolic markers.* Nature, 2013. **500**(7464): p. 541-6.

45. Ley, R.E., et al., *Microbial ecology: human gut microbes associated with obesity.* Nature, 2006. **444**(7122): p. 1022-3.

46. Jumpertz, R., et al., *Energy-balance studies reveal associations between gut microbes, caloric load, and nutrient absorption in humans.* Am J Clin Nutr, 2011. **94**(1): p. 58-65.

47. Duncan, S.H., et al., *Human colonic microbiota associated with diet, obesity and weight loss.* Int J Obes (Lond), 2008. **32**(11): p. 1720-4.

48. Ley, R.E., et al., *Obesity alters gut microbial ecology.* Proc Natl Acad Sci U S A, 2005. **102**(31): p. 11070-5.

49. Boursier, J., et al., *The severity of nonalcoholic fatty liver disease is associated with gut dysbiosis and shift in the metabolic function of the gut microbiota.* Hepatology, 2016. **63**(3): p. 764-75.

50. Le Roy, T., et al., *Intestinal microbiota determines development of non-alcoholic fatty liver disease in mice.* Gut, 2013. **62**(12): p. 1787-94.

51.   Grabherr, F., et al., *Gut Dysfunction and Non-alcoholic Fatty Liver Disease.* Front Endocrinol (Lausanne), 2019. **10**: p. 611.

52.   Turnbaugh, P.J., et al., *Diet-induced obesity is linked to marked but reversible alterations in the mouse distal gut microbiome.* Cell Host Microbe, 2008. **3**(4): p. 213-23.

53.   Daniel, H., et al., *High-fat diet alters gut microbiota physiology in mice.* ISME J, 2014. **8**(2): p. 295-308.

54.   Fleissner, C.K., et al., *Absence of intestinal microbiota does not protect mice from diet-induced obesity.* Br J Nutr, 2010. **104**(6): p. 919-29.

55.   Karlsson, F.H., et al., *Gut metagenome in European women with normal, impaired and diabetic glucose control.* Nature, 2013. **498**(7452): p. 99-103.

56.   Zhang, H., et al., *Human gut microbiota in obesity and after gastric bypass.* Proc Natl Acad Sci U S A, 2009. **106**(7): p. 2365-70.

57.   Ridaura, V.K., et al., *Gut microbiota from twins discordant for obesity modulate metabolism in mice.* Science, 2013. **341**(6150): p. 1241214.

58.   den Besten, G., et al., *Short-Chain Fatty Acids Protect Against High-Fat Diet-Induced Obesity via a PPARgamma-Dependent Switch From Lipogenesis to Fat Oxidation.* Diabetes, 2015. **64**(7): p. 2398-408.

59.   Fava, F., et al., *The type and quantity of dietary fat and carbohydrate alter faecal microbiome and short-chain fatty acid excretion in a metabolic syndrome 'at-risk' population.* Int J Obes (Lond), 2013. **37**(2): p. 216-23.

60.   Santacruz, A., et al., *Interplay between weight loss and gut microbiota composition in overweight adolescents.* Obesity (Silver Spring), 2009. **17**(10): p. 1906-15.

61.   Furet, J.P., et al., *Differential adaptation of human gut microbiota to bariatric surgery-induced weight loss: links with metabolic and low-grade inflammation markers.* Diabetes, 2010. **59**(12): p. 3049-57.

62.   Brignardello, J., et al., *Pilot study: alterations of intestinal microbiota in obese humans are not associated with colonic inflammation or disturbances of barrier function.* Aliment Pharmacol Ther, 2010. **32**(11-12): p. 1307-14.

63.   Karlsson, C.L., et al., *The microbiota of the gut in preschool children with normal and excessive body weight.* Obesity (Silver Spring), 2012. **20**(11): p. 2257-61.

64.   Cotillard, A., et al., *Dietary intervention impact on gut microbial gene richness.* Nature, 2013. **500**(7464): p. 585-8.

65.   Larsen, N., et al., *Gut microbiota in human adults with type 2 diabetes differs from non-diabetic adults.* PLoS One, 2010. **5**(2): p. e9085.

66.   Wu, X., et al., *Molecular characterisation of the faecal microbiota in patients with type II diabetes.* Curr Microbiol, 2010. **61**(1): p. 69-78.

67.   Qin, J., et al., *A metagenome-wide association study of gut microbiota in type 2 diabetes.* Nature, 2012. **490**(7418): p. 55-60.

68.   Zhang, X., et al., *Human gut microbiota changes reveal the progression of glucose intolerance.* PLoS One, 2013. **8**(8): p. e71108.

69.   Forslund, K., et al., *Disentangling type 2 diabetes and metformin treatment signatures in the human gut microbiota.* Nature, 2015. **528**(7581): p. 262-266.

70.   Walters, W.A., Z. Xu, and R. Knight, *Meta-analyses of human gut microbes associated with obesity and IBD.* FEBS Lett, 2014. **588**(22): p. 4223-33.

71.   Finucane, M.M., et al., *A taxonomic signature of obesity in the microbiome? Getting to the guts of the matter.* PLoS One, 2014. **9**(1): p. e84689.

72.   Sze, M.A. and P.D. Schloss, *Looking for a Signal in the Noise: Revisiting Obesity and the Microbiome.* MBio, 2016. **7**(4).

73.   Reijnders, D., et al., *Effects of Gut Microbiota Manipulation by Antibiotics on Host Metabolism in Obese Humans: A Randomized Double-Blind Placebo-Controlled Trial.* Cell Metab, 2016. **24**(2): p. 341.

74. Plovier, H., et al., *A purified membrane protein from Akkermansia muciniphila or the pasteurized bacterium improves metabolism in obese and diabetic mice.* Nat Med, 2017. **23**(1): p. 107-113.

75. Woting, A., et al., *Clostridium ramosum promotes high-fat diet-induced obesity in gnotobiotic mouse models.* MBio, 2014. **5**(5): p. e01530-14.

76. Fei, N. and L. Zhao, *An opportunistic pathogen isolated from the gut of an obese human causes obesity in germfree mice.* ISME J, 2013. **7**(4): p. 880-4.

77. *Obesity: preventing and managing the global epidemic. Report of a WHO consultation.* World Health Organ Tech Rep Ser, 2000. **894**: p. i-xii, 1-253.

78. Comuzzie, A.G. and D.B. Allison, *The search for human obesity genes.* Science, 1998. **280**(5368): p. 1374-7.

79. Hill, J.O. and J.C. Peters, *Environmental contributions to the obesity epidemic.* Science, 1998. **280**(5368): p. 1371-4.

80. Speakman, J.R., et al., *Set points, settling points and some alternative models: theoretical options to understand how genes and environments combine to regulate body adiposity.* Dis Model Mech, 2011. **4**(6): p. 733-45.

81. Xu, H., et al., *Chronic inflammation in fat plays a crucial role in the development of obesity-related insulin resistance.* J Clin Invest, 2003. **112**(12): p. 1821-30.

82. Cani, P.D., et al., *Metabolic endotoxemia initiates obesity and insulin resistance.* Diabetes, 2007. **56**(7): p. 1761-72.

83. Bournat, J.C. and C.W. Brown, *Mitochondrial dysfunction in obesity.* Curr Opin Endocrinol Diabetes Obes, 2010. **17**(5): p. 446-52.

84. Musso, G., R. Gambino, and M. Cassader, *Obesity, diabetes, and gut microbiota: the hygiene hypothesis expanded?* Diabetes Care, 2010. **33**(10): p. 2277-84.

85. Nakatsuji, H., et al., *Dysregulation of glucose, insulin, triglyceride, blood pressure, and oxidative stress after an oral glucose tolerance test in men with abdominal obesity.* Metabolism, 2010. **59**(4): p. 520-6.

86. Bays, H.E., et al., *Obesity, adiposity, and dyslipidemia: a consensus statement from the National Lipid Association.* J Clin Lipidol, 2013. **7**(4): p. 304-83.

87. Bramlage, P., et al., *Hypertension in overweight and obese primary care patients is highly prevalent and poorly controlled.* Am J Hypertens, 2004. **17**(10): p. 904-10.

88. Tuomilehto, J., et al., *Prevention of type 2 diabetes mellitus by changes in lifestyle among subjects with impaired glucose tolerance.* N Engl J Med, 2001. **344**(18): p. 1343-50.

89. Kahn, S.E., R.L. Hull, and K.M. Utzschneider, *Mechanisms linking obesity to insulin resistance and type 2 diabetes.* Nature, 2006. **444**(7121): p. 840-6.

90. Keller, U., *From obesity to diabetes.* Int J Vitam Nutr Res, 2006. **76**(4): p. 172-7.

91. Wright, S.D., et al., *CD14, a receptor for complexes of lipopolysaccharide (LPS) and LPS binding protein.* Science, 1990. **249**(4975): p. 1431-3.

92. Cani, P.D., et al., *Changes in gut microbiota control metabolic endotoxemia-induced inflammation in high-fat diet-induced obesity and diabetes in mice.* Diabetes, 2008. **57**(6): p. 1470-81.

93. Muccioli, G.G., et al., *The endocannabinoid system links gut microbiota to adipogenesis.* Mol Syst Biol, 2010. **6**: p. 392.

94. Everard, A., et al., *Responses of gut microbiota and glucose and lipid metabolism to prebiotics in genetic obese and diet-induced leptin-resistant mice.* Diabetes, 2011. **60**(11): p. 2775-86.

95. Brun, P., et al., *Increased intestinal permeability in obese mice: new evidence in the pathogenesis of nonalcoholic steatohepatitis.* Am J Physiol Gastrointest Liver Physiol, 2007. **292**(2): p. G518-25.

96. Kaliannan, K., et al., *Intestinal alkaline phosphatase prevents metabolic syndrome in mice.* Proc Natl Acad Sci U S A, 2013. **110**(17): p. 7003-8.

97. Lam, Y.Y., et al., *Increased gut permeability and microbiota change associate with mesenteric fat inflammation and metabolic dysfunction in diet-induced obese mice.* PLoS One, 2012. **7**(3): p. e34233.

98.   Serino, M., et al., *Metabolic adaptation to a high-fat diet is associated with a change in the gut microbiota.* Gut, 2012. **61**(4): p. 543-53.

99.   de La Serre, C.B., et al., *Propensity to high-fat diet-induced obesity in rats is associated with changes in the gut microbiota and gut inflammation.* Am J Physiol Gastrointest Liver Physiol, 2010. **299**(2): p. G440-8.

100.   Suzuki, T. and H. Hara, *Dietary fat and bile juice, but not obesity, are responsible for the increase in small intestinal permeability induced through the suppression of tight junction protein expression in LETO and OLETF rats.* Nutr Metab (Lond), 2010. **7**: p. 19.

101.   Kless, C., et al., *Diet-induced obesity causes metabolic impairment independent of alterations in gut barrier integrity.* Mol Nutr Food Res, 2015. **59**(5): p. 968-78.

102.   Muller, V.M., et al., *Gut barrier impairment by high-fat diet in mice depends on housing conditions.* Mol Nutr Food Res, 2016. **60**(4): p. 897-908.

103.   Nier, A., et al., *Markers of intestinal permeability are already altered in early stages of non-alcoholic fatty liver disease: Studies in children.* PLoS One, 2017. **12**(9): p. e0183282.

104.   Younossi, Z.M., et al., *Global epidemiology of nonalcoholic fatty liver disease-Meta-analytic assessment of prevalence, incidence, and outcomes.* Hepatology, 2016. **64**(1): p. 73-84.

105.   Mouzaki, M., et al., *Intestinal microbiota in patients with nonalcoholic fatty liver disease.* Hepatology, 2013. **58**(1): p. 120-7.

106.   Raman, M., et al., *Fecal microbiome and volatile organic compound metabolome in obese humans with nonalcoholic fatty liver disease.* Clin Gastroenterol Hepatol, 2013. **11**(7): p. 868-75 e1-3.

107.   Michail, S., et al., *Altered gut microbial energy and metabolism in children with non-alcoholic fatty liver disease.* FEMS Microbiol Ecol, 2015. **91**(2): p. 1-9.

108.   Hofmann, A.F. and L.R. Hagey, *Bile acids: chemistry, pathochemistry, biology, pathobiology, and therapeutics.* Cell Mol Life Sci, 2008. **65**(16): p. 2461-83.

109.   Lin, H., et al., *Alterations of Bile Acids and Gut Microbiota in Obesity Induced by High Fat Diet in Rat Model.* J Agric Food Chem, 2019. **67**(13): p. 3624-3632.

110.   Wewalka, M., et al., *Fasting serum taurine-conjugated bile acids are elevated in type 2 diabetes and do not change with intensification of insulin.* J Clin Endocrinol Metab, 2014. **99**(4): p. 1442-51.

111.   Cariou, B., et al., *Fasting plasma chenodeoxycholic acid and cholic acid concentrations are inversely correlated with insulin sensitivity in adults.* Nutr Metab (Lond), 2011. **8**(1): p. 48.

112.   Haeusler, R.A., et al., *Human insulin resistance is associated with increased plasma levels of 12alpha-hydroxylated bile acids.* Diabetes, 2013. **62**(12): p. 4184-91.

113.   Mouzaki, M., et al., *Bile Acids and Dysbiosis in Non-Alcoholic Fatty Liver Disease.* PLoS One, 2016. **11**(5): p. e0151829.

114.   Eiseman, B., et al., *Fecal enema as an adjunct in the treatment of pseudomembranous enterocolitis.* Surgery, 1958. **44**(5): p. 854-9.

115.   van Nood, E., M.G. Dijkgraaf, and J.J. Keller, *Duodenal infusion of feces for recurrent Clostridium difficile.* N Engl J Med, 2013. **368**(22): p. 2145.

116.   Weingarden, A.R., et al., *Microbiota transplantation restores normal fecal bile acid composition in recurrent Clostridium difficile infection.* Am J Physiol Gastrointest Liver Physiol, 2014. **306**(4): p. G310-9.

117.   Kassam, Z., et al., *Fecal microbiota transplantation for Clostridium difficile infection: systematic review and meta-analysis.* Am J Gastroenterol, 2013. **108**(4): p. 500-8.

118.   Moayyedi, P., et al., *Fecal Microbiota Transplantation Induces Remission in Patients With Active Ulcerative Colitis in a Randomized Controlled Trial.* Gastroenterology, 2015. **149**(1): p. 102-109 e6.

119.   Rossen, N.G., et al., *Findings From a Randomized Controlled Trial of Fecal Transplantation for Patients With Ulcerative Colitis.* Gastroenterology, 2015. **149**(1): p. 110-118 e4.

120.   Vaughn, B.P., et al., *Increased Intestinal Microbial Diversity Following Fecal Microbiota Transplant for Active Crohn's Disease.* Inflamm Bowel Dis, 2016. **22**(9): p. 2182-90.

121. Fischer, M., et al., *Fecal Microbiota Transplantation is Safe and Efficacious for Recurrent or Refractory Clostridium difficile Infection in Patients with Inflammatory Bowel Disease.* Inflamm Bowel Dis, 2016. **22**(10): p. 2402-9.

122. Cui, B., et al., *Fecal microbiota transplantation through mid-gut for refractory Crohn's disease: safety, feasibility, and efficacy trial results.* J Gastroenterol Hepatol, 2015. **30**(1): p. 51-8.

123. Smith, M.I., et al., *Gut microbiomes of Malawian twin pairs discordant for kwashiorkor.* Science, 2013. **339**(6119): p. 548-54.

124. Kootte, R.S., et al., *Improvement of Insulin Sensitivity after Lean Donor Feces in Metabolic Syndrome Is Driven by Baseline Intestinal Microbiota Composition.* Cell Metab, 2017. **26**(4): p. 611-619 e6.

125. Smits, L.P., et al., *Effect of Vegan Fecal Microbiota Transplantation on Carnitine- and Choline-Derived Trimethylamine-N-Oxide Production and Vascular Inflammation in Patients With Metabolic Syndrome.* J Am Heart Assoc, 2018. **7**(7).

126. Li, S.S., et al., *Durable coexistence of donor and recipient strains after fecal microbiota transplantation.* Science, 2016. **352**(6285): p. 586-9.

127. de Groot, P., et al., *Donor metabolic characteristics drive effects of faecal microbiota transplantation on recipient insulin sensitivity, energy expenditure and intestinal transit time.* Gut, 2019.

128. Liou, A.P., et al., *Conserved shifts in the gut microbiota due to gastric bypass reduce host weight and adiposity.* Sci Transl Med, 2013. **5**(178): p. 178ra41.

129. Tremaroli, V., et al., *Roux-en-Y Gastric Bypass and Vertical Banded Gastroplasty Induce Long-Term Changes on the Human Gut Microbiome Contributing to Fat Mass Regulation.* Cell Metab, 2015. **22**(2): p. 228-38.

130. Blanton, L.V., et al., *Gut bacteria that prevent growth impairments transmitted by microbiota from malnourished children.* Science, 2016. **351**(6275).

131. Backhed, F., et al., *Mechanisms underlying the resistance to diet-induced obesity in germ-free mice.* Proc Natl Acad Sci U S A, 2007. **104**(3): p. 979-84.

132. Zhang, L., et al., *Environmental spread of microbes impacts the development of metabolic phenotypes in mice transplanted with microbial communities from humans.* ISME J, 2017. **11**(3): p. 676-690.

133. Peters, B.A., et al., *A taxonomic signature of obesity in a large study of American adults.* Sci Rep, 2018. **8**(1): p. 9749.

134. Jackson, M.A., et al., *Detection of stable community structures within gut microbiota co-occurrence networks from different human populations.* PeerJ, 2018. **6**: p. e4303.

135. Lim, M.Y., et al., *The effect of heritability and host genetics on the gut microbiota and metabolic syndrome.* Gut, 2017. **66**(6): p. 1031-1038.

136. Di Luccia, B., et al., *Rescue of Fructose-Induced Metabolic Syndrome by Antibiotics or Faecal Transplantation in a Rat Model of Obesity.* PLoS One, 2015. **10**(8): p. e0134893.

137. Soderborg, T.K., et al., *The gut microbiota in infants of obese mothers increases inflammation and susceptibility to NAFLD.* Nat Commun, 2018. **9**(1): p. 4462.

138. Rabot, S., et al., *High fat diet drives obesity regardless the composition of gut microbiota in mice.* Sci Rep, 2016. **6**: p. 32484.

139. Ehses, J.A., et al., *Toll-like receptor 2-deficient mice are protected from insulin resistance and beta cell dysfunction induced by a high-fat diet.* Diabetologia, 2010. **53**(8): p. 1795-806.

140. Caricilli, A.M., et al., *Gut microbiota is a key modulator of insulin resistance in TLR 2 knockout mice.* PLoS Biol, 2011. **9**(12): p. e1001212.

141. Lagkouvardos, I., et al., *Gut metabolites and bacterial community networks during a pilot intervention study with flaxseeds in healthy adult men.* Mol Nutr Food Res, 2015. **59**(8): p. 1614-28.

142. Klindworth, A., et al., *Evaluation of general 16S ribosomal RNA gene PCR primers for classical and next-generation sequencing-based diversity studies.* Nucleic Acids Res, 2013. **41**(1): p. e1.

143. Berry, D., et al., *Barcoded primers used in multiplex amplicon pyrosequencing bias amplification.* Appl Environ Microbiol, 2011. **77**(21): p. 7846-9.

144.   Lagkouvardos, I., et al., *IMNGS: A comprehensive open resource of processed 16S rRNA microbial profiles for ecology and diversity studies.* Sci Rep, 2016. **6**: p. 33721.

145.   Edgar, R.C., *UPARSE: highly accurate OTU sequences from microbial amplicon reads.* Nat Methods, 2013. **10**(10): p. 996-8.

146.   Wang, Q., et al., *Naive Bayesian classifier for rapid assignment of rRNA sequences into the new bacterial taxonomy.* Appl Environ Microbiol, 2007. **73**(16): p. 5261-7.

147.   Lagkouvardos, I., et al., *Rhea: a transparent and modular R pipeline for microbial profiling based on 16S rRNA gene amplicons.* PeerJ, 2017. **5**: p. e2836.

148.   Jost, L., *Partitioning diversity into independent alpha and beta components.* Ecology, 2007. **88**(10): p. 2427-39.

149.   Chen, J., et al., *Associating microbiome composition with environmental covariates using generalized UniFrac distances.* Bioinformatics, 2012. **28**(16): p. 2106-13.

150.   Chun, J., et al., *EzTaxon: a web-based tool for the identification of prokaryotes based on 16S ribosomal RNA gene sequences.* Int J Syst Evol Microbiol, 2007. **57**(Pt 10): p. 2259-61.

151.   Livak, K.J. and T.D. Schmittgen, *Analysis of relative gene expression data using real-time quantitative PCR and the 2(-Delta Delta C(T)) Method.* Methods, 2001. **25**(4): p. 402-8.

152.   Sellmann, C., et al., *Diets rich in fructose, fat or fructose and fat alter intestinal barrier function and lead to the development of nonalcoholic fatty liver disease over time.* J Nutr Biochem, 2015. **26**(11): p. 1183-92.

153.   Kleiner, D.E., et al., *Design and validation of a histological scoring system for nonalcoholic fatty liver disease.* Hepatology, 2005. **41**(6): p. 1313-21.

154.   Han, J., et al., *An isotope-labeled chemical derivatization method for the quantitation of short-chain fatty acids in human feces by liquid chromatography-tandem mass spectrometry.* Anal Chim Acta, 2015. **854**: p. 86-94.

155.   Hold, G.L., et al., *Oligonucleotide probes that detect quantitatively significant groups of butyrate-producing bacteria in human feces.* Appl Environ Microbiol, 2003. **69**(7): p. 4320-4.

156.   Martin, R., et al., *Functional Characterization of Novel Faecalibacterium prausnitzii Strains Isolated from Healthy Volunteers: A Step Forward in the Use of F. prausnitzii as a Next-Generation Probiotic.* Front Microbiol, 2017. **8**: p. 1226.

157.   Dao, M.C., et al., *Akkermansia muciniphila and improved metabolic health during a dietary intervention in obesity: relationship with gut microbiome richness and ecology.* Gut, 2016. **65**(3): p. 426-36.

158.   Dao, M.C., et al., *Akkermansia muciniphila abundance is lower in severe obesity, but its increased level after bariatric surgery is not associated with metabolic health improvement.* Am J Physiol Endocrinol Metab, 2019. **317**(3): p. E446-E459.

159.   Earley, H., et al., *The abundance of Akkermansia muciniphila and its relationship with sulphated colonic mucins in health and ulcerative colitis.* Sci Rep, 2019. **9**(1): p. 15683.

160.   Schneeberger, M., et al., *Akkermansia muciniphila inversely correlates with the onset of inflammation, altered adipose tissue metabolism and metabolic disorders during obesity in mice.* Sci Rep, 2015. **5**: p. 16643.

161.   Lazo, M. and J.M. Clark, *The epidemiology of nonalcoholic fatty liver disease: a global perspective.* Semin Liver Dis, 2008. **28**(4): p. 339-50.

162.   Gaemers, I.C., et al., *Lipotoxicity and steatohepatitis in an overfed mouse model for non-alcoholic fatty liver disease.* Biochim Biophys Acta, 2011. **1812**(4): p. 447-58.

163.   Kayser, B.D., M.I. Goran, and S.G. Bouret, *Perinatal overnutrition exacerbates adipose tissue inflammation caused by high-fat feeding in C57BL/6J mice.* PLoS One, 2015. **10**(3): p. e0121954.

164.   Wellen, K.E. and G.S. Hotamisligil, *Inflammation, stress, and diabetes.* J Clin Invest, 2005. **115**(5): p. 1111-9.

165.   Weisberg, S.P., et al., *Obesity is associated with macrophage accumulation in adipose tissue.* J Clin Invest, 2003. **112**(12): p. 1796-808.

166.   Hartstra, A.V., et al., *Infusion of donor feces affects the gut-brain axis in humans with metabolic syndrome.* Mol Metab, 2020. **42**: p. 101076.

167. Nicholson, A., et al., *Diet-induced obesity in two C57BL/6 substrains with intact or mutant nicotinamide nucleotide transhydrogenase (Nnt) gene.* Obesity (Silver Spring), 2010. **18**(10): p. 1902-5.

168. Neuman, V., et al., *Human gut microbiota transferred to germ-free NOD mice modulate the progression towards type 1 diabetes regardless of the pace of beta cell function loss in the donor.* Diabetologia, 2019.

169. Gonzalez, L.M., A.J. Moeser, and A.T. Blikslager, *Porcine models of digestive disease: the future of large animal translational research.* Transl Res, 2015. **166**(1): p. 12-27.

170. Pang, X., et al., *Inter-species transplantation of gut microbiota from human to pigs.* ISME J, 2007. **1**(2): p. 156-62.

171. Zhang, C., et al., *Structural resilience of the gut microbiota in adult mice under high-fat dietary perturbations.* ISME J, 2012. **6**(10): p. 1848-57.

172. Panek, M., et al., *Methodology challenges in studying human gut microbiota - effects of collection, storage, DNA extraction and next generation sequencing technologies.* Sci Rep, 2018. **8**(1): p. 5143.

173. Marotz, C.A. and A. Zarrinpar, *Treating Obesity and Metabolic Syndrome with Fecal Microbiota Transplantation.* Yale J Biol Med, 2016. **89**(3): p. 383-388.

174. Cammarota, G., et al., *International consensus conference on stool banking for faecal microbiota transplantation in clinical practice.* Gut, 2019. **68**(12): p. 2111-2121.

175. Wang, J.W., et al., *Fecal microbiota transplantation: Review and update.* J Formos Med Assoc, 2019. **118 Suppl 1**: p. S23-S31.

176. Clavel, T., I. Lagkouvardos, and A. Hiergeist, *Microbiome sequencing: challenges and opportunities for molecular medicine.* Expert Rev Mol Diagn, 2016. **16**(7): p. 795-805.

177. Falony, G., et al., *Population-level analysis of gut microbiome variation.* Science, 2016. **352**(6285): p. 560-4.

178. Rintala, A., et al., *Gut Microbiota Analysis Results Are Highly Dependent on the 16S rRNA Gene Target Region, Whereas the Impact of DNA Extraction Is Minor.* J Biomol Tech, 2017. **28**(1): p. 19-30.

179. Turnbaugh, P.J., et al., *The effect of diet on the human gut microbiome: a metagenomic analysis in humanized gnotobiotic mice.* Sci Transl Med, 2009. **1**(6): p. 6ra14.

180. Respondek, F., et al., *Short-chain fructo-oligosaccharides modulate intestinal microbiota and metabolic parameters of humanized gnotobiotic diet induced obesity mice.* PLoS One, 2013. **8**(8): p. e71026.

181. Kibe, R., et al., *Movement and fixation of intestinal microbiota after administration of human feces to germfree mice.* Appl Environ Microbiol, 2005. **71**(6): p. 3171-8.

182. Kubeck, R., et al., *Dietary fat and gut microbiota interactions determine diet-induced obesity in mice.* Mol Metab, 2016. **5**(12): p. 1162-1174.

183. Backhed, F., et al., *Host-bacterial mutualism in the human intestine.* Science, 2005. **307**(5717): p. 1915-20.

184. Rabot, S., et al., *Germ-free C57BL/6J mice are resistant to high-fat-diet-induced insulin resistance and have altered cholesterol metabolism.* FASEB J, 2010. **24**(12): p. 4948-59.

185. Parks, B.W., et al., *Genetic control of obesity and gut microbiota composition in response to high-fat, high-sucrose diet in mice.* Cell Metab, 2013. **17**(1): p. 141-52.

186. Scott, K.P., et al., *The influence of diet on the gut microbiota.* Pharmacol Res, 2013. **69**(1): p. 52-60.

187. Warden, C.H. and J.S. Fisler, *Comparisons of diets used in animal models of high-fat feeding.* Cell Metab, 2008. **7**(4): p. 277.

188. Dalby, M.J., et al., *Dietary Uncoupling of Gut Microbiota and Energy Harvesting from Obesity and Glucose Tolerance in Mice.* Cell Rep, 2017. **21**(6): p. 1521-1533.

189. Borody, T.J., S. Paramsothy, and G. Agrawal, *Fecal microbiota transplantation: indications, methods, evidence, and future directions.* Curr Gastroenterol Rep, 2013. **15**(8): p. 337.

190. Vermeire, S., et al., *Donor Species Richness Determines Faecal Microbiota Transplantation Success in Inflammatory Bowel Disease.* J Crohns Colitis, 2016. **10**(4): p. 387-94.

191. de Vos, W.M., *Fame and future of faecal transplantations--developing next-generation therapies with synthetic microbiomes.* Microb Biotechnol, 2013. **6**(4): p. 316-25.

192. Nguyen, T.L., et al., *How informative is the mouse for human gut microbiota research?* Dis Model Mech, 2015. **8**(1): p. 1-16.

193. Kasai, C., et al., *Comparison of the gut microbiota composition between obese and non-obese individuals in a Japanese population, as analyzed by terminal restriction fragment length polymorphism and next-generation sequencing.* BMC Gastroenterol, 2015. **15**: p. 100.

194. Wos-Oxley, M., et al., *Comparative evaluation of establishing a human gut microbial community within rodent models.* Gut Microbes, 2012. **3**(3): p. 234-49.

195. Chung, H., et al., *Gut immune maturation depends on colonization with a host-specific microbiota.* Cell, 2012. **149**(7): p. 1578-93.

196. Lundberg, R., *Humanizing the gut microbiota of mice: Opportunities and challenges.* Lab Anim, 2019. **53**(3): p. 244-251.

197. Damman, C.J., et al., *The microbiome and inflammatory bowel disease: is there a therapeutic role for fecal microbiota transplantation?* Am J Gastroenterol, 2012. **107**(10): p. 1452-9.

198. Thingholm, L.B., et al., *Obese Individuals with and without Type 2 Diabetes Show Different Gut Microbial Functional Capacity and Composition.* Cell Host Microbe, 2019. **26**(2): p. 252-264 e10.

199. Murphy, E.F., et al., *Composition and energy harvesting capacity of the gut microbiota: relationship to diet, obesity and time in mouse models.* Gut, 2010. **59**(12): p. 1635-42.

200. Gart, E., et al., *Diet-Independent Correlations between Bacteria and Dysfunction of Gut, Adipose Tissue, and Liver: A Comprehensive Microbiota Analysis in Feces and Mucosa of the Ileum and Colon in Obese Mice with NAFLD.* Int J Mol Sci, 2018. **20**(1).

201. Mulder, P., et al., *Surgical removal of inflamed epididymal white adipose tissue attenuates the development of non-alcoholic steatohepatitis in obesity.* Int J Obes (Lond), 2016. **40**(4): p. 675-84.

202. Fontana, L., et al., *Aging promotes the development of diet-induced murine steatohepatitis but not steatosis.* Hepatology, 2013. **57**(3): p. 995-1004.

203. Kim, I.H., et al., *Aging increases the susceptibility of hepatic inflammation, liver fibrosis and aging in response to high-fat diet in mice.* Age (Dordr), 2016. **38**(4): p. 291-302.

204. Wu, D., et al., *Aging up-regulates expression of inflammatory mediators in mouse adipose tissue.* J Immunol, 2007. **179**(7): p. 4829-39.

205. Tchkonia, T., et al., *Fat tissue, aging, and cellular senescence.* Aging Cell, 2010. **9**(5): p. 667-84.

206. Johansson, M.E., et al., *Normalization of Host Intestinal Mucus Layers Requires Long-Term Microbial Colonization.* Cell Host Microbe, 2015. **18**(5): p. 582-92.

Publications and Presentations

Publications

- Hartstra AV, **Schüppel V**, Imangaliyev S, Schrantee A, Prodan A, Collard D, Levin E, Dallinga-Thie G, Ackermans MT, Winkelmeijer M, Havik SR, Metwaly A, Lagkouvardos I, Nier A, Bergheim I, Heikenwälder M, Dunkel A, Nederveen AJ, Liebisch G, Mancano G, Claus S, Benitez-Paez A, la Fleur SE, Bergman JJ, Sanz Y, Booij J, Kemper E, Groen AK, Serlie MJ, Haller, Nieuwdorp M. (2020). Infusion of donor feces affects the gut-brain axis in humans with metabolic syndrome. Molecular Metabolism; 42:101076.

- Olivares M, **Schüppel V**, Hassan AM, Beaumont M, Neyrinck AM, Bindels LB, Benitez-Paez A, Sanz Y, Haller D, Holzer P, Delzenne NM. (2018). The potential role of the dipeptidyl peptidase-4-like activity by the gut microbiota: consequences for the host health. Frontiers in Microbiology; 9:1900.

- Neyrinck AM, **Schüppel VL**, Lockett T, Haller D, Delzenne NM. (2016). Microbiome and metabolic disorders related to obesity: Which lessons to learn from experimental models. Trends in Food Science & Technology; 57:256–264.

- Kübeck R, Bonet-Ripoll C, Hoffmann C, Walker A, Müller VM, **Schüppel VL**, Lagkouvardos I, Scholz B, Engel KH, Daniel H, Schmitt-Kopplin P, Haller D, Clavel T, Klingenspor M. (2016). Dietary fat and gut microbiota interactions determine diet-induced obesity in mice. Molecular Metabolism; 5(12):1162-1174.

- **Schüppel V**, Haller D. (2016). Das Mikrobiom bei chronischen Erkrankungen. Der Diabetologe; 12(6):420-427.

- Gruber L, Hemmerling J, **Schüppel V**, Müller M, Boekschoten MV, Haller D. (2015). Maternal high-fat diet accelerates development of Crohn's Disease-like ileitis in TNFΔARE/WT offspring. Inflammatory Bowel Diseases; 21(9):2016-25.

- Kless C*, Müller VM*, **Schüppel VL***, Lichtenegger M, Rychlik M, Daniel H, Klingenspor M, Haller D. (2015). Diet-induced obesity causes metabolic impairment independent of alterations in gut barrier integrity. Molecular Nutrition & Food Research; 59(5):968-78. *shared first authorship

- Rauschmeier M, **Schüppel V**, Tetsch L, Jung K. (2014). New insights into the interplay between the lysine transporter LysP and the pH sensor CadC in Escherichia coli. Journal of Molecular Biology; 426(1):215-29.

Published abstracts

- **24. – 26.06.2016**: 9th Seeon Conference, Microbiota, Probiota and Host; "Role of intestinal microbiota on gut barrier, metabolic function and inflammation in a humanized mouse model of diet-induced obesity".

- **05. – 08.03.2017**: 5th Joint Conference of the DGHM & VAAM, Würzburg; "Role of Intestinal Microbiota on Gut Barrier, Metabolic Function and Inflammation in a Humanized Mouse Model of Diet-Induced Obesity".

Grants

Poster award, Seeon conference, 2016, "Role of intestinal microbiota on gut barrier, metabolic function and inflammation in a humanized mouse model of diet-induced obesity".

Acknowledgements

An dieser Stelle möchte ich mich von Herzen bei allen Personen bedanken, die mich unterstützt und das Zustandekommen der vorliegenden Arbeit ermöglicht haben.

Zu allererst danke ich meinem Doktorvater und Erstgutachter Prof. Dirk Haller für die Möglichkeit, die Doktorarbeit an diesem Lehrstuhl zu absolvieren. Vielen Dank auch für die zahlreichen und konstruktiven Denkanstöße und Diskussionen!

Bei Prof. Martin Klingenspor möchte ich mich in erster Linie für die tolle Zusammenarbeit im BMBF Projekt inklusive reger Diskussionen und konstruktivem Input herzlich danken. Außerdem danke ich vielmals für die Übernahme des Zweitprüfersitzes.

Prof. Michael Schemann danke ich für die sofortige Bereitschaft, den Vorsitz der Prüfungskommission zu übernehmen.

Ich danke von tiefstem und ganzem Herzen meiner „Mädels-Crew" für die intensive und tolle Zeit, auch außerhalb des Labors. Vielen, lieben Dank für die stetigen mutmachenden Worte, die offenen Ohren und die großartige Unterstützung von der ersten Sekunde der Doktorarbeit an: Sarah Just, Elena Lobner, Isabella Lengfelder und Monika Schaubeck!

Ich danke zudem meinem gesamten Lehrstuhl für die hilfsbereite und positive Teamarbeit, für die wissenschaftliche und technische Unterstützung sowie die zahlreichen Anregungen und Unterhaltungen. Besonders hervorheben möchte ich dabei folgende Alumni sowie Kollegen: Sandra Bierwirth, Gabi Hörmannsperger, Thomas Clavel, Ilias Lagkouvardos, Alexandra Buse, Sevana Khaloian, Brita Sturm, Sigrid Kisling, Ingrid, Schmöller, Amira Metwaly, Melanie Klein, Sandra Hennig, Caroline Ziegler, Simone Daxauer, Silvia Pitariu und Nico Gebhardt.

Ich danke Caroline Kless und Veronika Müller für die fantastische Zusammenarbeit im BMBF-Projekt. Zudem möchte ich mich bei allen Kooperationspartnern des MyNewGut-Projektes für die gute Zusammenarbeit und die intensiven Diskussionen bedanken.

Zuletzt gilt mein größter Dank meiner Familie und meinem Freund Alex. Danke, dass ihr mich immer zu 100 Prozent unterstützt habt und mit viel Geduld sowie Zuversicht den Weg gemeinsam mit mir gegangen seid! Vielen, lieben Dank!!!

Kollegen
Familie
Freunde
DANKE!
Betreuer
Prüfer/Vorsitz
Kooperationspartner

Eidesstattliche Erklärung

Ich erkläre an Eides statt, dass ich die bei der promotionsführenden Einrichtung

Fakultät TUM School of Life Sciences

der TUM zur Promotionsprüfung vorgelegte Arbeit mit dem Titel:

Role of the intestinal microbiota in metabolic and inflammatory phenotypes in a human microbiota-associated mouse model for metabolic disorders and diet-induced obesity

in **Freising-Weihenstephan, ZIEL – Zentralinstitut für Ernährungs- und Lebensmittelforschung, Lehrstuhl für Ernährung und Immunologie**

Fakultät, Institut, Lehrstuhl, Klinik, Krankenhaus, Abteilung

unter der Anleitung und Betreuung durch: **Prof. Dr. Dirk Haller** ohne sonstige Hilfe erstellt und bei der Abfassung nur die gemäß § 6 Ab. 6 und 7 Satz 2 angebotenen Hilfsmittel benutzt habe.

☒ Ich habe keine Organisation eingeschaltet, die gegen Entgelt Betreuerinnen und Betreuer für die Anfertigung von Dissertationen sucht, oder die mir obliegenden Pflichten hinsichtlich der Prüfungsleistungen für mich ganz oder teilweise erledigt.

☒ Ich habe die Dissertation in dieser oder ähnlicher Form in keinem anderen Prüfungsverfahren als Prüfungsleistung vorgelegt.

☐ Die vollständige Dissertation wurde in _____ veröffentlicht. Die promotionsführende Einrichtung

_____

hat der Veröffentlichung zugestimmt.

☒ Ich habe den angestrebten Doktorgrad noch nicht erworben und bin nicht in einem früheren Promotionsverfahren für den angestrebten Doktorgrad endgültig gescheitert.

☐ Ich habe bereits am _____ bei der Fakultät für _____

_____ der

Hochschule _____ unter

Vorlage einer Dissertation mit dem Thema _____

_____ die

Zulassung zur Promotion beantragt mit dem Ergebnis: _____

_____

Die öffentlich zugängliche Promotionsordnung der TUM ist mir bekannt, insbesondere habe ich die Bedeutung von § 28 (Nichtigkeit der Promotion) und § 29 (Entzug des Doktorgrades) zur Kenntnis genommen. Ich bin mir der Konsequenzen einer falschen Eidesstattlichen Erklärung bewusst.

Mit der Aufnahme meiner personenbezogenen Daten in die Alumni-Datei bei der TUM bin ich

☒ einverstanden,   ☐ nicht einverstanden.

_____

Ort, Datum, Unterschrift

Curriculum Vitae

PERSÖNLICHE DATEN

Name	Valentina Schüppel
geb.	03.10.1986, München
Familienstand	ledig
Staatsangehörigkeit	deutsch

BERUFLICHE TÄTIGKEITEN UND PRAKTIKA

10/2018 – heute	Embryologin am Kinderwunschzentrum an der Oper, München
03/2012 – 03/2018	Doktorarbeit, Lehrstuhl Ernährung und Immunologie, Technische Universität München, Prof. Dr. D. Haller
02/2010 – 08/2010	Arbeit als studentische Hilfskraft Praktikum Abteilung Mikrobiologie, Arbeitsgruppe Prof. Dr. T. Mascher, Ludwig-Maximilians-Universität München
11/2009 – 12/2009	Praktikum am "Department of Pathology and Laboratory Medicine", Tulane University (School of Medicine), New Orleans, PHD G. Morris
02/2009 – 03/2009 10/2009 – 11/2009	Arbeit als studentische Hilfskraft Praktikum Abteilung Mikrobiologie, Arbeitsgruppe Prof. Dr. K. Jung, Ludwig-Maximilians-Universität München
07/2008 – 09/2008	Praktikantin in der Fermentationsentwicklung, Roche Diagnostics GmbH, Penzberg

AUSBILDUNG

22.06.2011	Abschluss zur Diplom-Biologin Univ. (Gesamtnote: 1,3)
09/2010 – 06/2011	Diplomarbeit im Hauptfach Mikrobiologie, Arbeitsgruppe Prof. Dr. Kirsten Jung (Note: 1,0)
04/2008 – 09/2010	Hauptstudium der Biologie mit Schwerpunkt Mikrobiologie, Zellbiologie und Pharmakologie/Toxikologie (Note: 1,7)
10/2006 – 06/2011	Studium der Biologie an der Ludwig-Maximilians-Universität München
09/1997 – 06/2006	Abitur am Gymnasium Starnberg (Abiturnote: 2,1)